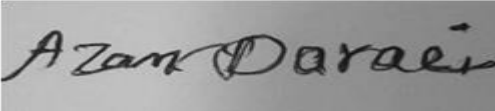




Faculty of Science and Technology

MASTER'S THESIS

Study program/ Specialization: Biological Chemistry	Spring semester, 2019 Open
Writer: Azam Daraei	 (Writer's signature)
Faculty Supervisor: Astrid Elisabeth Mork- Jansson	
Thesis title: Characterization of exosomes and synthesized exosome-based liposomes to establish a drug delivery scheme for the treatment of epilepsy.	
Credits (ECTS): 60	
Key words: Exosome, Liposome, Drug delivery system, Epilepsy	Pages: 70 pages + Appendix: 46 pages Stavanger, 15 th June 2019

Abstract

Epilepsy is one of the most prevalent, chronic, critical neurological diseases. Due to the ability of the blood-brain barrier (BBB) to prevent the entry of drugs into the brain, pharmaceutical treatment of central nervous system diseases is a challenge. The development of nanotechnology offers the ability to overcome this issue.

Our objective was to evaluate the possibility of an exosome-based drug delivery system program for an anti-epileptic drug (AED) to treat epileptic patients. For this purpose, we isolated exosomes by a size exclusion method (SEC), then exosomes were characterized by dynamic light scattering (DLS) and mass spectrometry (MS). Further, we synthesized exosome-based liposomes using Avanti extruder, and afterwards, liposomes were characterized by DLS. Finally, we isolated porcine brain endothelial cells (PBECS), as an *in vitro* BBB model, followed by a viability test.

We found that isolation and characterization of exosomes, and also preparing and characterization of liposomes by the presented approaches, was feasible and showed purity and homogeneity of yields. We found that several lipids were enriched in exosomes from blood plasma. Finally, we found that to achieve a proper *in vitro* BBB model for drug delivery studies, optimization of cell isolation procedures and cell culture conditions of individual models seems to be of essential importance.

Acknowledgment

I would like to express my deepest gratitude to my supervisor Astrid Elisabeth Mork-Jansson. Thank you for guiding me through every step of this project. Your advice and support during writing this master thesis are greatly appreciated.

I would like to thank Julie Nikolaisen for taking the time to train me on the technique of mass spectrometry and in the cell lab. Thank you for your valuable advice. Many thanks to Martin Jakubec of University of Bergen for conducting the experiment by mass spectrometry. Also, thanks to Jodi Maple Grodem for helpful written comments. Thanks to my fellow master students Saleha Akbari and Sussane Nesse for providing interesting discussion. Thanks to my friends Mojgan and Maryam for their support.

Finally, I would like to thank my dear sisters for providing me with consistent emotional support throughout my study in Norway.

June 2019

Azam Daraei

Table of Contents

Abstract.....	i
Acknowledgment.....	ii
List of Figures.....	vi
List of Tables	viii
Abbreviation.....	x
1. Introduction.....	1
1.1 Epilepsy	1
1.2 Blood brain barrier	2
1.3 Exosomes	4
1.3.1 Biogenesis of exosomes.....	4
1.3.2 Composition of exosomes	5
1.3.3 Exosomes as drug delivery vehicles.....	7
1.3.4 Isolation and characterization of exosomes.....	9
1.3.4.1 Mass spectrometry	10
1.3.4.2 Dynamic light scattering	12
1.4 Liposomes.....	13
1.4.1 Extrusion.....	14
1.5 Purpose	15

2.	Methods and materials	17
2.1	Materials.....	17
2.1.1	<i>Cell culture.....</i>	<i>17</i>
2.1.2	<i>Liposomes.....</i>	<i>18</i>
2.1.3	<i>Exosomes isolation.....</i>	<i>18</i>
2.2	Methods	18
2.2.1	<i>Cell culture.....</i>	<i>18</i>
2.2.1.1	<i>Isolation of brain capillaries.....</i>	<i>19</i>
2.2.1.2	<i>Resuscitation of frozen cell line</i>	<i>20</i>
2.2.2	<i>Liposomes preparation.....</i>	<i>21</i>
2.2.2.1	<i>Sonication.....</i>	<i>22</i>
2.2.3	<i>Exosomes isolation.....</i>	<i>22</i>
2.2.4	<i>Dynamic light scattering.....</i>	<i>23</i>
2.2.5	<i>Mass spectrometry.....</i>	<i>23</i>
3.	Results	25
3.1	Characterization of exosomes by DLS.....	25
3.2	Characterizing of exosomes with mass spectrometry.....	26
3.3	Characterization of liposomes by DLS	33
3.3.1	<i>Sonication.....</i>	<i>37</i>
3.4	Cell culture	39

3.4.1	<i>PBECs as an invitro BBB model</i>	39
4.	Discussion	42
4.1	<i>An in vitro</i> BBB model.....	42
4.2	Preparation and characterization of liposomes	44
4.3	Exosomes isolation and characterization.....	45
	Conclusion	48
	References:	49
	Appendix:	57

List of Figures

Figure 1-1 Schematic diagrams of the BBB and the transport mechanism across the BBB. Reprinted with permission from Sibel Bozdog Pehlivan [11].	3
Figure 1-2 Representation of EVs biogenesis and composition [27]. Reprinted with permission from Rufino-Ramos	5
Figure 1-3 Composition of exosomes. Exosomes are composed of various types of proteins, such as major histocompatibility complex (MHC)-II, integrin, cluster of differentiation (CD), tetraspanins, heat shock protein (Hsp), Ras-related protein (Rab), etc. Exosomes also contain various types of lipids, such as sphingomyelin and cholesterol. Lastly, exosomes are found to contain nucleic acid, including miRNA, mRNA and non-coding RNAs [15].	7
Figure 1-4 Components of a mass spectrometer. Adapted from (http://www.premierbiosoft.com/tech_notes/mass-spectrometry.html).(05.04.19).	11
Figure 1-5 Schematic showing the instrumentation of DLS. The figure is reprinted from the PhD degree of Dhiraj Kumar, University of Minnesota Twin Cities, with permission from the author.	12
Figure 1-6 A representation of the steric organization of a liposome [69].	14
Figure 1-7 Components of a Mini Extruder. Adapted from (https://avantilipids.com/divisions/equipment-products).(05.04.19).	15
Figure 2-1 The brain before removing the meninges, B: the brain after removing the meninges.	20
Figure 2-2 Avanti mini extruder device. adapted from (https://avantilipids.com/divisions/equipment-products).(10.04.19).	21
Figure 2-3 EV original size exclusion column. Adapted from (https://www.izon.com/exosome-isolation/qevoriginal). (10.04.19).	22

Figure 3-1 The intensity distribution result of exosome isolation. Fractions of seven to twelve (F7-F12) are determined.	26
Figure 3-2 The intensity distribution result for PC. A: Extruded at 25°C and extrusion cycle 11 and 16 times through the filter. B: Extruded at 41°C and extrusion cycle 11 and 16 times through the filter.	34
Figure 3-3 The intensity distribution result for PC extruded through polycarbonate membranes 50 nm and 100 nm.	35
Figure 3-4 The intensity distribution result for (PC-SM) extruded through polycarbonate membranes 50 nm and 100 nm.	36
Figure 3-5 : The intensity distribution result for PC-SM -PE combination, extruded at 41°C and at 63 °C.	37
Figure 3-6 The intensity distribution result for PC produced by extrusion and sonication methods.	38
Figure 3-7 The intensity distribution result for the PC-SM combination produced by extrusion and sonication methods.	39
Figure 3-8 Viability test results of isolation Batch I, A: After three days, B: After six days.	40
Figure 3-9 Viability test results of isolation Batch II, A: After three days, B: After six days	41
Figure 3-10 The result of the repeated viability test of isolation Batch II, A: After three days, B: After eight days.	41

List of Tables

Table 2-1 Reagents used in Cell isolation.....	17
Table 2-2 Reagents used in Cell culture.	17
Table 2-3 Reagents and phospholipids used to prepare liposomes.....	18
Table 3-1 Exosome isolation results, the fractions from seven to twelve (F7-F12). Based on size and size distribution of each of isolated exosome fraction.	25
Table 3-2 Most abundant lipid species in the fraction 10(80 nm) in positive (Pos) and negative (Neg) modes.....	28
Table 3-3 Most abundant lipid species in the fraction 11(65 nm) in positive (Pos) and negative (Neg) modes.....	29
Table 3-4 Most abundant lipid species for fraction 12 (55 nm) in positive (Pos) and negative (Neg) modes.	30
Table 3-5 Most abundant fatty acid (FA) chains of each headgroup in the fraction 10 (80 nm) in positive (Pos) and negative (Neg) modes.	31
Table 3-6 Most abundant fatty acid (FA) chains of each headgroup in the fraction 11 (65 nm) in positive (Pos) and negative (Neg) modes.	32
Table 3-7 Most abundant fatty acid (FA) chains of each headgroup in the fraction 12 (55 nm) in positive (Pos) and negative (Neg) modes.	33
Table 3-8 Results of size and size distribution for PC extruded at 25°C and 41 °C, with extrusion cycle 11 and 16 times through a 100 nm polycarbonate filter.....	34
Table 3-9 Results of size and size distribution for PC extruded through polycarbonate membranes 50 nm and 100 nm.....	34

Table 3-10 <i>Results of size and size distribution for PC-SM combination, extruded through polycarbonate membranes 50 nm and 100 nm.</i>	35
Table 3-11 <i>Results of size and size distribution for PC-SM -PE combination, extruded at 41°C and at 63 °C.</i>	36
Table 3-12 Results of size and size distribution for PC produced by Sonication and Extrusion methods.	37
Table 3-13 Results of size and size distribution for PC-SM combination produced by Sonication and Extrusion methods.....	38
Table 3-14 The schedule to change the culture media for cell cultures Batch I and Batch II.	40

Abbreviation

AEDs	Anti-Epileptic Drugs
ABs	Apoptotic Bodies
APCI	Atmospheric Pressure Chemical Ionization
BBB	Blood Brain Barrier
BCECs	Brain Capillary Endothelial Cells
DLS	Dynamic Light Scattering
ECs	Endothelial Cells
EVs	Extracellular vesicles
ESI	Electrospray Ionization
EX	Extrusion
FA	Fatty Acid
ILAE	International League Against Epilepsy
ILVs	Intraluminal Vesicles
MS	Mass Spectrometry
MVBs	Multivesicular Bodies
MVs	Micro Vesicles
MALDI	Matrix-Assisted Laser Desorption Ionization

PBECs	Porcine Brain Endothelial Capillary Cells
PC	Phosphatidylcholine
PM	Plasma membrane
PE	Phosphatidylethanolamine
PI	Phosphatidylinositol
PDI	Polydispersity Index
PA	Phosphatidic Acid
SEC	Size Exclusion Chromatography
Std Dev	Standard Deviation
SM	Sphingomyelin
TJs	Tight Junctions
Tm	Phase Transition Temperature
VNS	vagus nerve stimulation

Blank page

Chapter 1

Introduction

1.1 Epilepsy

Epilepsy is one of the most prevalent and incapacitating neurological illnesses. Epilepsy is characterized by periodic and unprovoked seizures [1]. According to the last report (8 February 2018) of the world health organization (WHO), about 50 million people worldwide suffer from this condition. One third of individuals suffering from epilepsy has no response to treatment [1, 2]. Epidemiological studies do not display differences in the prevalence of epilepsy between women and men and it can occur at any age [3, 4].

Epilepsy is characterized by seizures, but this symptom is not specific to epilepsy. Other conditions where seizures are present are febrile cramps, hypoglycemia and the side effect of medications [1, 2]. According to the definition of the International League Against Epilepsy (ILAE), an epileptic seizure is a temporary incident of signs or symptoms, because of atypical intense or synchronous neuronal activity in the brain [5]. A sudden surge of electrical activity in the brain is called a seizure. In other words, a seizure is the result of an imbalance in the electrical activity of the brain. Brain cells can excite or inhibit other brain cells from signaling. In normal conditions, there is a balance between these brain cells. While occurring seizures due to imbalance between exciting and inhibiting cells. Factors like genes or acquired elements can cause imbalance between exciting and inhibiting cells [1]. In the diagnosis of epilepsy, the history of disease and neurological studies such as neuroimaging and electroencephalography (EEG) are essential, while laboratory tests can be useful as supplementary assessments [1].

Available resources of more than 20 AEDs, show effective treatment in over 70% of people with epilepsy [1, 2]. AEDs reduce the electrical activity of the brain. In the cases, that initial AEDs are ineffective, the chance of responding to other AEDs that have been examined unsuccessfully is relatively low. Based on this information, ILAE described intractable epilepsy as failure in seizure control, despite the utilize of two AEDs [2]. If seizures are not controlled by AEDs, other options are dietary therapy (ketogenic diet) and surgery including resective epilepsy surgery (lesionectomy, hemispherotomy), and palliative epilepsy surgery (stimulation therapy, callostomy)[1] . The ketogenic diet (KD) is a high fat and low carbohydrate diet, which is applied in refractory epilepsy and is a principal remedy for children [6]. The role of immune therapy for intractable epilepsy is still being characterized [1].

1.2 Blood brain barrier

There are several protective systems in the brain to support neurons from circulating blood cells and pathogens. They consist of blood- cerebrospinal fluid (CSF) barrier, the blood- brain barrier (BBB), the blood- retinal barrier and the blood spinal cord barrier. Among these, the BBB is the most extensive and unique [7]. The BBB has the least permeable microvessels in the whole body because of tight junctions which act as a physical barrier, while in the external capillaries materials are transmitted easily between the bloodstream and tissues [8]. The BBB was discovered by Paul Ehrlich in 1885. He observed that stain injected into the vascular system was quickly distributed through all organs except the brain and spinal cord [8, 9].

Capillaries are the smallest cerebral blood vessels and are a major site of the BBB, considering that endothelial cells (ECs) and tight junctions (TJs) are the fundamental structure in the BBB [8, 10]. Although astrocytes and pericytes are significant parts of the BBB, but it is mostly formed by the special features of ECs .The TJs that join adjacent ECs and physically impede solute flux between the blood and the brain, which leads to the restricted passive diffusion to the brain for small lipophilic substances of molecular weight less than 400 to 500 Da, selective influx transfer of hydrophilic composites is allowed by transport proteins, biotransformation and detoxification

system is supplied by metabolic barriers, and inconsiderable pinocytotic activity are distinctive properties of ECs (Figure 1-1) [11].

Despite the limited transfer of substances through the BBB, the brain needs a lot of energy and nutrients. Hence, there are several mechanisms that mediate the uptake of endogenous substances. Some of the mechanisms can be used as the basic principles for the development of drug delivery methods. Generally, in normal condition, substances pass through the BBB via passive diffusion, carrier mediated transfer, receptor mediated transfer, and adsorptive transcytosis [3].

Because of the BBB, many large molecules cannot penetrate the brain. Only some small molecules (molecular weight less than 600 Da, chain length below 6 amino acids) and molecules dissolved in lipids could pass through the BBB and enter the brain [12, 13].

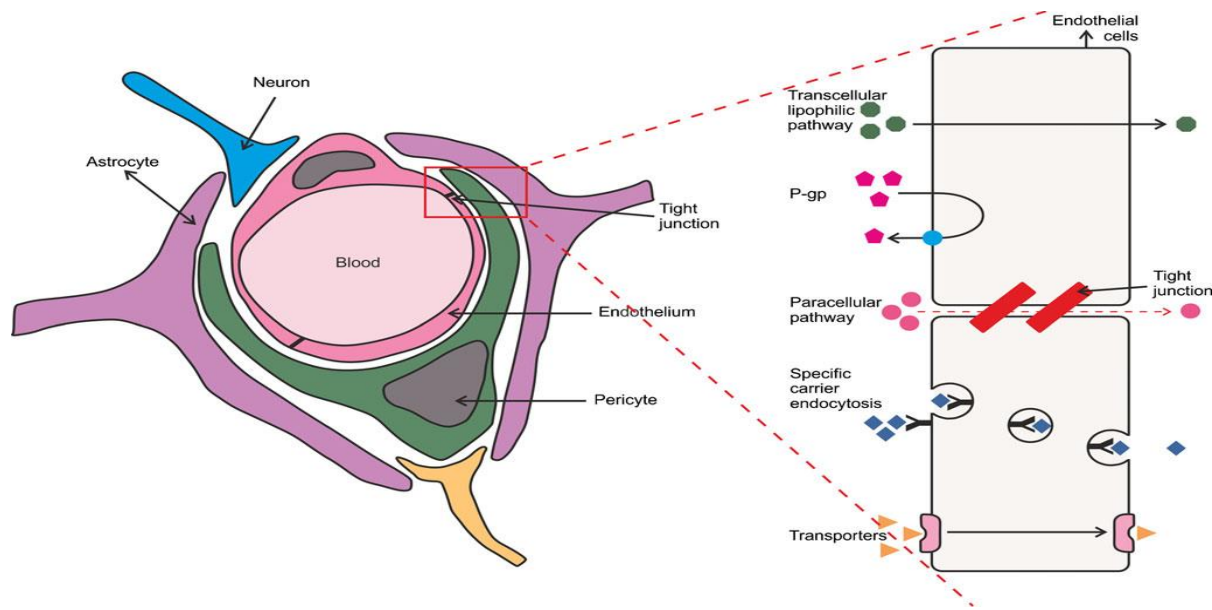


Figure 1-1 Schematic diagrams of the BBB and the transport mechanism across the BBB. Reprinted with permission from Sibel Bozdog Pehlivan [11].

Several methods have been used previously to cross the BBB, such as transcranial or nasal application, infiltrated hypertonic factors, and lipidation of micro molecule drugs. These techniques, besides their restrictions, are often invasive, they could increase the chance of infection

or brain damage. Moreover, by using these methods drugs are transmitted to the white matter that is not preferable [8]. The exploration of new methods has led to enhancement in BBB permeability and the reduction of side effects. The procedures involve the following fields: physical, chemical, biological and diverse nanoparticle mechanisms [8].

1.3 Exosomes

Exosomes are membrane-derived vesicles, which are generated within endosomes, with various contents and which participate in physiological and pathological processes [14, 15]. They are produced by most cells and can be found in body fluids such as blood, urine, amniotic liquid, breast milk and saliva [15]. Exosomes have been considered recently due to their desirable features as drug delivery vehicles.

The discovery of exosomes in the 1980s was the result of researchers' observations during working with maturing reticulocytes. They observed that small vesicles were created by inward budding in an intracellular endosome, following the formation of a multivesicular body (MVB), then the MVB could merge into the plasma membrane (PM) and exosomes are these internal vesicles which are secreted outside [16, 17].

1.3.1 Biogenesis of exosomes

Exosomes belong to a larger group of cell- derived vesicles defined as extracellular vehicles (EVs) [18, 19]. EVs are membrane –comprised small vesicles that are released by all types of prokaryotic and eukaryotic cells [20, 21]. Apoptotic Bodies (ABs), Shedding Micro Vesicles (MVs) and Exosomes, are the three major groups of EVs. (Figure 1-2). ABs are the result of cell death (apoptosis) and are heterogenous in shape with sizes between 50-5000 nm. They are generated from PM and they include DNA, RNA, histones, and signaling molecules [22]. MVs are generated due to vesiculation of the cell membrane with integration of cytosolic proteins, and subject to the source cells and the technique utilized for their isolation from cell media, their dimension range are 20-1000 nm [23]. Exosomes are a category of vesicles that are more homogenous than MVs in terms of size and shape, and their size range between 50-100 nm. They

are formed by growing into MVBs. The combination of MVBs to the PM leads to secretion of the exosomes [22, 24].

Exosomes are generally formed in three steps. In the first step, early endosomes are created from the PM, then they are developed into late endosomes. The inward budding of late endosomes leads to the formation of intraluminal vesicles (ILVs). MVBs are the result of the accumulation of these ILVs in late endosomes. MVBs are formed during two procedures. During a procedure endosomal sorting complexes are required for transporting (ESCRT) and another procedure is ESCRT independent. Finally, MVBs can be degraded after fusing with the lysosome or can secrete ILVs into the extracellular area after fusing with the PM and these released ILVs are designated as exosomes (Figure 1-2) [25].

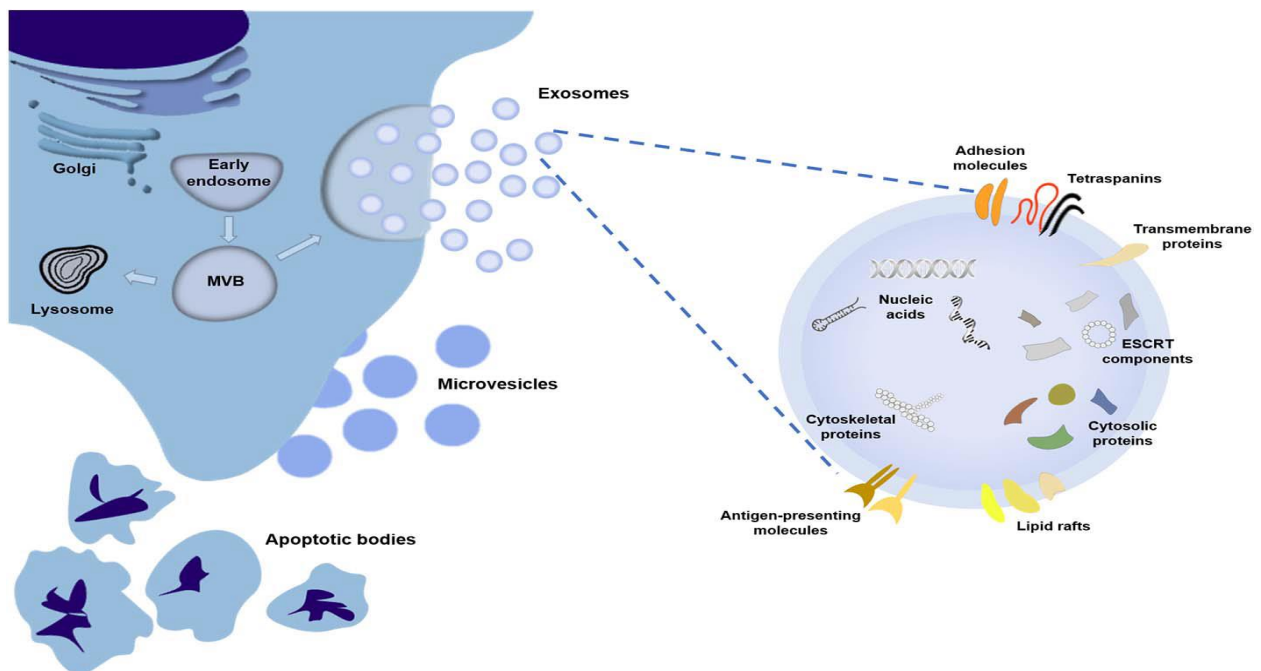


Figure 1-2 Representation of EVs biogenesis and composition [27]. Reprinted with permission from Rufino-Ramos

1.3.2 Composition of exosomes

Exosomes, regardless of their morphological and physical characteristics, are usually distinguished based on their protein and lipid contents [25]. The nanospherical membrane-derived framework of exosomes is shaped with a lipid bilayer. Exosomes also consist of different kinds of

proteins and lipids that originate from the ancestral cells of the exosomes. (Figures 1-2 and Figure1-3). Based on information from ExoCarta, an exosome database, approximately 8000 proteins and 194 lipids have been identified in exosomes [26]. Since, exosomes are derived from intracellular constituent “endosome”, they contain proteins such as heat shock proteins (Hsp70 and Hsp90), membrane transport and fusion proteins (GTPases, Annexins and flotillin), and tetraspanins (CD9, CD63, CD81, and CD82) [26]. Heat shock proteins, annexins, and proteins of the Rab family are highly found in exosomes and are involved in their intracellular assembly and trafficking. Tetraspanins, a group of transmembrane proteins, are often identified in exosomes. In a cell, tetraspanins are involved in fusion, cell migration, cell-cell adhesion, and signaling. However, their role in exosomes is not recognized [24].

Integrins are other proteins found abundantly in exosomes. They are adhesion molecules that promote the binding of cells to the extracellular matrix and their function in exosomes is to connect the vesicles to their target cells [28]. Other proteins include thrombospondin, CD55, CD59, lactadherin, ALIX, and TSG101 [24, 29]. During exosome generation, these various groups of proteins are incorporated with exosomes and act as a cargo for cell-cell communication [15].

In addition to proteins, exosomes also contain many lipids, with various kinds of exosomes, containing different groups of lipids. The lipid bilayer of exosomes is largely comprised of cell PM type of lipids including sphingomyelin, phosphatidylcholine, phosphatidylethanolamine, phosphatidylserine, monosialotetrahexosylganglioside (GM3), and phosphatidylinositol [30]. The rigidity and stability of exosomes is determined by sphingomyelin and GM3 [31]. Phosphatidylserine is appeared on the PM of exosomes by a variety of phospholipid transportation enzymes. Its role includes docking the outer plasma, enabling the signaling and integration of the exosome to the PM [32]. Other types of lipids that are associated with exosomes are lipid rafts such as cholesterol, ceramide, and phosphoglycerides, with long and saturated fatty-acid chains

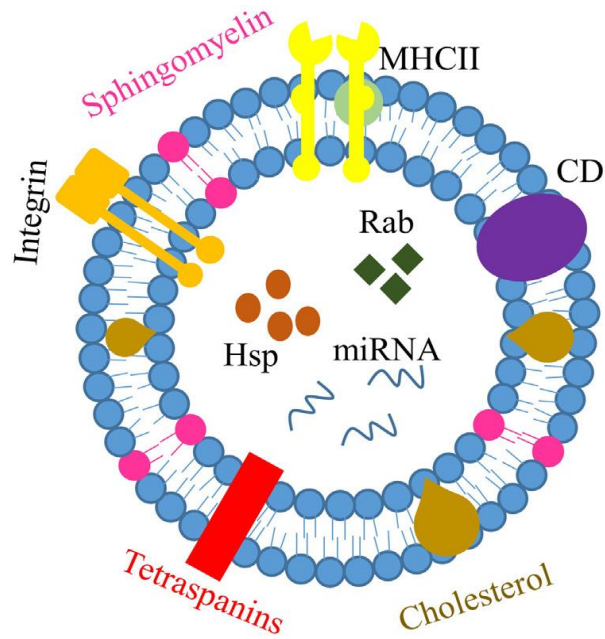


Figure 1-3 Composition of exosomes. Exosomes are composed of various types of proteins, such as major histocompatibility complex (MHC)-II, integrin, cluster of differentiation (CD), tetraspanins, heat shock protein (Hsp), Ras-related protein (Rab), etc. Exosomes also contain various types of lipids, such as sphingomyelin and cholesterol. Lastly, exosomes are found to contain nucleic acid, including miRNA, mRNA and non-coding RNAs [15].

Other components of exosomes include nucleic acid, such as micro RNA (miRNA), messenger RNA (mRNA), and non-coding RNAs (Figure 1-3) [15, 26]. Furthermore, exosomes include many other types of RNA (adhesion and signaling). Exosomes comprise specific subsets of cellular RNA. Some sets are particular or tissue specific, while other sets of RNA exist in exosomes regardless of cellular source [33].

1.3.3 Exosomes as drug delivery vehicles

The drug delivery systems that are currently most promising are liposomes and polymeric nanoparticles. A liposome is an artificial vesicle with a phospholipid membrane that self-assembles into different sizes and forms in an aqueous milieu [34]. Liposomes exploited as drug delivery systems have some advantages like long circulation, wide range of techniques for high concentration drug loading and artificial preparing possibility. Although, immunocompatibility of liposomes is debatable and their targeting capability *in vivo* are not sufficient [35]. Polymeric

nanoparticles as drug delivery systems are involved in entrapment, encapsulation or incorporation of drug molecules [36]. Application of polymeric nanoparticles as a nanocarrier has the following profits: ordered and constant release of the drug while carrying, reduced toxicity and preferable drug usage. But because of the smaller size of the nanoparticles and their large surface area, particles accumulation makes physical control of nanoparticles demanding in liquid and dry shape [37].

Compared to liposomes and polymeric nanoparticles exosomes are more stable in circulation because of their endogenous source and unique surface content [38, 39]. Due to their small size and bubble shape, exosomes can move from one cell to another, release its contents through the cell membrane and link to each other [39]. Exosomes with many special characteristics appear to be a remarkable choice not only as an intercellular communicator but also a potential replacement for other nanoparticle methods as drug delivery vehicles. Due to their protein content and genetic material, biological and small drugs can be incorporated into exosomes. Exosomes as a nanocarrier have more extensive spreading in biologic fluids which probably result in a long circulating half-life and greater efficacy, and exosomes extracted from tissue-specific cells can pass through physiological barriers and access the tissue by their superficial proteins [24, 39, 40].

Despite these advantages, exosomes have some drawbacks: there are currently no manufacturing techniques or employed methods for incorporation drugs into exosomes. These disadvantages result in low drug loading capacity and retention. Finally, after *in vivo* establishment, their clearance from blood is fast [35].

Different types of drugs have been employed using exosome-based delivery to specific tissues. Most investigations are related to transfer of small interfering RNA (siRNAs), while less research has been done on the capacity of incorporation of other types of drugs [38]. Due to the presence of a bilayer lipid membrane and an aqueous core in exosomes like liposomes, both hydrophilic and lipophilic drugs could be potentially incorporated into the exosome. However, typical exosome as a nanocarrier should be modified for encapsulation of therapeutic agents by some *in vitro* approaches [38].

1.3.4 Isolation and characterization of exosomes

Exosomes are isolated from cells and biological fluids by several various principles, including ultracentrifugation, immunoaffinity, ultrafiltration, SEC, and precipitation [35]. In each technique a special feature of exosomes is employed to assist isolation, such as size, form, density or surface antigens. Obtaining more percentage of purified exosomes is the challenge of different methods [41, 42]. The principle for exosome isolation is the same for cells and biological fluids, but due to high viscosity of some fluids, they need to be diluted, and in some samples, large particles should be separated from them, moreover, using protease inhibitors to impede likely degeneration of exosomes proteins [43].

Ultracentrifugation is regarded as the gold standard for isolation of exosome [41, 42, 44]. Ultracentrifugation mainly depends on vesicle size therefore, refinement of exosomes from other extracellular vesicles such as microvesicles that are similar in exosomes is troublesome [35]. Immunoaffinity capture- based methods utilize interaction between antibodies and selective exosome surface proteins to isolate them. Compared to ultracentrifugation methods, immunoaffinity utilizes much less sample volume and extracts larger volumes of purified exosomes, regardless of vesicle size variations [35]. Size-exclusion methods are not only faster than ultracentrifugation, but also do not need specialized equipment [35, 42]. In precipitation method, exosomes can be isolated from biological fluids by changing their solubility. Different techniques apply polymers that can precipitate exosomes based on their surface features [41, 42]. In precipitation method, the results of exosome isolation in some of biological fluids are more acceptable than ultracentrifugation. Although, an important limitation of this technique is the co-precipitation of other non-exosomal particles, including the polymeric substance employed [41, 45].

Exosomes can be characterized regarding their size, protein and lipid composition. Several techniques can be applied to characterize exosomes such as flow cytometry, western blotting, nanoparticle tracking analysis, DLS, MS, and some microscopy techniques [46]. The International Society for Extracellular Vesicles (ISEV) issued a position paper in 2014, wherein the existence

of exosome-associated surface markers, also the lack of proteins not associated with exosomes, is suggested for exosome characterization. Exosomal surface markers contain TSG101, Alix, flotillin 1, tetraspanins (CD9, CD63, CD81), integrins and cell adhesion molecules [47].

Lipids are important components of exosomal membranes. Exosomes are generally enriched in cholesterol, SM, and phosphatidylserine. In exosomes, the fatty acids are mainly saturated or monounsaturated. Lipids not only have a structural function in exosomal membrane, but also are essential agents in exosome formation and release to extracellular area [48, 49]. The exosomal lipid content is consistent with the composition of a lipid bilayer. There is an asymmetry distribution of lipid classes in the PM, such that SM, other sphingolipids and PC are mainly present in the outer leaflet, whereas other classes are mostly located in the inner leaflet [50]. Therefore, exosomes are also can be characterized regarding their lipid classes and species.

1.3.4.1 Mass spectrometry

MS is one of the most powerful analytical techniques which is used in various scientific fields such as chemistry, medicine, biomedical and pharmaceutical research [51, 52]. In other words, it is an indispensable tool in different research areas due to its high sensitivity, accuracy, differentiation, and high performance [53]. Structural data of the sample are obtained by MS through calculating the mass-to-charge ratio (m/z) values of the charged molecules and tandem mass spectrometric (MS/MS) fractions. The main components of the machines are the ionization source, the mass analyzer, and the detector [54] (Figure 1-4).

Diverse ionization methods have been employed with MS such as electrospray ionization (ESI), atmospheric pressure chemical ionization (APCI) and matrix-assisted laser desorption ionization (MALDI). The results of the MS analysis are notably influenced by the ionization source [53].

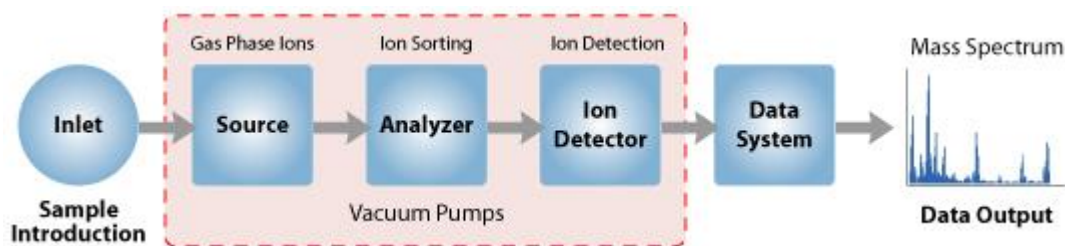


Figure 1-4 Components of a mass spectrometer. Adapted from
 (http://www.premierbiosoft.com/tech_notes/mass-spectrometry.html).(05.04.19).

The first procedure in the MS is to convert the specimen from solid or liquid state to the gaseous phase. This molecular ion typically goes through fragmentation. Each primary ionic product can be fragmented consecutively. The ions are sorted in the MS based on their mass-to-charge ratio and are identified relative to their abundance. Therefore, a mass spectrum of the molecule is formed. The result is presented as a plot of ion abundance versus mass-to-charge ratio. Thus, the ion analysis determines the character and structure of molecular precursor [55].

Regardless of the numerous advantages of the MS, there are several limitations due to the type of ion source. For instance, the streaming type of ESI implies that a sample continually is being consumed. But no mass spectrometer continually analyses ions, as a result, some of the specimen is wasted [56, 57]. The other limitation of ESI is its capability to ion inhibition results. When salt concentration in solutions is high (more than 1mM), analyte ion production is usually impeded, therefore, most biological specimens should be desalted before analysis [58]. In APC, ionization is thermodynamically controlled, and some mixtures can totally inhibit analyte ion generation. It is also difficult to analyze complex compounds in APC [58]. In MALDI, although the pulsed type of method is one origin of its sensitivity, it also causes problems when pairing to some mass analyzers. Therefore, only definite mass spectrometers are simply paired with MALDI. Besides, apply a matrix which promotes ionization, produce a great extent of chemical background to be found at m/z ratio below 500 Da. Consequently, samples with low molecular weight is generally hard to analyze by MALDI [59, 60].

1.3.4.2 Dynamic light scattering

DLS, also referred to as photon correlation spectroscopy (PCS) or quasi-elastic light scattering, is an important instrument for characterizing diffusion action of macromolecules in solution. The measurement of light scattering as a useful technique is used in several scientific fields. Special characteristic of molecules is investigated subject to the light source and detector. Typically, in a light scattering procedure a monochromator wave of light passes through a sample and the signal is detected by a suitable detector (Figure 1-5) [61].

DLS initially measures the Brownian motion of the molecules in a solution that happens because of bombardment from solvent molecules and links this movement to the size of particles. The velocity of Brownian motion of particles is influenced by their size, temperature and solvent viscosity [62]. Since, the viscosity of solvent is influenced by temperature therefore the temperature must be precisely known [63]. When particle motion is considered over a period of time, data about size of molecules are acquired, because small particles move faster, they tend to change the light frequency more than larger particles [61].

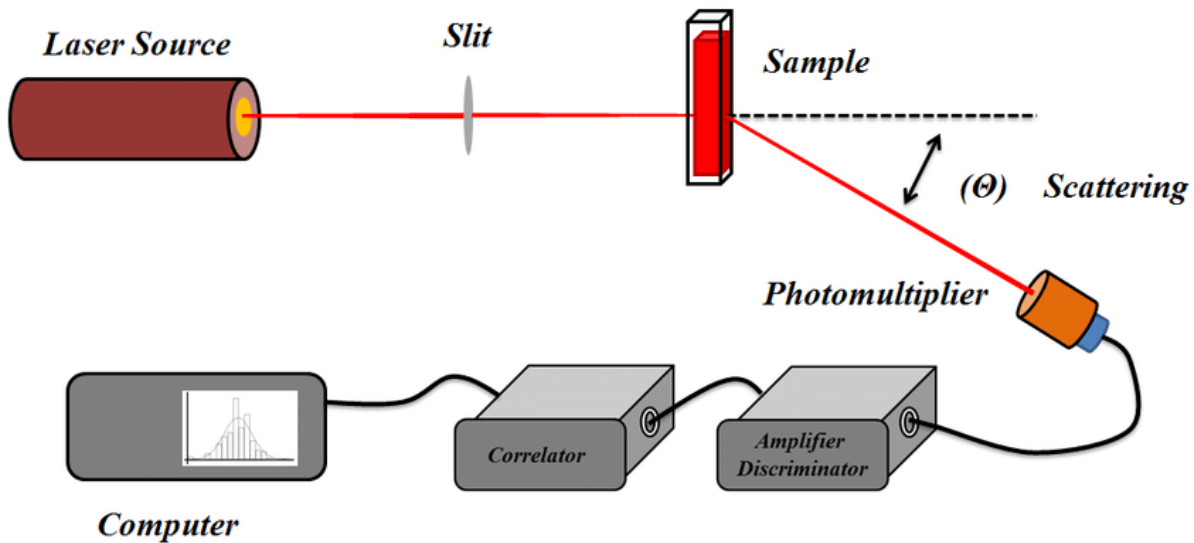


Figure 1-5 Schematic showing the instrumentation of DLS. The figure is reprinted from the PhD degree of Dhiraj Kumar, University of Minnesota Twin Cities, with permission from the author.

Since, DLS has high sensitivity and needs a small amount of sample, it is commonly employed in several scientific areas. Additionally, it is considered as the gold standard for measuring, in a rapid and precise way, size distribution of suspensions, due to the simplicity of utilize of DLS [64, 65]. Although, DLS is very practical in measuring homogenous suspensions of small particles, some disadvantages have been mentioned in the measure of compounds, because larger particles scatter more light, the smaller particles become nearly indistinguishable [66].

1.4 Liposomes

Liposomes are spherical vesicles with multilamellar or unilamellar bilayer membrane composed of cholesterol and phospholipids, the essential constituent of cell membranes. The phospholipids have a hydrophilic head and two non-polar chains (Figure1-6) [67, 68]. Their size can vary from 30 and 50 nm to several micrometers [67].

In general, all of liposomes have a compartmental construction that allows them to be involved in storage and delivery process for different materials. The application of liposomes as a carrier vehicle is due to their contents is preserved from incidents that typically occur, for instance, enzymic degeneration and chemical and immunological inactivation [69]. When the molecules of interest are introduced into the liposomes, at least one interposed lipidic layer isolates them from their area. Moreover, the lipidic structure of the liposomal membranes ensures their biocompatibility and biodegradability [70]. In addition, liposomal composition allows insufficiently soluble lipophilic and amphiphilic drugs to be better solubilized in aqueous solutions [71].

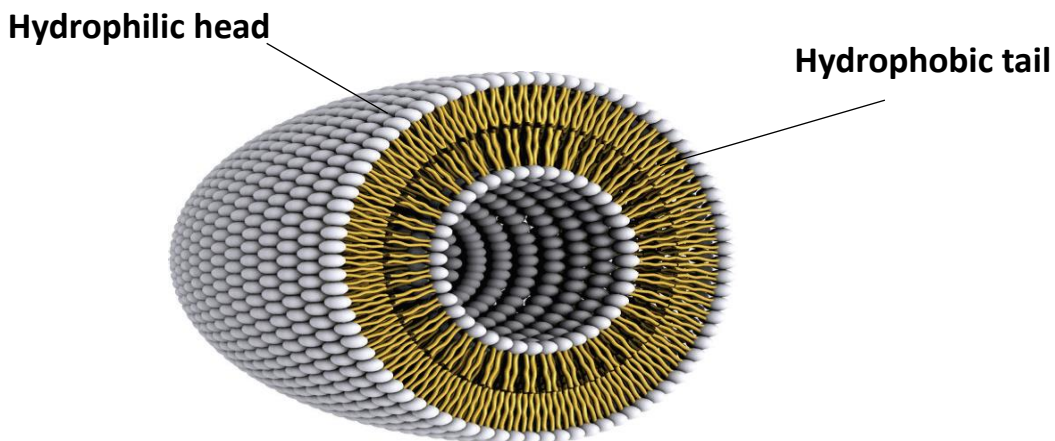


Figure 1-6 A representation of the steric organization of a liposome [69].

Because, liposomes are artificially prepared vesicles, there are different methods for nanosizing liposomes. Some of these techniques include extrusion, ultrasonication, freeze-thaw sonication (FTS), sonication and homogenization [72]. Among these methods, extrusion technique has many advantages, extrusion produces liposomes with a comparatively homogeneous size distribution, is renewable, the operation is quick, and the technique is relatively mild [73].

1.4.1 Extrusion

Extrusion is a technique by which micrometer liposomes are structurally converted to large unilamellar vesicles or nanoliposomes based on pore-size of the filters applied [74]. During extrusion the liposome suspension is moved through a membrane filter with a characteristic pore size [75]. An extruder is a machine which presses suspension through the membrane by a pump, therefore vesicles are extruded under physical force across polycarbonate filters of specified pore size [76].

Extruder (Avanti Polar Lipids, Inc.) components include gas tight or Hamilton syringes, heating block, filter support, polycarbonate membrane, internal membrane support, extruder outer casing (Figure 1-7). During the extrusion process factors such as the force used, the number of pass

through the membrane and the pore size can affect the average diameter and size distribution (polydispersity) of the produced liposomes [73, 77].

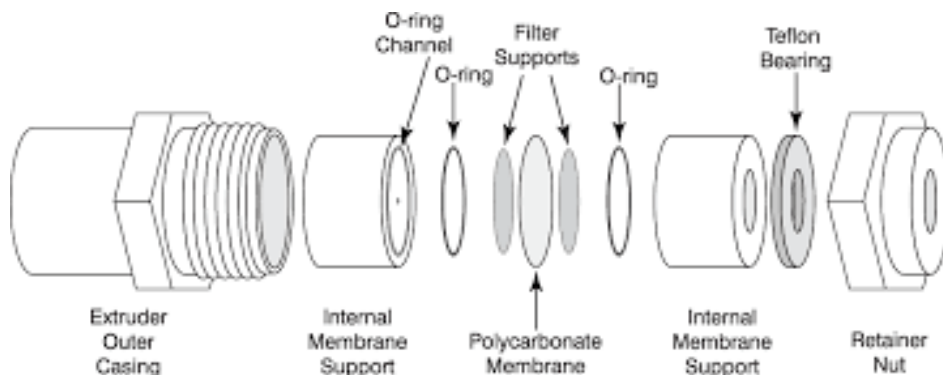


Figure 1-7 Components of a Mini Extruder. Adapted from (<https://avantilipids.com/divisions/equipment-products>).(05.04.19).

1.5 Purpose

Epilepsy is defined as the condition of frequent, unprovoked seizures. There are several methods to treat epilepsy, pharmacological treatment is one of them. In which, AEDs are prescribed for the patient to control seizures. AEDs must be able to pass through the BBB and deliver the drug to the brain to control the seizures. While the number of accessible AEDs has increased in recent years, approximately 30% of patients are resistant to pharmacological treatment. In these cases, other therapies can be effective, for instance ketogenic diet, brain surgery and vagus nerve stimulation (VNS). Surgery and VNS are not only invasive, they also involve special devices and are therefore expensive. Consequently, there is a need to establish a delivery system to develop more efficient therapy for epilepsy, which has less side effects and is accessible to all patients.

With appearance of nanotechnologies, nanoparticles have been recommended as an interesting implement to potentially improve drug delivery through the BBB. In this regard, exosomes nanosized vesicles secreted by various cells, demonstrate an essential tool for therapeutic plans. Considering that exosomal carriers can afford advantages of both cell-based drug delivery and nanotechnology, interest in utilizing exosomes for therapeutic purposes has increased quickly in latest years. Exosomes can travel from one cell to another, readily pass their contents across the

cell membrane owing to their specific features and deliver their contents in a biologically active form. Noticeable, exosomes can pass through biological barriers including the BBB. Exosomes have been employed to carry small molecules, proteins and nucleic acids to cross the BBB. The

main advantage of exosomes against other artificial nanoparticles is their non-immunogenic character, causing a long and lasting circulation. Nevertheless, essential complications and impediments are present for exosomes as a drug carrier, containing exosome donor cell selection, loading process improvement, formulation purification, and toxicity and pharmacokinetic studies.

The aim of this study is to investigate the feasibility of using exosomes as a nano-carrier in the drug delivery system to treat epilepsy. For this purpose, exosomes was isolated from blood plasma and then characterizes in terms of their size and lipid content. Furthermore, PBECs were isolated to serve as an *in vitro* BBB model. The exosome-based liposomes were then synthesized and characterized to test in the BBB model. I hope this project as a part of the larger drug delivery system study, will aid in providing a therapeutic approach with minimal side effects and accessible to all epileptic patients.

Chapter 2

Methods and materials

2.1 Materials

2.1.1 Cell culture

PBECs were used in the present study, for this purpose, pig brains were prepared from Horsens Slaughterhouse and then isolation of brain capillaries and cell culture were performed in the Center for Organelle Research (CORE) laboratories. Reagents that were used in cell isolation and cell culture are summarized in Table 2-1 and Table 2-2 respectively.

Table 2-1 Reagents used in Cell isolation.

Compound	Concentration	Use	Manufacturer	Cat number
DMEM/F12	450 ml	Cell isolation	biowest	L0093_
penicillin/streptomycin	1%	Culture medium	Merck	A2212
Trypsin/ EDTA	10%	Digestion medium	Sigma	T4049
Sterile PBS	500 ml	Washing&Storage	-	-
Sterile DMSO	10%	Freezing medium	-	-

Table 2-2 Reagents used in Cell culture.

Compound	Concentration	Use	Manufacturer	Cat number
DMEM(1X+GlutaMAX)	17.3 ml	Cell culture	gibco	3196-021
Collagen I, Rat Tail	300 µg/ml	Coating	gibco	A10483-01
Fibronectin	1 µg/ml	Coating	Corning	354008
DPBS	10%	Culture medium	HyClone	SH30028.02
Heparin	1%	Culture medium	Sigma	H3149
penicillin/streptomycin	1%	Culture medium	Merck	A2212
Puromycin	4 µg/ml	Culture medium	Sigma	P8833
Hank's PBS	1X	Washing	PAA	H15-008
Distilled Water	-	Culture medium	gibco	15230-071

2.1.2 Liposomes

Reagents and phospholipids that were used to prepare liposomes, are summarized in Table 2-3.

Table 2-3 Reagents and phospholipids used to prepare liposomes

Compound	Concentration	Use	Manufacturer	Cat number
Phosphatidylcholine	2.5 mg/ml	Liposome	Avanti Polar	850356P
Sphingomyelin	2.5 mg/ml	Liposome	Sigma	85615
Phosphatidylethanolamine	10 mg/ml	Liposome	Sigma	P7943
Chloroform	10 ml	Solvent	Merck	102445
Sterile Distilled water	-	Solvent	-	-

2.1.3 Exosomes isolation

In this study exosomes were isolated from blood plasma samples that were prepared from Stavanger Hospital. Exosome isolation was performed by Izon qEV columns.

The materials will be as the following:

- Blood plasma
- Degassed Ethanol 20 %
- Degassed PBS 1x
- Izon qEV columns

2.2 Methods

2.2.1 Cell culture

In this study PBECs were utilized as an *in vitro* BBB model to study of drug delivery to the brain by exosomes. First, brain capillaries were isolated. All the following methods were performed according to aseptic technique. All procedures were performed in a biosafety cabinet which was sterilized before and after work with an 70% ethanol solution and UV light decontamination. All solutions, media and equipment were first sterilized and then placed inside the cabinet.

2.2.1.1 Isolation of brain capillaries

Ten porcine brains were used in the present study. At first the meninges were removed from the brain. For this purpose, the washing and the storage beakers were placed on ice inside the cabinet. Initially, the brain was washed gently with PBS and then the meninges were removed from the brain by a sterile fine-tip curved forceps. The clean brain was transferred to the storage beaker containing PBS. (Figure 2-1). This procedure was repeated with all the brains.

The gray matter from the brain was scraped with a sterile scalpel. In this process white matter was not gotten as much as possible. The gray matter was transferred to a petri dish with 5-10 ml DMEM/F12-comp. When the petri dish was full, the content was transferred to a 500 ml flask which was on the ice.

To homogenize the material, the grinder tube was filled to the limit and were made 8 down/up strokes with the loose pestle and 8 down/up strokes with the tight pestle. The homogenate was transferred to the new 500 ml flask and the procedure was repeated with the rest of the material. The homogenate was diluted to approximately 450 ml with DMEM/F12-comp.

In the next step, the homogenate was filtered and then transferred to the petri dishes with digestion media. The dishes were incubated on a shaker at 37 degrees for one hour.

The media with the material from the dishes were transferred to the tubes (50 ml) and each dish was washed with 10 ml DMEM/F12-comp. The tubes were centrifuged at 4°C, 250g for five minutes, then the supernatant was removed and each of the pellets resuspended in 10 ml DMEM/F12-comp. Centrifugation has been repeated twice. The tubes were incubated on ice for five minutes after the last resuspension. Then the supernatant from each tube was carefully transferred into the new tubes, centrifuged at 4°C, 250g for five minutes. The supernatant was removed, and the pellets resuspended in a total of 7-9 ml freezing media. The cell suspension (1 ml) was transferred to each of the labeled cryo- tubes, placed overnight in a freezing box at (-80° C) and then moved to the liquid nitrogen tank the next day for long-term storage.

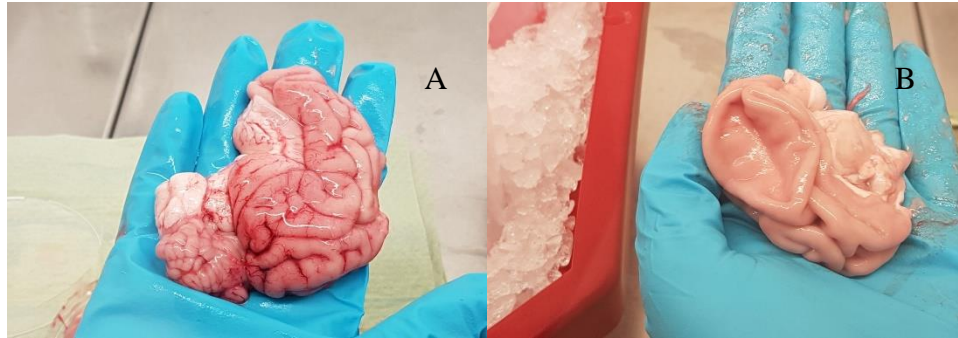


Figure 2-1 A: the brain before removing the meninges, B: the brain after removing the meninges.

2.2.1.2 Resuscitation of frozen cell line

In the beginning, 1ml of prewarmed collagen at room temperature was diluted with 9 ml PBS, then two T75 flasks were coated with 5ml of 300 μ g/ml collagen and incubated at 37°C overnight. But since collagen was completely dried in the flask after 24 hours, the coating was repeated the next day and the flasks were incubated for two hours. Collagen was aspirated, and the flasks were washed twice with 4ml HBSS. Then prewarmed fibronectin (1 μ g/ml) was added, 4 ml to each flask, the flasks were incubated at room temperature for two hours. Fibronectin was removed and the flasks were washed twice with 4 ml HBSS, the second HBSS wash was not removed.

The cryotube comprising PBECs (Batch I) was thawed quickly (twisting quickly in hand). The thawed PBECs were added gently drop-wise into the 20 ml prewarmed medium (at 37°C), that was prepared the same day. The last HBSS wash was removed from the flasks, 10 ml of medium with cells were added to each flask and kept in a humidified 37°C, 5% CO₂ incubator for three days. To prevent cell contamination, the flasks were stored in the incubator in a special box.

After three days, cell cultures were monitored by a microscope. But because the cells had poor viability, the culture medium was changed and incubated. Next day cultures were microscopically controlled for cell viability.

Resuscitation of frozen cells was repeated with another batch of PBECs (Batch II). The media were changed for each flask the next day, and the flasks were incubated for six days. During this period, the flasks were microscopically controlled, and the media were changed after four days.

Resuscitation of frozen cells was repeated with Batch II of PBECS. The flasks were incubated for seven days and after four days the culture medium was renewed. During incubation, cultures were monitored in terms of contamination and cell viability by a microscope. It should be noted that new medium has been used in all processes.

2.2.2 Liposomes preparation

Liposomes were prepared by extrusion method. Briefly 2.5 mg of PC was dissolved in 1 ml of distilled water. Extrusion was carried out under distinct circumstances. First, the suspension was sequentially extruded 11 times through a 100 nm polycarbonate filter at 25°C by an Avanti mini extruder (Figure 2-2). Then, the suspension was extruded 16 times, but other conditions were like the past one. The suspension was also extruded 11 and 16 times through a 100 nm polycarbonate filter at phase transition temperature (T_m) 41°C.



Figure 2-2 Avanti mini extruder device. adapted from (<https://avantilipids.com/divisions/equipment-products>).(10.04.19).

To prepare the next phospholipids PC – SM, 2.5 mg of SM was dissolved in 1 ml of distilled water. SM is soluble in chloroform and methanol, but as these substances can harm the Hamilton syringes of the device's, distilled water has been used as a solvent. Therefore, the SM suspension was intensively vortexed to be well dissolved. Then, 200 μ l of SM with 800 μ l of PC, which was already ready, were mixed. The mixture was extruded 20 times through a 100 nm polycarbonate filter at 41°C. Repeated liposome preparation with PC and PC – SM combination, using a 50 nm polycarbonate filter.

A concentration of 10mg/ml of phosphatidylethanolamine (PE) in chloroform was prepared to preparation of other phospholipids, a mixture of PC-SM and PE. The mixture of PC-SM-PE was extruded at 41°C through a 50 nm polycarbonate filter with a 30 times exclusion cycle number. This experiment was repeated; thus, 2.5 mg of SM was dissolved in 1 ml of chloroform. Then the mixture of PC-SM-PE was then extruded at 63°C (T_m of PE) through a 50 nm polycarbonate filter.

2.2.2.1 Sonication

The liposomal suspensions were sonicated respectively: PC (2.5mg/ml), and the mixture of PC-SM-PE was sonicated respectively. The lipid solution was placed in a round- bottomed plastic tube and sonicated at the condition such as a pulse of 60s on and 60s off, on ice in ten cycles, at an amplitude of 20%.

2.2.3 Exosomes isolation

In this study exosomes were isolated by SEC method, using Izon qEV columns (Figure 2-3).



Figure 2-3 EV original size exclusion column. Adapted from (<https://www.izon.com/exosome-isolation/qevoriginal>). (10.04.19).

Human plasma has been used as a sample. First, plasma was removed from the freezer (-80°C) and was heated at room temperature on the ice, to be fully thawed. The plasma (500µl) was then centrifuged at 4°C twice and once for 15 minutes at a speed of 2500 rpm.

The column was placed in a holder and checked vertically. The top cap was removed carefully and degassed ethanol 20% was removed gently from the beads in the column. It should be noted, degassed ethanol 20% is used as a bacteriostatic to store the column at 4°C to 8°C. In order to column equilibration, the lower cap was removed, and the column was rinsed with at least 12 ml of elution buffer (Degassed PBS 1x). Then, the buffer was removed from the top of filter with the bottom cap on, after that plasma (500µl) was loaded and immediately the bottom cap was removed and promptly the fractions were collected (0.5 ml). Elution buffer was added as the last plasma just entered the top filter of the column. Generally, the first six fractions do not contain vesicles, therefore, are usually not analyzed. Finally, the column was rinsed with 20 ml PBS, then the bottom cap was put and 2ml of degassed ethanol 20% was added to the top filter of the column, the top cap was put, and the column was returned to the refrigerator.

2.2.4 Dynamic light scattering

A Zetasizer Nano ZS (Malvern Instrument Inc.) was used to characterize the particle size by dynamic light scattering. In this study, liposomes and exosomes were measured by DLS. To characterize of liposomes, a cuvette (ZEN 2112) was used with a sample volume of 100µl, at specific phase transition temperature. Size was measured at standard setting for vesicles using three cycles at three minutes.

To characterize of exosomes, a cuvette (ZEN 2112) was used with a sample volume of 100µl, at 25°C. Size was measured at standard setting for vesicles using three cycles at three minutes. The measurement was subsequently analyzed with Malvern Zetasiser software which processes the measurement data to produce the results.

2.2.5 Mass spectrometry

In the present study, mass spectrometry was used for lipid analysis in exosomes. The experiment was conducted at the university of Bergen.

In this study three fractions, tenth fraction (F10), eleventh fraction (F11) and twelfth fraction (F12) which had been collected from exosome isolation, were examined by MS. Two samples (F10, F11) were examined in five runs (R1-R5), and F12, was examined in three runs (R1-R3) by MS. Based on the charge of ions identified on MS, some lipids are better identified in positive mode and some of them in negative mode. Therefore, there were two folders (positive and negative) for each sample and both folders were interpreted together to analyze the results. The Lip Mat files included a file contains identified lipid species, which are sorted by highest score. Score more than 30, is relatively confident lipid species identification, however, this information was also confirmed by a manual check of fragmentation figures. The following files contain the abundance of fatty acids components of each headgroup in the sample, area for each distinctive fatty acid chain in one lipid group and region from chromatogram for each unique lipid. Furthermore, five most abundant fatty acid chains were plotted in a diagram and five most abundant individual lipid species were shown in a chromatogram.

Regarding Lip Mat data, each sample was analyzed in each run and in both positive and negative modes. Lipid headgroups included: PC, SM, PE, and phosphatidylinositol (PI). After comparing the results of the identified lipid species file with abundant individual lipid species chromatogram, lipid species with a score less than 30 were recognized. Moreover, the abundance of fatty acid chains for each headgroup in the sample, was determined.

Chapter 3

Results

3.1 Characterization of exosomes by DLS

Exosomes were isolated by SEC. Fractions collected were measured by DLS. Because, the first six fractions are the void volume which does not contain exosomes, is usually not analyzed. Therefore, the fractions from seven to twelve were analyzed. The results are displayed in Table 3-1 and Figure 3-1. Parameters that have been measured include average size (Z-average), polydispersity index (PDI), and standard deviation (Std Dev). Std Dev of PDI (0.08-0.7), is the range over which the distribution algorithms best operate over. All fractions showed PDI less than 0.7, however, according to size distribution and Z-average, the result of tenth fraction (F10) is more acceptable.

Table 3-1 Exosome isolation results, the fractions from seven to twelve (F7-F12). Based on size and size distribution of each of isolated exosome fraction.

Exosome Isolation	F7	F8	F9	F10	F11	F12
Zaverage (d. nm)	158.2±11.43	116.1±0.7095	87.31±0.7831	66.7±0.0557	54.5±0.2007	49.82±2.721
PDI- Value	0.314±0.049	0.237±0.007	0.237±0.005	0.237±0.003	0.224±0.002	0.261±0.054

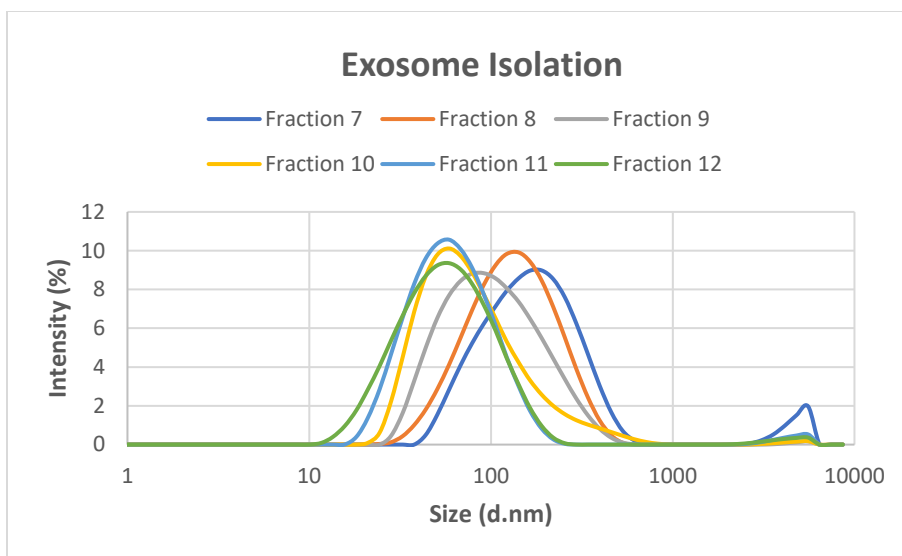


Figure 3-1 The intensity distribution result of exosome isolation. Fractions of seven to twelve (F7-F12) are determined.

3.2 Characterizing of exosomes with mass spectrometry

Mass spectrometry progressively being utilized to identify the structure of biomolecules. In this study lipid contents of exosomes were characterized using MS.

Most abundant lipid species for each sample were determined and the results are summarized in Tables 3-2, Table 3-3 and Table 3-4. For each headgroup, the lipid species that had a high abundance in the chromatogram but scored less than 30 in the identified lipid species file, were listed in red on the tables. As shown in the tables, most lipid species were identified in the positive mode and in most cases, the lipids identified in the negative mode have score of less than 30, which means low reliability in the identification. In all samples the most abundant PC lipid was PC 16:0/18:1 sodium adduct (PC+Na 16:0/18:1). This conclusion was confirmed by comparing the PC chromatogram and the identified lipid species file, this lipid is in the first place in the identified lipid species list with a score 50, its number of hits is two which means it has been found two times.

In SM headgroup, the most abundant SM lipid is SM d22:1/15:1 potassium adduct (SM kd22:1/15:1) in the SM chromatogram, but this lipid has a score 21 in the identified lipid species

file. In addition, in the fragmentation figure only headgroup fragment has been identified. These facts indicate that SM kd22:1/15:1 is probably not the most abundant SM lipid species, and it is misidentified with a lipid which produces resembling fragments. The second SM species in the chromatogram is SM 14:1/20:1 sodium adduct (SM+Na 14:0/20:1) with the much lower area, however, this lipid has a score 48.9 in the identified lipid species file, which is a reliable identification. We thus concluded that SM+Na 14:0/20:1 is the most abundant SM lipid species in this study.

PE species are only detected in F10 and F11, based on chromatogram PE 16:0/23:4 sodium adduct (PE+Na 16:0/23:4) is the most abundant PE lipid, however, this lipid has a score about 20 in the identified lipid species file, which reflects low reliability in identification. On the other hand, PE 18:0/20:4 sodium adduct (PE+Na 18:0/20:4), has a score 35, which means confident identification, though with the much lower area in the chromatogram.

In PI species, PI 18:0/20:4 sodium adduct (PI+Na 18:0/20:4), is the most abundant PI lipid in samples F10 and F11, compared to chromatogram and the identified lipid species file. However, in F12, PI species was only detected in one run, and it was PI Lyso+Na 18:0/0:0 with score nearly 23, which means low confident in the identification. It should be noted that, Phosphatidic acid (PA) species, was only detected in sample F11 and only in one run in the negative mode.

The abundance of fatty acid chains of each headgroup in the sample have analyze, considering area for each specific fatty acid chains in one lipid headgroup. After calculating the abundance and drawing the chart, the results are summarized in Tables 3-5, 3.6 and 3-7.

Table 3-2 Most abundant lipid species in the fraction 10(80 nm) in positive (Pos) and negative (Neg) modes.

F10 80 nm Pos Mode	Run 1	Run 2	Run 3	Run 4	Run 5
PC species	PC+Na 16:0/18:1 PC+Na 16:0/18:2 PC+H 16:0/18:1 PC+H 16:0/18:2 PC+Na 16:0/20:4	PC+Na 16:0/18:1 PC+Na 16:0/18:2 PC+H 16:0/18:2 PC+Na 16:0/20:4 PC+Na 16:0/20:2	PC+Na 16:0/18:1 PC+H 16:0/18:1 PC Lyso+Na 16:0/0:0 PC Lyso+H16:0/0:0 PC+Na 16:0/18:2	PC+Na 16:0/18:1 PC+Na 16:0/18:2 PC+H 16:0/18:1 PC+H 16:0/18:2 PC+Na 16:0/20:4	PC+Na 16:0/18:1 PC+H 16:0/18:1 PC+Na 16:0/18:2 PC Lyso+Na 16:0/0:0 PC Lyso+H16:0/0:0
SM species	SM+kd 22:1/15:1 SM+Nad 14:0/20:1 SM+kd 14:0/27:6 SM+Nad 14:0/28:2 SM+Nad 16:1/26:2	SM+kd 15:0/22:2 SM+Nad 14:0/20:1 SM+Na d 18:0/24:2 SM+Nad 14:0/28:2 SM+Nad 15:0/25:2	SM+Nad 14:0/20:1 SM+Nad 14:0/28:2 SM+Nad 14:0/28:3 SM+Nad 17:0/23:2 SM+NH4d14:0/29:6	SM+kd 14:1/23:1 SM+Kd 15:2/24:2 SM+Nad 14:0/20:1 SM+Nad 14:0/28:2 SM+Nad 15:0/27:3	SM+Nad 15:0/19:1 SM+Nad 19:0/23:2 SM+Nad 19:0/23:3 SM+Nad 16:0/24:1 SM+Nad 14:0/20:2
PE species	PE+Na 16:0/23:4 PE+Na 18:0/20:4	PE+Na 16:0/23:4		PE+Na 18:0/23:4 PE+Na 17:1/19:1 PE+Na 18:0/20:4	PE+Na 16:0/23:4
PI species	PI+Na 18:0/20:4 PI+Na 16:0/20:4	PI+Na 18:0/20:4 PI+Na 16:0/20:4	PI Lyso+Na 18:0/0:0 PI Lyso+Na 16:0/0:0	PI+Na 18:0/20:4 PI+Na 16:1/20:4	PI Lyso+Na 18:0/0:0 PI+Na 18:0/20:4 PI+Na 10:0/26:2 PI+Na 10:0/24:1 PI Lyso+Na 16:0/0:0
Neg Mode					
PC species	PC-CH3CO2 16:0/18:2 PC-CH3CO2 18:1/18:2				
SM species	SM-CH3CO2d 14:0/20:1		SM-CH3CO2d 14:0/20:1	SM-CH3CO2 d14:0/20:1	
PE species	PE Lyso-H 16:0/0:0				
PI species	PI-H 18:0/20:4 PI Lyso-H 18:0/0:0	PI-H 18:0/20:4	PI Lyso-H 18:0/0:0	PI-H 18:0/20:4 PI Lyso-H 18:0/0:0	PI Lyso-H 18:0/0:0 PI -H 18:0/20:4

Table 3-3 Most abundant lipid species in the fraction 11(65 nm) in positive (Pos) and negative (Neg) modes.

F11 65 nm Pos Mode	Run 1	Run 2	Run 3	Run 4	Run 5
PC species	PC Lyso+H16:0/0:0 PC Lyso+Na 16:0/0:0 PC+Na 16:0/18:1 PC+H 16:0/18:1 PC Lyso+H18:0/0:0	PC+Na 16:0/18:1 PC+H 16:0/18:1 PC+Na 16:0/18:2 PC+H 16:0/18:2 PC Lyso+H16:0/0:0	PC+Na 16:0/18:1 PC+Na 16:0/18:2 PC+H 16:0/18:1 PC+H 16:0/18:2 PC+Na 18:0/18:2	PC+Na 16:0/18:1 PC+Na 16:0/18:2 PC+H 16:0/18:1 PC+H 16:0/18:2 PC+Na 16:0/20:2	PC+Na 16:0/18:1 PC Lyso+H 16:0/0:0 PC Lyso+Na 16:0/0:0 PC Lyso+H 18:0/0:0 PC+Li 10:2/27:5
SM species	SM+kd 16:0/21:1 SM+Nad 14:0/20:1 SM+Nad 16:0/26:2 SM+Nad 15:2/25:5 SM+Nad 17:0/23:6	SM+kd 17:0/20:1 SM+Nad 14:0/20:1 SM+Nad 14:0/28:2 SM+Nad 14:0/28:3 SM+Nad 15:0/25:2	SM+kd 16:1/21:1 SM+kd 21:0/16:2 SM+Nad 15:0/19:1 SM+Nad 14:0/28:2 SM+Nad 14:0/28:3	SM+kd 16:0/21:2 SM+Nad 14:0/20:1 SM+Nad 14:0/28:2 SM+Nad 15:0/27:3 SM+Nad 14:0/26:2	SM+Nad 14:1/20:0 SM+Nad 14:0/28:2 SM+Nad 14:0/26:2 SM+Hd 17:0/25:4 SM+Nad 14:0/20:2
PE species		PE+Na 16:0/23:4	PE+Na 16:0/23:4 PE Lyso+H 18:0/0:0	PE+Na 16:0/23:4 PE+Na 10:0/28:4	
PI species	PI Lyso+Na 18:0/0:0 PI Lyso+Na 16:0/0:0 PI+Na 11:0/23:1	PI Lyso+Na 18:0/0:0 PI+Na 18:0/20:4 PI+Na 13:0/23:2 PI+Na 10:0/24:1 PI Lyso+Na 16:0/0:0	PI+Na 18:0/20:4 PI Lyso+Na 18:0/0:0 PI+Na 16:0/20:4	PI+Na 18:0/20:4 PI+Na 16:0/20:4 PI Lyso+Na 18:0/0:0	PI Lyso+Na 18:0/0:0 PI Lyso+Na 16:0/0:0
Neg Mode					
PC species				PC-CH3CO2 18:0/20:3	
SM species	SM-CH3CO2 d14:0/20:2 SM-CH3CO2 d14:0/20:2 SM-CH3CO2 d14:0/18:1	SM-CH3CO2 d14:0/20:2 SM-CH3CO2 d14:0/20:2 SM-CH3CO2 d14:0/18:1	SM-CH3CO2 d14:0/20:2 SM-CH3CO2 d14:0/18:1	SM-CH3CO2 d14:0/20:1	SM-CH3CO2 d14:0/20:1
PE species	PE Lyso-H 18:0/0:0		PE Lyso-H 18:0/0:0 PE Lyso-H 16:0/0:0		PE Lyso-H 20:0/0:0
PI species	PI Lyso-H 18:0/0:0 PI Lyso-H 16:0/0:0 PI Lyso-CH3CO2 20:3/0:0	PI Lyso-H 18:0/0:0 PI-H 18:0/20:4 PI Lyso-H 16:0/0:0	PI-H 18:0/20:4 PI Lyso-H 18:0/0:0 PI-H 16:0/20:4 PI Lyso-H 16:0/0:0	PI-H 18:0/20:4 PI-H 16:0/20:4 PI Lyso-H 18:0/0:0	PI Lyso-H 18:0/0:0 PI Lyso-H 16:0/0:0
PA species	PA Lyso-H 18:0/0:0				

Table 3-4 Most abundant lipid species for fraction 12 (55 nm) in positive (Pos) and negative (Neg) modes.

F12 55 nm Pos Mode	Run 1	Run 2	Run 3
PC species	PC+Na 16:0/18:1 PC+Na 16:0/18:2 PC+Na 18:0/18:2 PC+H 16:0/18:2 PC+Na 16:0/20:4	PC Lyso+Na 16:0/0:0 PC+Na 16:0/18:1 PC Lyso+Na 18:0/0:0 PC+Li 10:2/27:5 PC+Na 11:0/25:1	PC+Na 17:0/17:2 PC+H 20:2/18:5 PC+Na 24:0/12:1
SM species	SM+Kd 14:0/23:2 SM+Nad 14:0/28:2 SM+Nad 20:0/14:1 SM+Nad 14:0/28:3 SM+Nad 14:0/26:2	SM+Nad 14:0/20:1 SM+Nad 14:0/28:2 SM+Nad 14:0/26:2 SM+Nad 14:0/26:1 SM+Nad 15:0/27:3	SM+Nad 14:0/20:1
PE species			
PI species		PI Lyso+Na 18:0/0:0	
Neg Mode			
PC species			
SM species			
PE species			
PI species	PI-H 18:0/20:4	PI Lyso+H 18:0/0:0	

Table 3-5 Most abundant fatty acid (FA) chains of each headgroup in the fraction 10 (80 nm) in positive (Pos) and negative (Neg) modes.

F10 80 nm Pos Mode	Run1	Run 2	Run 3	Run 4	Run 5
PC- FA	16:0 18:1 18:2 20:4 20:2	16:0 18:1 18:2 20:4 20:2	18:1 16:0 18:2 17:5 10:0	18:1 16:0 18:2 19:3 20:4	18:1 16:0 18:2 11:5 18:0
SM- FA	22:1 d22:1 15:1 d14:0 20:1	d15:0 22:2 d14:0 20:1 d18:0	d14:0 20:1 28:2 28:3 d17:0	d14:1 23:1 d15:2 24:2 d14:0	d15:0 19:1 d19:0 23:2 23:3
PE- FA	23:4 16:0 20:4 18:0	23:4 16:0		23:4 18:0 19:1 17:1 20:4	23:4 16:0
PI -FA	20:4 18:0 16:0	20:4 18:0 16:0	18:0 16:0	20: 4 18:0 16:0	18:0 20:4 26:2 10:0 24:1
Neg Mode					
PC- FA	18:2 16:0 18:1				
SM -FA	d14:0 20:1		d14:0 20:1	d14:0 20:1	
PE- FA	16:0				
PI- FA	20:4 18:0	20:4 18:0	18:0	20:4 18:0	18:0 20:4

Table 3-6 Most abundant fatty acid (FA) chains of each headgroup in the fraction 11 (65 nm) in positive (Pos) and negative (Neg) modes.

F11 65 nm Pos Mode	Run 1	Run 2	Run 3	Run 4	Run 5
PC- FA	16:0 18:1 18:0 22:1 13:4	18:1 16:0 18:2 22:4 13:1	18:1 16:0 18:2 18:0 17:4	18:1 16:0 18:2 20:2 20:4	18:1 16:0 18:0 27:5 10:2
SM- FA	d16:0 21:1 d14:0 20:1 26:2	d17:0 20:1 d14:0 28:2 28:3	21:0 16:1 d16:1 d21:0 16:2	d16:0 21:2 d14:0 20:1 28:2	d14:1 20:0 d14:0 28:2 26:2
PE- FA		23:4 16:0	23:4 16:0 18:0	23:4 16:0 28:4 10:0	
PI -FA	18:0 16:0 23:1 11:0	18:0 20:4 23:2 13:0 24:1	20:4 18:0 16:0	20:4 18:0 16:0	18:0 16:0
Neg Mode					
PC- FA				20:3 18:0	
SM -FA	d14:0 20:1 20:2 18:1	d14:0 20:1 20:2 18:1	d14:0 20:1 18:1	d14:0 20:1	d14:0 20:1
PE- FA	18:0		18:0 16:0		20:0
PI- FA	18:0 16:0 20:3	18 20:4 16:0	20:4 18:0 16:0	20:4 18:0 16:0	18:0 16:0
PA-FA	18:0				

Table 3-7 Most abundant fatty acid (FA) chains of each headgroup in the fraction 12 (55 nm) in positive (Pos) and negative (Neg) modes.

F12 55 nm Pos Mode	Run 1	Run 2	Run 3
PC- FA	16:0 18:1 18:2 18:0 20:4	16:0 18:1 18:0 27:5 10:2	17:2 17:0 20:2 18:5 24:0
SM- FA	d14:0 23:2 28:2 d20:0 14:1	d14:0 20:1 28:2 26:2 26:1	d14:0 20-1
PE- FA			
PI -FA		18:0	
Neg Mode			
PC- FA			
SM -FA			
PE- FA			
PI- FA	20:4 18:0	18:0	

3.3 Characterization of liposomes by DLS

The average size and size distribution are essential factors in characterization of liposomes. DLS is one of the available methods for determining the liposome size and size distribution. The results of PC extrusion are summarized in Table 3-8. and Figure 3-2. The DLS measurement showed a relative difference between the extruded PC at 41°C and at 25 °C. While the extruded PC at 41°C showed a Z-average of 131.9 nm, the extruded PC at 25 °C showed a Z-average of 133.5 nm. Therefore, the more homogenous PC is shown in Figure 3-2 B. Although a minimum of eleven pass through the extruder membrane is recommended for most lipid, but the DLS measurement showed that the size of liposomes was decreased when the number of extrusion cycle was increased.

Table 3-8 Results of size and size distribution for PC extruded at 25°C and 41 °C, with extrusion cycle 11 and 16 times through a 100 nm polycarbonate filter.

PC 16:0 (2.5 mg/ml)	25°C, 11 times Ex	25°C, 16 times Ex	41°C, 11 times Ex	41°C, 16 times Ex
Z-average (d. nm)	133.5±6.987	121.1±6.987	131.9±4.967	122.8±4.967
PDI-Value	0.185±0.003	0.131±0.003	0.137±0.013	0.124±0.013

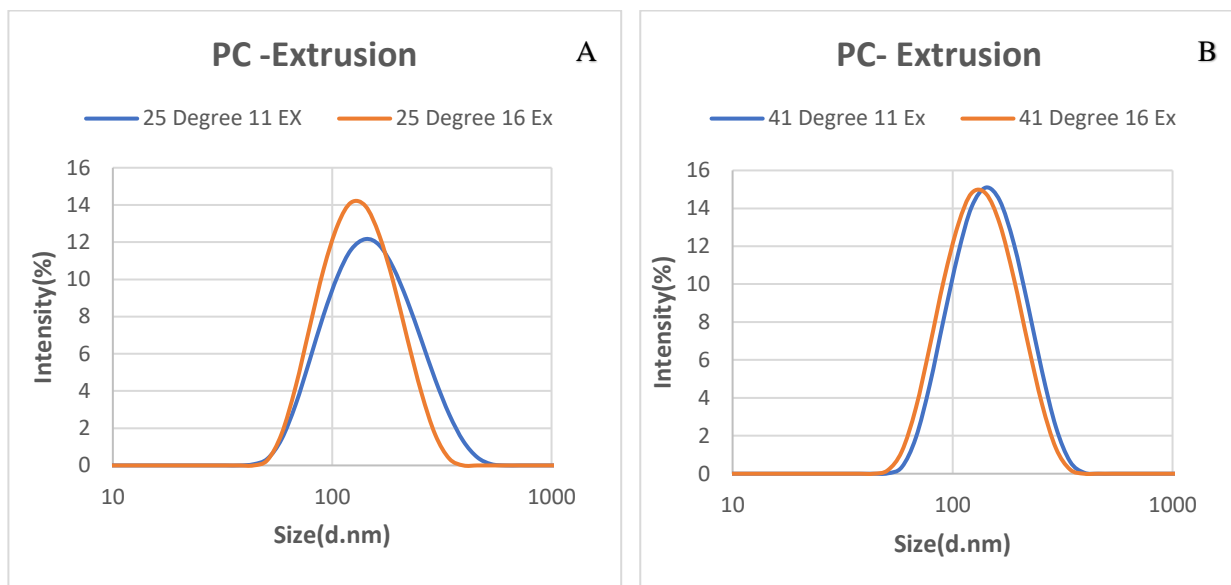


Figure 3-2 The intensity distribution result for PC. A: Extruded at 25°C and extrusion cycle 11 and 16 times through the filter. B: Extruded at 41°C and extrusion cycle 11 and 16 times through the filter.

Preparation of liposome with PC was repeated using a 50 nm polycarbonate filter. The DLS measurements showed a significant difference between liposomes that were extruded with two different membranes. The extrusion results are presented in Table 3-9 and Figure 3-3. The liposomes extruded through a 50 nm polycarbonate filter, are smaller in diameters and more homogenous.

Table 3-9 Results of size and size distribution for PC extruded through polycarbonate membranes 50 nm and 100 nm.

PC 16:0 (2.5 mg/ml)	Extruder membrane (100 nm)	Extruder membrane (50 nm)
Z-average (d. nm)	122.8±4.967	83.19±0.5484
PDI-Value	0.124±0.013	0.094±0.009

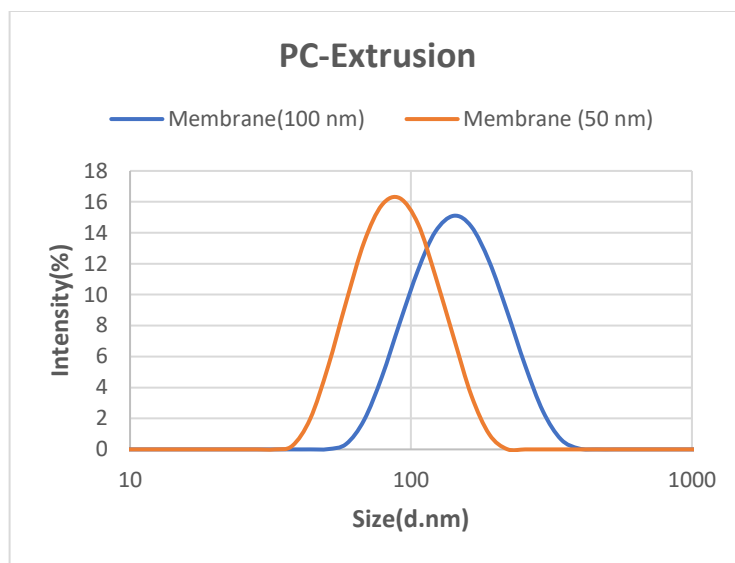


Figure 3-3 The intensity distribution result for PC extruded through polycarbonate membranes 50 nm and 100 nm.

The next phospholipid was a PC-SM combination. The results of PC-SM extrusion at 41°C, through the extruder membranes 50 nm and 100 nm, are presented in Table 3-10 and Figure 3-4. The z-average and PDI- values show a meaningful difference in the characteristic of the produced liposomes. Therefore, a 50 nm filter was considered in liposome preparation.

Table 3-10 Results of size and size distribution for PC-SM combination, extruded through polycarbonate membranes 50 nm and 100 nm.

PC -SM (2.5 mg/ml)	Extruder membrane (100 nm)	Extruder membrane (50 nm)
Z-average (d. nm)	122.7±1.35	82.51±0.2052
PDI-Value	0.159±0.01	0.103±0.008

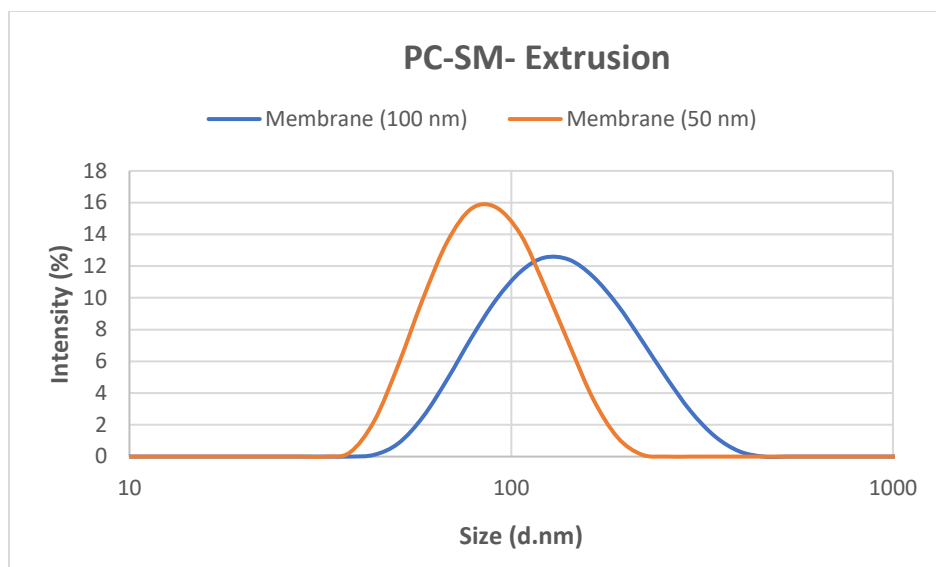


Figure 3-4 The intensity distribution result for (PC-SM) extruded through polycarbonate membranes 50 nm and 100 nm.

The other liposome was a PC-SM-PE combination. The suspension was extruded at 41°C and at 63 °C. The results are displayed in Table 3-11 and Figure 3-5. According to the size distribution analysis, at 41°C, three peaks are observed and at 63 °C, two peaks are shown (Figure 3-5), indicating the presence some large particles. The PC-SM-PE suspension was clearly aggregated and significantly larger in size. It should be noted that the mean intensity values in the table are the sum of the peaks. The extruded liposome at 41°C showed a Z-average size of 524 nm and PDI-value 0.621, and the extruded liposome at 63°C had a Z-average size of 1564 nm and PDI -value of 0.659. In other words, although the size of the extruded liposome at 41°C, had a smaller size, according to the graph, the liposomes extruded at 63°C had more homogeneity.

Table 3-11 Results of size and size distribution for PC-SM -PE combination, extruded at 41°C and at 63 °C.

PC-SM-PE	Tm (41°C)	Tm (63°C)
Z-average (d. nm)	524±20.33	1564.3±34.08
PDI-Value	0.621±0.045	0.659±0.05

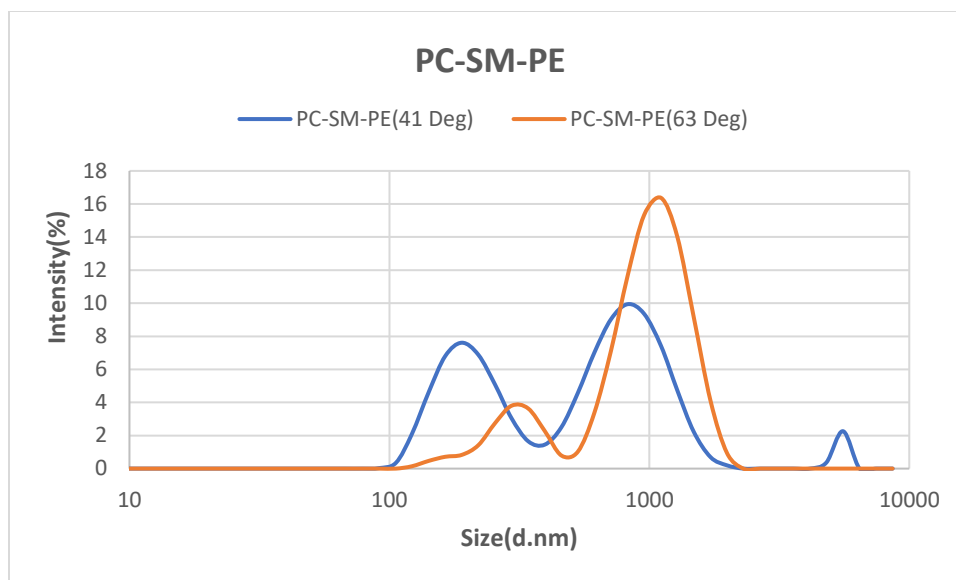


Figure 3-5 : The intensity distribution result for PC-SM -PE combination, extruded at 41°C and at 63 °C.

3.3.1 Sonication

In addition to extrusion, the sonication method was also used to prepare liposomes. The results of the comparison of sonication and extrusion methods are shown in Table 3-12 and Figure 3-6. Considering the size distribution, it is concluded that a more homogenous liposome is produced using the extrusion method. In addition, the extruded liposomes are somewhat smaller than the sonicated liposomes.

Table 3-12 Results of size and size distribution for PC produced by Sonication and Extrusion methods.

PC 16:0 (2.5 mg/ml)	Sonication	Extrusion
Z-average (d. nm)	87.1±0.9402	83.19±0.5484
PDI -Value	0.194±0.004	0.094±0.009

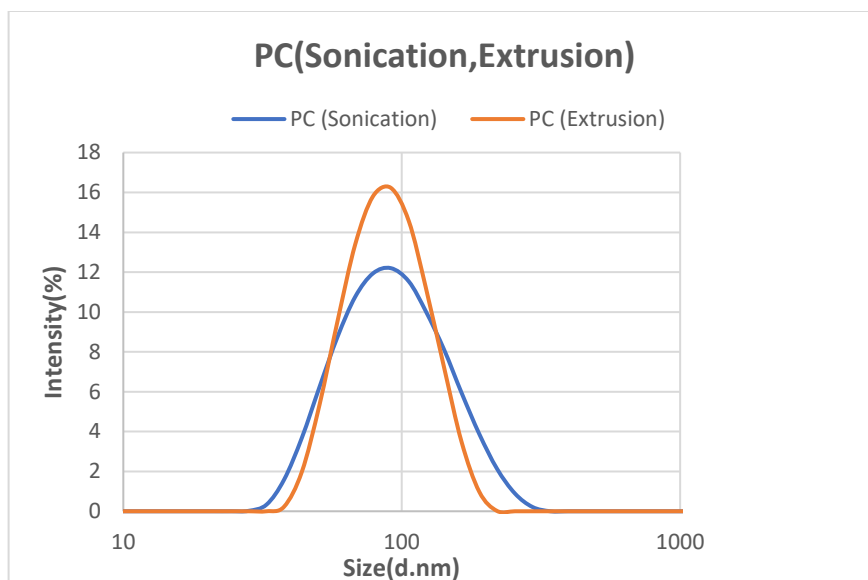


Figure 3-6 The intensity distribution result for PC produced by extrusion and sonication methods.

A combination of PC-SM was sonicated. The results of the comparison between the methods of sonication and extrusion are shown in the Table 3-13 and Figure 3-7. The homogeneity of the liposomes produced by the extrusion method, was also confirmed by the size distribution analysis. Finally, liposomes were synthesized by extrusion method to examine in the BBB model.

Table 3-13 Results of size and size distribution for PC-SM combination produced by Sonication and Extrusion methods.

PC -SM (2.5 mg/ml)	Sonication	Extrusion
Z-average (d. nm)	101.2±0.4651	82.51±0.2052
PDI -Value	0.181±0.012	0.103±0.008

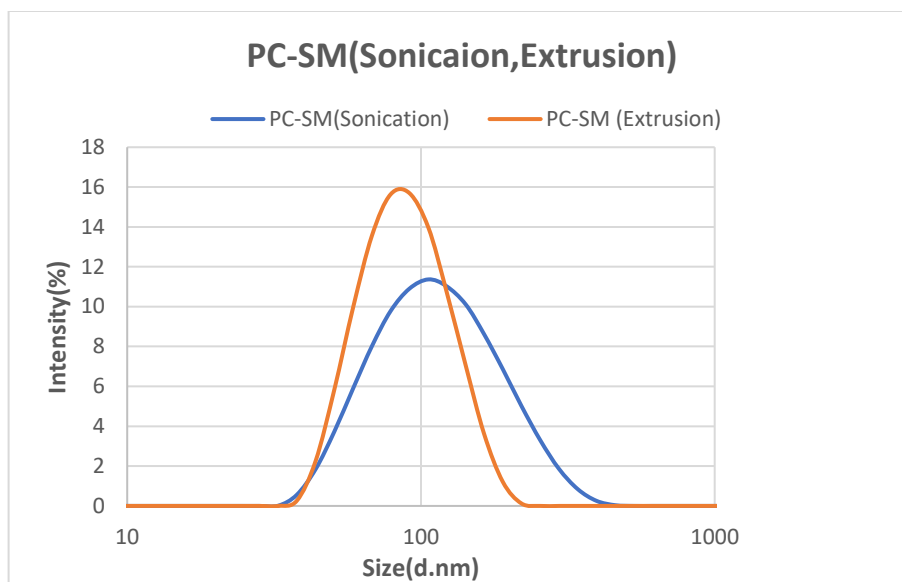


Figure 3-7 The intensity distribution result for the PC-SM combination produced by extrusion and sonication methods.

3.4 Cell culture

The long-term goal of this study was to utilize of exosomes as drug delivery vehicles for treatment of epilepsy. Epilepsy is one of the neurological diseases. Since, the BBB is the obstacle to deliver advantageous drugs to treat CNS (central nervous system) diseases, thus in this study the PBECs were used as an *in vitro* BBB model, to permeability assay.

3.4.1 PBECs as an *in vitro* BBB model

To enable set up of the PBECs model, isolation of PBECs was performed as described in methods (2.2.1.1). Following isolation of PBECs, the viability of two separate isolations (Batch I and II), were tested as described in methods (2.2.1.2). Results showed that the isolated PBECs were of poor quality, viability results of Batch I are shown in Figure 3-8, and viability results of Batch II are shown in Figures 3-9 and 3.10. It should be noted that the cultivation of Batch II, was repeated to evaluate the effect of changing the culture medium on the viability of cells. The schedule for changing the culture media is shown in Table 3-14.

Table 3-14 The schedule to change the culture media for cell cultures Batch I and Batch II.

Cell culture Batch	Time to change the culture medium	
Cell culture Batch I	On the third day	On the sixth day
Cell culture Batch II	On the first day	On the fourth day
Cell culture Batch II (Repeated)	On the third day	On the sixth day

Since, brain microvessel endothelial cell culture are very sensitive to changes in culture conditions, any modification in coating culture surface, washing cultures and substances such as DMSO, can influence the viability of the cells. Moreover, homogenization and digestion of homogenate in isolation procedure may be factors that influence the cell viability. It is clear that isolation protocol needs to be optimized. If we have more time, we would continue with optimizing PBECs isolation and viability at the same time. Then, we would continue with permeability assay and liposome uptake assay in the cell line

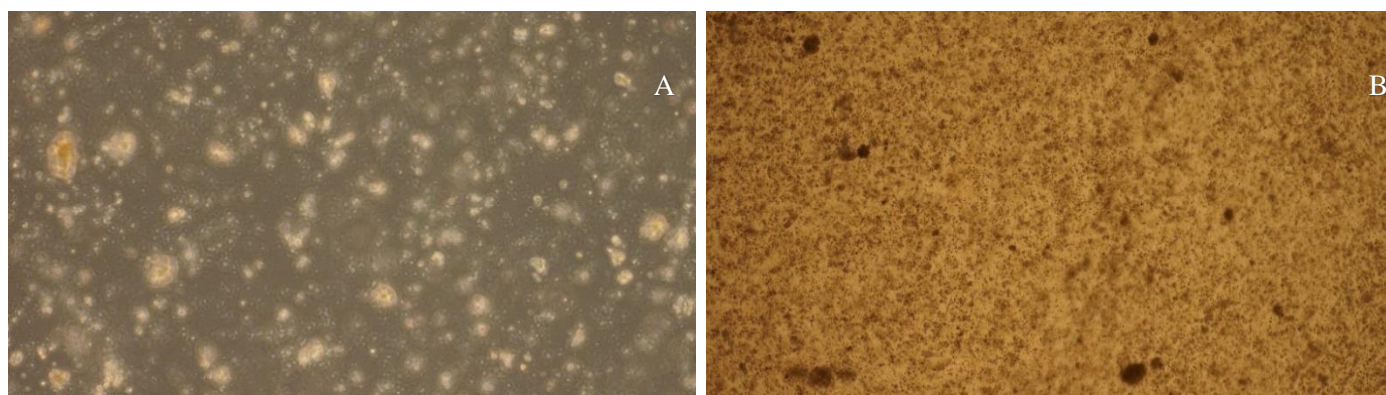


Figure 3-8 Viability test results of isolation Batch I, A: After three days, B: After six days.

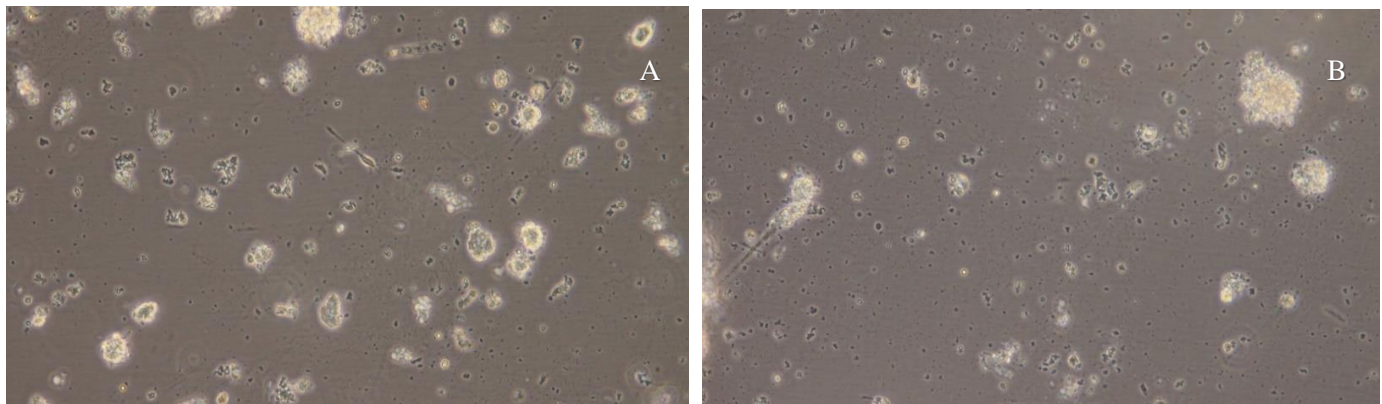


Figure 3-9 Viability test results of isolation Batch II, A: After three days, B: After six days

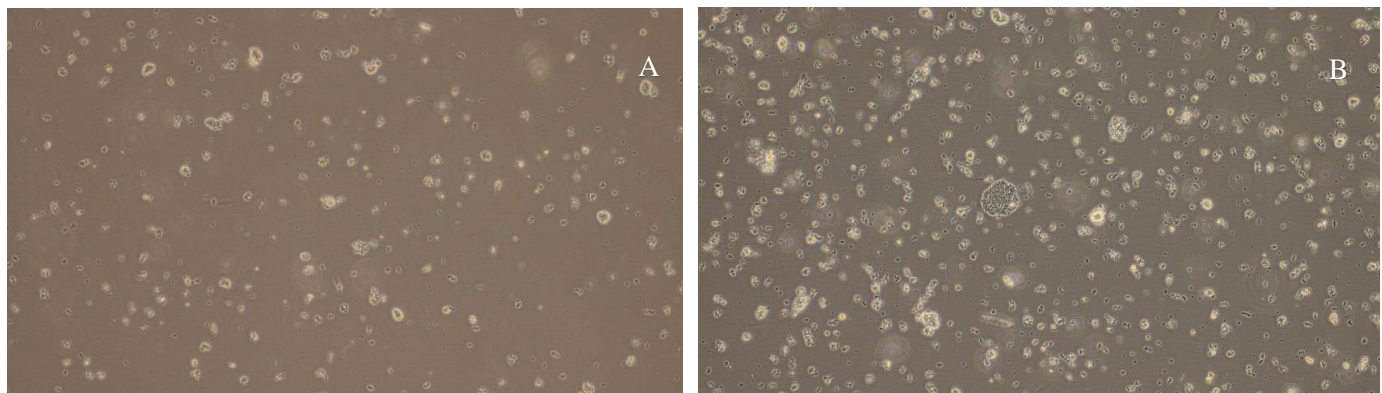


Figure 3-10 The result of the repeated viability test of isolation Batch II, A: After three days, B: After eight days.

Chapter 4

Discussion

In this study, the isolation and primary cultivation of PBECs was performed. The purpose was to use PBECs as a culture model of the BBB. In addition, exosome-based liposomes were synthesized using the Avanti micro extruder. The size, homogeneity and stability of liposomes was characterized by DLS. Exosomes were also isolated by Izon qEV columns, based on the SEC method, and exosome characterization was performed by DLS and MS.

4.1 *An in vitro* BBB model

An *in vitro* BBB model developed on PBECs has various benefits compared with *in vitro* rodent BBB models: higher cellular production per animal; PBECs reserve many of the essential BBB characteristics; porcine brains are by-products from the slaughterhouse and thus affordable; and their use for research is more ethically admissible [78].

In 1989, Misccheck et al, isolated PBECs [79]. For this purpose, two isolation protocols have been established and adjusted in separate laboratories. The first protocol was developed using homogenization of whole brain hemispheres after the meninges have been removed using sterile scalpels, afterwards a dispase digestion. The digested suspension was centrifuged in dextran to isolate microvessels from low-density substances, then they were incubated with collagenase/dispase to release endothelial cells. The cells were separated by centrifugation on a percoll gradient and then subcultured for one passage to raise cell production and purity [79-81].

Helmut Franke et al, isolated PBECs based on this protocol [80]. The second protocol was established using mechanical homogenization of separated gray matter and size-selective filtering across consecutively smaller nylon mesh (150 and 60 μm) to segregate microvessels. The microvessels digestion was performed with collagenase/DNAse/trypsin, and finally endothelial

cells were acquired by culturing microvessel extracts [82, 83]. Both protocols have been employed and described considerably and, even though different, they have some typical features [84].

In our study, PBECs isolation was performed based on the second protocol. In several studies cell culture was performed in a variety of procedures. Franke et al, cultivated PBECs immediately after isolation. They coated culture flasks (75 cm²) with collagen and allowed to dry for several days at 37°C. The cells were plated onto collagen-coated surfaces. On the following day, they washed cultures twice with PBS (37°C) to remove cell debris and non-adherent cells. Subcultivation of preconfluent endothelial cell cultures was performed on the third day after initial seeding. They used penicillin, streptomycin and gentamicin as antibiotics, to prepare the culture medium [80].

Thomsen et al, isolated PBECs using a somewhat altered protocol earlier explained [85-87]. They cultivated the isolated microvessel fragments onto 60 mm² plastic dishes coated with collagen IV and fibronectin. PBECs were sustained in DMEM/F12 supplemented with plasma-derived serum, basic fibroblast growth factor, heparin, insulin, transferrin, sodium selenite and gentamicin sulphate and cultured in an incubator. They added puromycin to the media for the first three days to acquire a pure culture of PBECs. They passaged and plated the cells after three days [87].

In this study, our method of isolation and cell culture is relatively similar to that of Patabendige et al. They also first coated culture surface with collagen, followed by fibronectin for two hours [78]. While, Franke et al, coated culture surface with collagen and allowed to dry for several days at 37°C. Thomsen et al, also used collagen and fibronectin to coat the culture surface, but they did not mention the duration of the coating. Despite the variety of methods used, they have often achieved relatively acceptable results [78, 80, 87]. In general, the cells should reach 50-80% confluency in 4-5 days. Although we maintained the cells for more than five days, there was no change in their growth. Because we had twice isolated the PBECs, therefore, we cultivated the two isolated cell batches. Consequently, due to high sensitivity of PBECs to alterations in the culture conditions, production and maintaining of PBECs requires special care [80]. For instance, the tendency of PBECs to aggregate should be considered in isolation, and also optimization of the

collagen coating of culture surfaces in cultivation step should be noticed [78, 80, 87]. Although in this study, all the essential points for isolation and cell culture were considered in accordance with the mentioned methods, however, the presence of problems in each step of isolation and cell culture may lead to a lack of PBECs growth.

4.2 Preparation and characterization of liposomes

Liposomes have made significant impression on therapeutics owing to their advantages as drug delivery systems. In fact, besides their non-toxic and biocompatible character that can adapt high cargos of drugs, they have the ability of loading multiple drugs to supply defense of drugs from degeneration, and to improve drug endocytosis into cells [88].

The liposome size is one of the crucial parameters that can impact the *in vivo* activity of liposomes. Former researches have displayed that liposomes with diameters more than 0.1 μm are opsonized more speedily and at the higher range than their smaller counterparts and, thus, are removed more quickly by the reticuloendothelial system [89, 90]. Accordingly, to extend the liposome circulation time, several methods, including sonication, extrusion, and homogenization have been invented in order to diminish the liposome size [91-94]. Among these, extrusion technique possesses some advantages: it produces liposomes with rather homogenous size distributions, it is reproducible, the processing is quick, and it is comparatively a mild procedure [73]. Ong et al also evaluated capability of various nanosizing methods, subsequent techniques were employed to nanosize the liposome: extrusion, ultrasonication, freeze-thaw sonication (FTS), sonication and homogenization. The extrusion method was discovered to be the most effective, afterwards FTS, ultrasonication, sonication and homogenization [72].

In our study, liposomes were prepared by extrusion and using the Avanti micro extruder (Figure 1-7, Figure 2-2). The phospholipids that were used in this experiment included: PC, SM and PE. The liposome size and size distribution were determined by DLS (Zetasizer, Malvern Instrument Ltd). Our results showed that raising the extrusion temperature only led to very slightly reduce in the liposome size and size distribution (Table 3-1 and Figure 3-4). It should be noted that the extrusion temperature employed in the present study were all about the transition temperature to facilitate

the extrusion procedure. This is in agreement with a previous study by Ong et al. Moreover, the effect of membrane pore size on the particle size and size distribution of the liposomes is exhibited in (Table 3-2, Table 3-3, Figure 3-5 and Figure 3-6). It is obvious from the results that reducing the membrane pore size caused in corresponding reduce in the size and size distribution of the liposomes. Previous studies which explored the relationship between the particle size of the liposomes and the pore size of the extruding device, have reported similar results [72-74, 77]. Experiment was followed by sonication technique for nanosizing liposomes. Sonication employs acoustic energy to generate pressure waves that disrupt large, multilamellar vesicles and accumulations into smaller vesicles. The application time and the strength of the pressure waves mainly ascertain the size of the produced vesicles, and overall sonication is more rapid and less intensive than extrusion [95, 96]. Our results showed a remarkable difference in the size and size distribution of the liposomes produced by sonication and extrusion (Table 3-5, Table 3-6, Figure 3-8 and Figure 3-9). From the tables and plots, size and size distribution of the extruded liposomes are more less than of the sonicated liposomes. This finding is consistent with a previous report of Ong et al [72].

The result of the extruded liposome of PC-SM-PE, displays a nonhomogeneous plot and increase in size and size distribution of the liposome (Table 3-4 and Figure 3-7). Although, extrusion was performed in two different temperatures 41°C and 63 °C, according to the transition temperature of PC -SM and PE respectively, but in general the result for this liposome is not satisfactory.

4.3 Exosomes isolation and characterization

Exosomes are isolated from cells and biological fluids using several different methods. Each method utilizes a particular characteristic of exosomes such as their size, figure, density or surface antigens to assist isolation [35]. One of the size-based exosome isolation techniques is size exclusion chromatography. SEC is a technique in which a solution including a heterogeneous group of diversely sized constituents is isolated based on their size. A column consisting of heterosporous beads is employed in SEC, constituents including different vesicles and impurities in a solution with a smaller hydrodynamic radius, can cross the many small pores, subsequent in a longer time to separate. Ingredients with a larger hydrodynamic radius such as exosomes are

incapable pass through as many pores, and therefore elute earlier from the column. Thus, exosomes may be isolated from other vesicles and impurities of various sizes. The advantages of SEC are that it maintains the unity and biological activity of exosomes and other molecules being isolated, due to SEC is generally accomplished employing gravity flow, vesicle structure and unity stay intact [97]. Baranyai et al explored efficiency and purity of exosome isolated with two methods: differential ultracentrifugation and SEC. They reported that it is possible to isolate exosomes from blood plasma by SEC without noticeable albumin contamination although with low vesicle yield [98]. In our study, exosomes were isolated from blood plasma by SEC, and then size and size distribution of exosomes were measured by DLS (Table 3-7 and Figure 3-10). The results are in agreement with previous reports that with SEC exosome isolation can be accomplished without considerable contaminants [97, 99-101].

Mass spectrometry with its specificity and sensitivity has capability to recognize and characterize molecular contents of extracellular vesicles such as exosomes. MS is a main instrument to evaluate protein content of EVs. Along with protein, lipid and metabolite contents of vesicles might also be best evaluated by MS, nevertheless there are a few efforts so far in this way [102]. The objective of our study was to characterize the lipid content of exosomes by MS. As previously mentioned, MS technique was performed at the university of Bergen, and then we analyzed the results according to manual curation.

According to the studies issued as yet, exosomes are comprised of a high range of membrane lipids [49, 103]. Thus, the exosomal lipid content should typically correspond to the content of a lipid bilayer. It is well-documented there is an inequality distribution of lipid classes in the two leaflets of plasma membrane. Therefore, sphingolipids and phosphatidylcholine are mainly existent in the outer leaflet, and the other lipid classes are mostly found in the inner leaflet [50]. An identical inequality in exosomal membrane is expected, at least presently after exosomes are delivered from cells [49]. Exosomes in biological fluids comprise a heterogenous population deriving from many various cell types. The lipid content of extracellular vesicles in biological fluids is less well identified and has as yet only been reported from EVs from seminal fluids (prostasome) and from urine [49, 103]. In respect of prostasomes, two prostatesome compound

(50nm and 100nm) isolated from human seminal fluid have been analyzed by MS [104]. And, the lipid content of exosomes isolated from human urine has lately been reported [105]. Cells include thousands of various molecular lipid species, and there has been a rising number of cases explaining particular cellular functions for one single lipid species [106]. While the exosomal numbers of various lipid classes has been detected in several studies, there are only a few studies where molecular lipid species have been evaluated and even fewer where they have been measured [103]. Liorente et al, reported that in their study of prostate cancer cells (PC-3 cell line) about 280 species from 18 lipid classes were quantified [107].

In our study, approximately 85 species from 4 lipid classes were quantified. In PC class, PC 16:0/18:1 and 16:0/18:2 were most abundant PC species. Previous researchers that have compared the saturation level of fatty acyl groups in lipids in exosomes with that in parent cells approved that there is an enrichment of phospholipid species with two saturated fatty acyl groups. For PC, this is mostly owing to a rise in PC 14:0/16:0 and 16:0/16:0 [107, 108]. On the other hand, Liorente et al emphasized that exosomes include plentiful monosaturated fatty acyl groups. PC 16:0/18:1 and PC 16:0/16:1 were the two abundant PC species in exosomes from PC-3 cells [107]. Sphingolipids, and particularly the main sphingolipid SM, are essential for the structure of exosomes [103]. In our study, in SM classes, SM d14:0/20:1 and d14:0/28:2 were dominant. SM d18:1/16:0, SM d18:1/24:0 and SM d18:1/24:1 were reported as SM species in exosomes from PC-3 cells [107]. In our study, in PE class, none of the species were dominant, and in PI class, two species PI 18:0/20:4, PI 16:0/20:4 approximately were dominant. However, in general the majority was with PC species and SM species.

Conclusion

We have demonstrated that isolation and characterization of exosomes and preparing and characterization of liposomes by the presented approaches, was feasible and showed purity and homogeneity of yields.

Some lipid species, PC 16:0/18:1 and 16:0/18:2 in PC class and SM d14:0/20:1 and d14:0/28:2 in SM class, were dominant, and should be preferentially used in further studies of exosomes from human plasma. MS is a high output method which provides a general overview of the lipid content of exosomes. Different steps of the MS, such as the nature of the lipids, sample preparation, software used, and data processing might affect the results.

As an *in vitro* BBB model, PBECs has various advantages. Although it showed poor viability in our project, therefore, further work seems necessary to optimize isolation and viability of PBECs. Furthermore, continuing the experiment with liposome uptake assay in the cell line would yield useful results.

References:

1. Stafstrom, C.E. and L.J.C.S.H.p.i.m. Carmant, *Seizures and epilepsy: an overview for neuroscientists*. 2015. **5**(6): p. a022426.
2. Moshé, S.L., et al., *Epilepsy: new advances*. 2015. **385**(9971): p. 884-898.
3. Grabrucker, A.M., et al., *Nanoparticle transport across the blood brain barrier*. 2016. **4**(1): p. e1153568.
4. Mifsud, J.J.J.o.t.M.C.o.P.P., *Gender differences in epilepsy: perceived or real?* 2014: p. 28.
5. Falco-Walter, J.J., I.E. Scheffer, and R.S.J.E.R. Fisher, *The new definition and classification of seizures and epilepsy*. 2018. **139**: p. 73-79.
6. Martin, K., et al., *Ketogenic diet and other dietary treatments for epilepsy*. 2016(2).
7. Saraiva, C., et al., *Nanoparticle-mediated brain drug delivery: overcoming blood–brain barrier to treat neurodegenerative diseases*. 2016. **235**: p. 34-47.
8. He, Q., et al., *Towards improvements for penetrating the blood–brain barrier—recent progress from a material and pharmaceutical perspective*. 2018. **7**(4): p. 24.
9. Gao, H.J.A.P.S.B., *Progress and perspectives on targeting nanoparticles for brain drug delivery*. 2016. **6**(4): p. 268-286.
10. Abbott, N.J., et al., *Structure and function of the blood–brain barrier*. 2010. **37**(1): p. 13-25.
11. Pehlivan, S.B.J.P.r., *Nanotechnology-based drug delivery systems for targeting, imaging and diagnosis of neurodegenerative diseases*. 2013. **30**(10): p. 2499-2511.
12. Leybaert, L., et al., *Neurobarrier coupling in the brain: adjusting glucose entry with demand*. 2007. **85**(15): p. 3213-3220.
13. Yang, T., et al., *Exosome delivered anticancer drugs across the blood-brain barrier for brain cancer therapy in *Danio rerio**. 2015. **32**(6): p. 2003-2014.
14. Simons, M. and G.J.C.o.i.c.b. Raposo, *Exosomes–vesicular carriers for intercellular communication*. 2009. **21**(4): p. 575-581.

15. Ha, D., N. Yang, and V.J.A.P.S.B. Nadithe, *Exosomes as therapeutic drug carriers and delivery vehicles across biological membranes: current perspectives and future challenges*. 2016. **6**(4): p. 287-296.
16. Harding, C., J. Heuser, and P.J.T.J.o.c.b. Stahl, *Receptor-mediated endocytosis of transferrin and recycling of the transferrin receptor in rat reticulocytes*. 1983. **97**(2): p. 329-339.
17. Pan, B.-T., et al., *Electron microscopic evidence for externalization of the transferrin receptor in vesicular form in sheep reticulocytes*. 1985. **101**(3): p. 942-948.
18. Abels, E.R. and X.O. Breakefield, *Introduction to extracellular vesicles: biogenesis, RNA cargo selection, content, release, and uptake*. 2016, Springer.
19. Lugli, G., et al., *Plasma exosomal miRNAs in persons with and without Alzheimer disease: altered expression and prospects for biomarkers*. 2015. **10**(10): p. e0139233.
20. Ellis, T.N. and M.J.J.M.M.B.R. Kuehn, *Virulence and immunomodulatory roles of bacterial outer membrane vesicles*. 2010. **74**(1): p. 81-94.
21. Silverman, J.M. and N.E.J.C.m. Reiner, *Exosomes and other microvesicles in infection biology: organelles with unanticipated phenotypes*. 2011. **13**(1): p. 1-9.
22. Van der Pol, E., et al., *Classification, functions, and clinical relevance of extracellular vesicles*. 2012. **64**(3): p. 676-705.
23. Cocucci, E., G. Racchetti, and J.J.T.i.c.b. Meldolesi, *Shedding microvesicles: artefacts no more*. 2009. **19**(2): p. 43-51.
24. Kooijmans, S.A., et al., *Exosome mimetics: a novel class of drug delivery systems*. 2012. **7**: p. 1525.
25. Urbanelli, L., et al., *Signaling pathways in exosomes biogenesis, secretion and fate*. 2013. **4**(2): p. 152-170.
26. Vlassov, A.V., et al., *Exosomes: current knowledge of their composition, biological functions, and diagnostic and therapeutic potentials*. 2012. **1820**(7): p. 940-948.
27. Rufino-Ramos, D., et al., *Extracellular vesicles: novel promising delivery systems for therapy of brain diseases*. 2017. **262**: p. 247-258.
28. Théry, C., et al., *Indirect activation of naïve CD4+ T cells by dendritic cell-derived exosomes*. 2002. **3**(12): p. 1156.

29. Kalani, A., A. Tyagi, and N.J.M.n. Tyagi, *Exosomes: mediators of neurodegeneration, neuroprotection and therapeutics*. 2014. **49**(1): p. 590-600.
30. Subra, C., et al., *Exosome lipidomics unravels lipid sorting at the level of multivesicular bodies*. 2007. **89**(2): p. 205-212.
31. Parolini, I., et al., *Microenvironmental pH is a key factor for exosome traffic in tumor cells*. 2009. **284**(49): p. 34211-34222.
32. Piccin, A., W.G. Murphy, and O.P.J.B.r. Smith, *Circulating microparticles: pathophysiology and clinical implications*. 2007. **21**(3): p. 157-171.
33. Gibbins, D.J., et al., *Multivesicular bodies associate with components of miRNA effector complexes and modulate miRNA activity*. 2009. **11**(9): p. 1143.
34. Sercombe, L., et al., *Advances and challenges of liposome assisted drug delivery*. 2015. **6**: p. 286.
35. Antimisiaris, S., S. Mourtas, and A.J.P. Marazioti, *Exosomes and exosome-inspired vesicles for targeted drug delivery*. 2018. **10**(4): p. 218.
36. Agrawal, U., et al., *Is nanotechnology a boon for oral drug delivery?* 2014. **19**(10): p. 1530-1546.
37. Jawahar, N., S.J.I.J.o.H. Meyyanathan, and A. Sciences, *Polymeric nanoparticles for drug delivery and targeting: A comprehensive review*. 2012. **1**(4): p. 217.
38. Lai, R.C., et al., *Exosomes for drug delivery—a novel application for the mesenchymal stem cell*. 2013. **31**(5): p. 543-551.
39. Lakhal, S. and M.J.J.B. Wood, *Exosome nanotechnology: an emerging paradigm shift in drug delivery: exploitation of exosome nanovesicles for systemic in vivo delivery of RNAi heralds new horizons for drug delivery across biological barriers*. 2011. **33**(10): p. 737-741.
40. Jang, S.C., et al., *Bioinspired exosome-mimetic nanovesicles for targeted delivery of chemotherapeutics to malignant tumors*. 2013. **7**(9): p. 7698-7710.
41. Kang, H., et al., *Methods to isolate extracellular vesicles for diagnosis*. 2017. **5**(1): p. 15.
42. Li, P., et al., *Progress in exosome isolation techniques*. 2017. **7**(3): p. 789.
43. Marbán, E.J.J.o.t.A.C.o.C., *The secret life of exosomes: what bees can teach us about next-generation therapeutics*. 2018. **71**(2): p. 193-200.

44. Théry, C., et al., *Isolation and characterization of exosomes from cell culture supernatants and biological fluids*. 2006. **30**(1): p. 3.22. 1-3.22. 29.
45. Shin, H., et al., *High-yield isolation of extracellular vesicles using aqueous two-phase system*. 2015. **5**: p. 13103.
46. Van der Pol, E., et al., *Particle size distribution of exosomes and microvesicles determined by transmission electron microscopy, flow cytometry, nanoparticle tracking analysis, and resistive pulse sensing*. 2014. **12**(7): p. 1182-1192.
47. Lötvall, J., et al., *Minimal experimental requirements for definition of extracellular vesicles and their functions: a position statement from the International Society for Extracellular Vesicles*. 2014, Taylor & Francis.
48. Aalberts, M., et al., *Identification of distinct populations of prostasomes that differentially express prostate stem cell antigen, annexin A1, and GLIPR2 in humans*. 2012. **86**(3): p. 82, 1-8.
49. Skotland, T., et al., *Exosomal lipid composition and the role of ether lipids and phosphoinositides in exosome biology*. 2019. **60**(1): p. 9-18.
50. Van Meer, G., D.R. Voelker, and G.W.J.N.r.M.c.b. Feigenson, *Membrane lipids: where they are and how they behave*. 2008. **9**(2): p. 112.
51. Hopfgartner, G., et al., *High-resolution mass spectrometry for integrated qualitative and quantitative analysis of pharmaceuticals in biological matrices*. 2012. **402**(8): p. 2587-2596.
52. Persike, M. and M.J.R.C.i.M.S.A.I.J.D.t.t.R.D.o.U.t.t.M.R.i.M.S. Karas, *Rapid simultaneous quantitative determination of different small pharmaceutical drugs using a conventional matrix-assisted laser desorption/ionization time-of-flight mass spectrometry system*. 2009. **23**(22): p. 3555-3562.
53. Awad, H., M.M. Khamis, and A.J.A.S.R. El-Aneed, *Mass spectrometry, review of the basics: ionization*. 2015. **50**(2): p. 158-175.
54. El-Aneed, A., A. Cohen, and J.J.A.S.R. Banoub, *Mass spectrometry, review of the basics: electrospray, MALDI, and commonly used mass analyzers*. 2009. **44**(3): p. 210-230.
55. De Hoffmann, E., J. Charette, and V. Stroobant, *Mass Spectrometry: Principles and Applications*. 1997.
56. Berggren, W.T., M.S. Westphall, and L.M.J.A.c. Smith, *Single-pulse nanoelectrospray ionization*. 2002. **74**(14): p. 3443-3448.

57. Lu, Y., et al., *Pulsed electrospray for mass spectrometry*. 2001. **73**(19): p. 4748-4753.
58. Glish, G.L. and R.W.J.N.r.d.d. Vachet, *The basics of mass spectrometry in the twenty-first century*. 2003. **2**(2): p. 140.
59. Shen, Z., et al., *Porous silicon as a versatile platform for laser desorption/ionization mass spectrometry*. 2001. **73**(3): p. 612-619.
60. Thomas, J.J., et al., *Desorption/ionization on silicon (DIOS): a diverse mass spectrometry platform for protein characterization*. 2001. **98**(9): p. 4932-4937.
61. Stetefeld, J., S.A. McKenna, and T.R.J.B.r. Patel, *Dynamic light scattering: a practical guide and applications in biomedical sciences*. 2016. **8**(4): p. 409-427.
62. Harding, S.E. and K.J.C.p.i.p.s. Jumel, *Light scattering*. 1998. **11**(1): p. 7.8. 1-7.8. 14.
63. Harding, S., *Protein Hydrodynamics. Protein: a comprehensive treatise*. 1999, JAI Press, Greenwich.
64. Bassi, F.A., et al., *Self-similarity properties of alpha-crystallin supramolecular aggregates*. 1995. **69**(6): p. 2720-2727.
65. Parasassi, T., et al., *Low density lipoprotein misfolding and amyloidogenesis*. 2008. **22**(7): p. 2350-2356.
66. Filipe, V., A. Hawe, and W.J.P.r. Jiskoot, *Critical evaluation of Nanoparticle Tracking Analysis (NTA) by NanoSight for the measurement of nanoparticles and protein aggregates*. 2010. **27**(5): p. 796-810.
67. Antimisiaris, S.G., et al., *Liposomes and drug delivery*. 2010: p. 1-91.
68. Kshirsagar, N., et al., *Liposomal drug delivery system from laboratory to clinic*. 2005. **51**(5): p. 5.
69. Bitounis, D., et al., *Optimizing druggability through liposomal formulations: new approaches to an old concept*. 2012. **2012**.
70. Immordino, M.L., F. Dosio, and L.J.I.j.o.n. Cattel, *Stealth liposomes: review of the basic science, rationale, and clinical applications, existing and potential*. 2006. **1**(3): p. 297.
71. Dupont, B.J.J.o.A.C., *Overview of the lipid formulations of amphotericin B*. 2002. **49**(1): p. 31-36.
72. Ong, S., et al., *Evaluation of extrusion technique for nanosizing liposomes*. 2016. **8**(4): p. 36.

73. Mayer, L., M. Hope, and P.J.B.e.B.A.-B. Cullis, *Vesicles of variable sizes produced by a rapid extrusion procedure*. 1986. **858**(1): p. 161-168.
74. Berger, N., et al., *Filter extrusion of liposomes using different devices: comparison of liposome size, encapsulation efficiency, and process characteristics*. 2001. **223**(1-2): p. 55-68.
75. Olson, F., et al., *Preparation of liposomes of defined size distribution by extrusion through polycarbonate membranes*. 1979. **557**(1): p. 9-23.
76. Liu, R., *Water-insoluble drug formulation*. 2000: CRC press.
77. Hunter, D. and B.J.B.j. Frisken, *Effect of extrusion pressure and lipid properties on the size and polydispersity of lipid vesicles*. 1998. **74**(6): p. 2996-3002.
78. Patabendige, A., et al., *A detailed method for preparation of a functional and flexible blood–brain barrier model using porcine brain endothelial cells*. 2013. **1521**: p. 16-30.
79. Mischeck, U., et al., *Characterization of γ -glutamyl transpeptidase activity of cultured endothelial cells from porcine brain capillaries*. 1989. **256**(1): p. 221-226.
80. Franke, H., H.-J. Galla, and C.T.J.B.R.P. Beuckmann, *Primary cultures of brain microvessel endothelial cells: a valid and flexible model to study drug transport through the blood–brain barrier in vitro*. 2000. **5**(3): p. 248-256.
81. Hoheisel, D., et al., *Hydrocortisone reinforces the blood–brain barrier properties in a serum free cell culture system*. 1998. **244**(1): p. 312-316.
82. Patabendige, A., R.A. Skinner, and N.J.J.B.r. Abbott, *Establishment of a simplified in vitro porcine blood–brain barrier model with high transendothelial electrical resistance*. 2013. **1521**: p. 1-15.
83. Schulze, C., et al., *Lysophosphatidic acid increases tight junction permeability in cultured brain endothelial cells*. 1997. **68**(3): p. 991-1000.
84. Helms, H.C., et al., *In vitro models of the blood–brain barrier: an overview of commonly used brain endothelial cell culture models and guidelines for their use*. 2016. **36**(5): p. 862-890.
85. Fazakas, C., et al., *Transmigration of melanoma cells through the blood-brain barrier: role of endothelial tight junctions and melanoma-released serine proteases*. 2011. **6**(6): p. e20758.
86. Nakagawa, S., et al., *A new blood–brain barrier model using primary rat brain endothelial cells, pericytes and astrocytes*. 2009. **54**(3-4): p. 253-263.

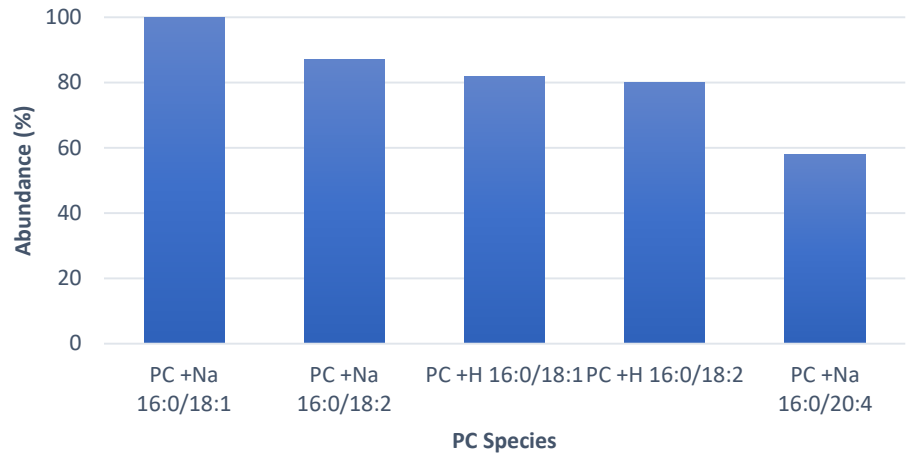
87. Thomsen, L.B., A. Burkhart, and T.J.P.o. Moos, *A triple culture model of the blood-brain barrier using porcine brain endothelial cells, astrocytes and pericytes*. 2015. **10**(8): p. e0134765.
88. Deshpande, P.P., S. Biswas, and V.P.J.N. Torchilin, *Current trends in the use of liposomes for tumor targeting*. 2013. **8**(9): p. 1509-1528.
89. Harashima, H., et al., *Enhanced hepatic uptake of liposomes through complement activation depending on the size of liposomes*. 1994. **11**(3): p. 402-406.
90. Szoka, J.F.J.B. and a. biochemistry, *The future of liposomal drug delivery*. 1990. **12**(5): p. 496-500.
91. Barnadas-Rodríguez, R. and M.J.I.j.o.p. Sabés, *Factors involved in the production of liposomes with a high-pressure homogenizer*. 2001. **213**(1-2): p. 175-186.
92. Fatouros, D., et al., *Preparation and properties of arsonolipid containing liposomes*. 2001. **109**(1): p. 75-89.
93. Hope, M.J., et al., *Reduction of liposome size and preparation of unilamellar vesicles by extrusion techniques*. 1993. **1**: p. 123-139.
94. Jousma, H., et al., *Characterization of liposomes. The influence of extrusion of multilamellar vesicles through polycarbonate membranes on particle size, particle size distribution and number of bilayers*. 1987. **35**(3): p. 263-274.
95. Maulucci, G., et al., *Particle size distribution in DMPC vesicles solutions undergoing different sonication times*. 2005. **88**(5): p. 3545-3550.
96. Richardson, E.S., W.G. Pitt, and D.J.J.B.j. Woodbury, *The role of cavitation in liposome formation*. 2007. **93**(12): p. 4100-4107.
97. Muller, L., et al., *Isolation of biologically-active exosomes from human plasma*. 2014. **411**: p. 55-65.
98. Baranyai, T., et al., *Isolation of exosomes from blood plasma: qualitative and quantitative comparison of ultracentrifugation and size exclusion chromatography methods*. 2015. **10**(12): p. e0145686.
99. Böing, A.N., et al., *Single-step isolation of extracellular vesicles by size-exclusion chromatography*. 2014. **3**(1): p. 23430.
100. Lobb, R.J., et al., *Optimized exosome isolation protocol for cell culture supernatant and human plasma*. 2015. **4**(1): p. 27031.

101. Nordin, J.Z., et al., *Ultrafiltration with size-exclusion liquid chromatography for high yield isolation of extracellular vesicles preserving intact biophysical and functional properties*. 2015. **11**(4): p. 879-883.
102. Pocsfalvi, G., et al., *Mass spectrometry of extracellular vesicles*. 2016. **35**(1): p. 3-21.
103. Skotland, T., K. Sandvig, and A.J.P.i.l.r. Llorente, *Lipids in exosomes: current knowledge and the way forward*. 2017. **66**: p. 30-41.
104. Brouwers, J.F., et al., *Distinct lipid compositions of two types of human prostatesomes*. 2013. **13**(10-11): p. 1660-1666.
105. Skotland, T., et al., *Molecular lipid species in urinary exosomes as potential prostate cancer biomarkers*. 2017. **70**: p. 122-132.
106. Kimura, T., W. Jennings, and R.M.J.P.i.l.r. Epanand, *Roles of specific lipid species in the cell and their molecular mechanism*. 2016. **62**: p. 75-92.
107. Llorente, A., et al., *Molecular lipidomics of exosomes released by PC-3 prostate cancer cells*. 2013. **1831**(7): p. 1302-1309.
108. Trajkovic, K., et al., *Ceramide triggers budding of exosome vesicles into multivesicular endosomes*. 2008. **319**(5867): p. 1244-1247.

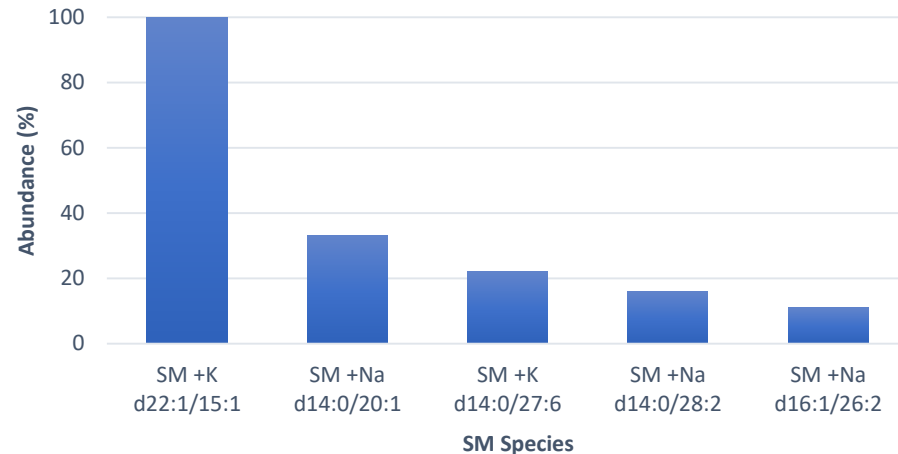
Appendix:

The summarized results in *the characterization of exosomes by MS (3.2)* section, are obtained by analyzing the MS results and drawing the attached diagrams. As previously mentioned, three fractions (F10, F11 and F12), collected from exosome isolation, were analyzed by MS. F10 and F11, were measured in five runs (R1-R5) and F12 in three runs (R1-R3). The abundance of lipid species and fatty acid (FA) chains were plotted in positive and negative modes for each headgroups.

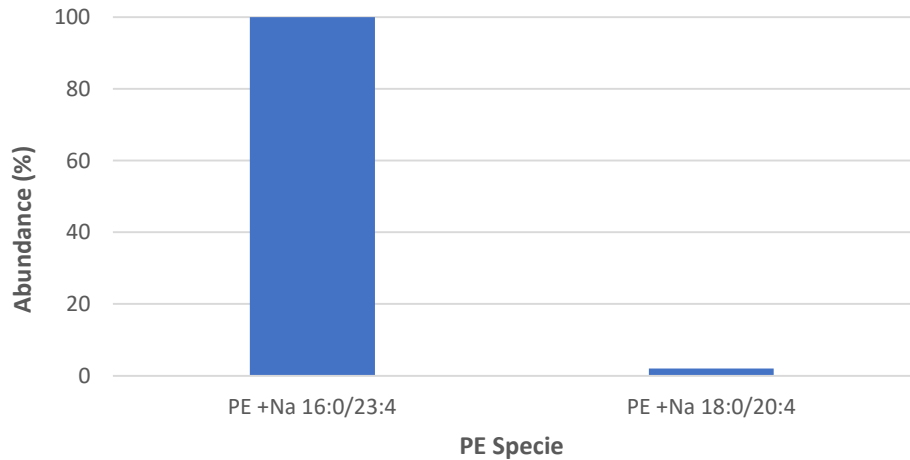
F10-PC-R1



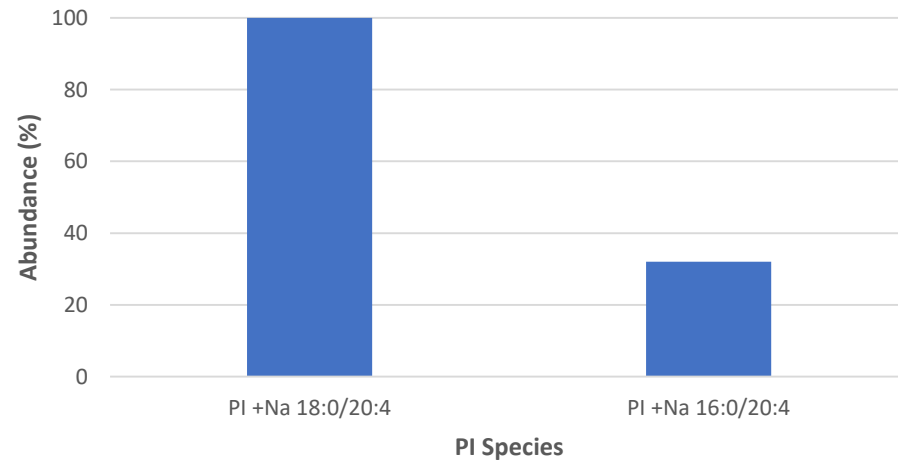
F10-SM-R1

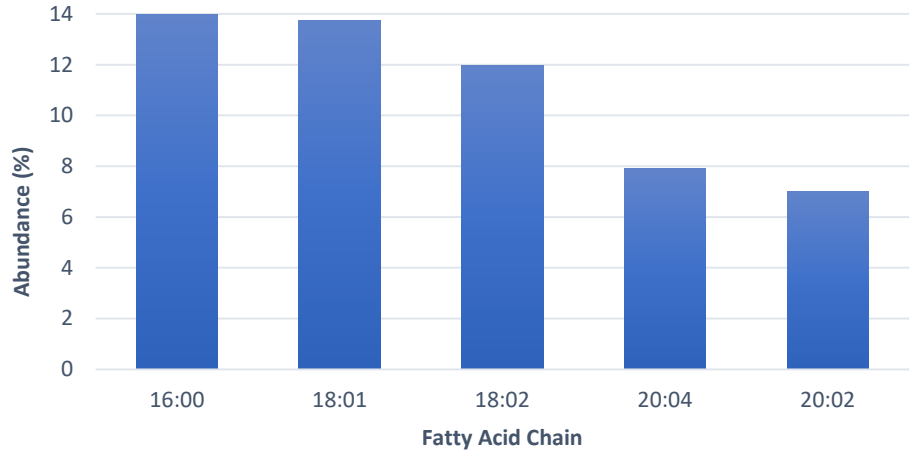
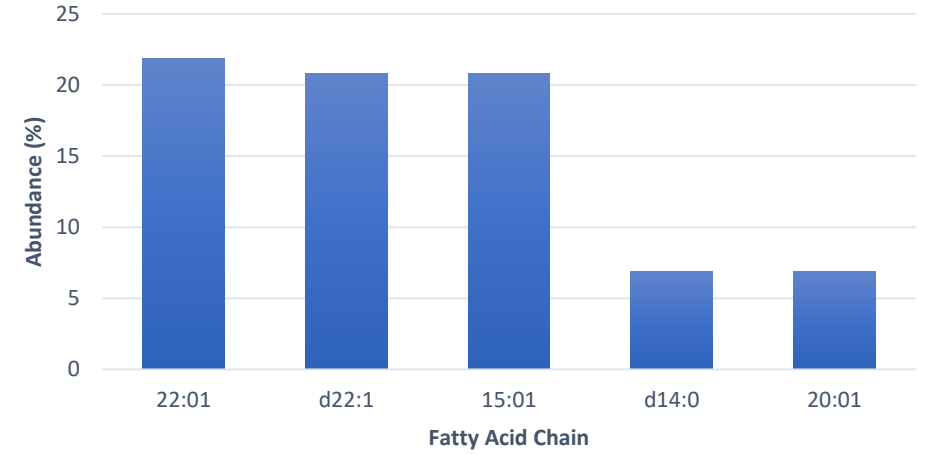
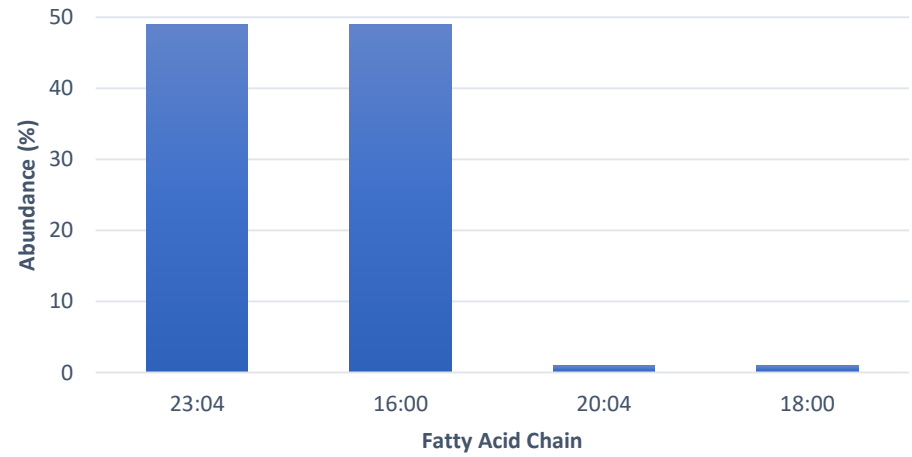
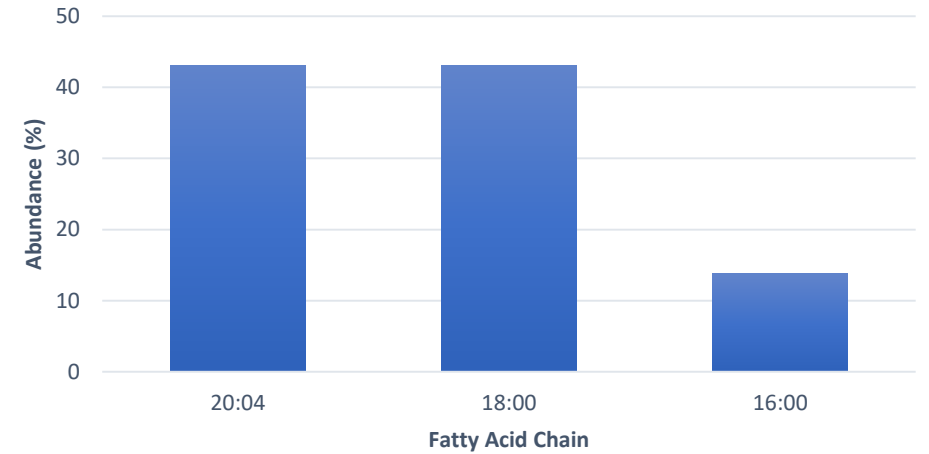


F10-PE-R1

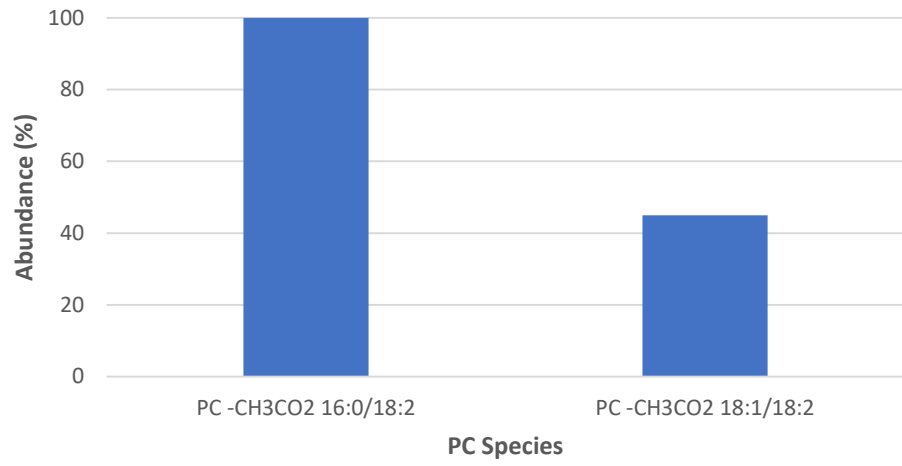


F10-PI-R1

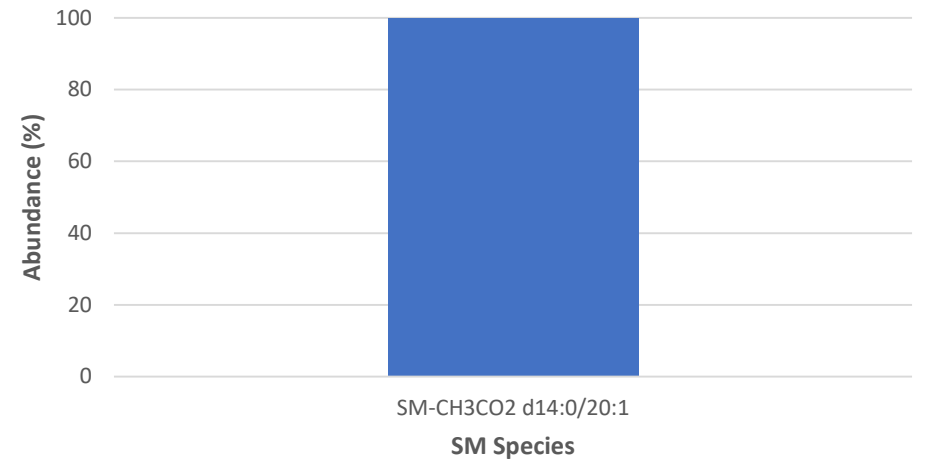


F10-PC-FA-R1**F10-SM-FA-R1****F10-PE-FA-R1****F10-PI-FA-R1**

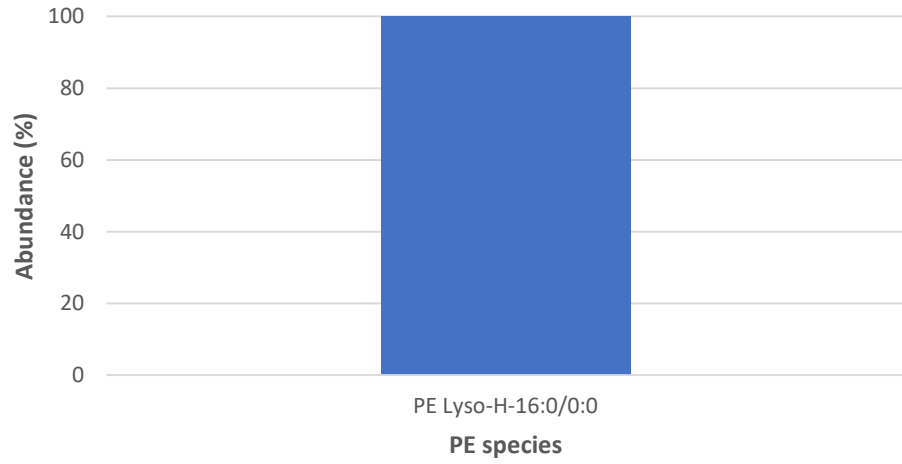
F10-PC-R1-Neg



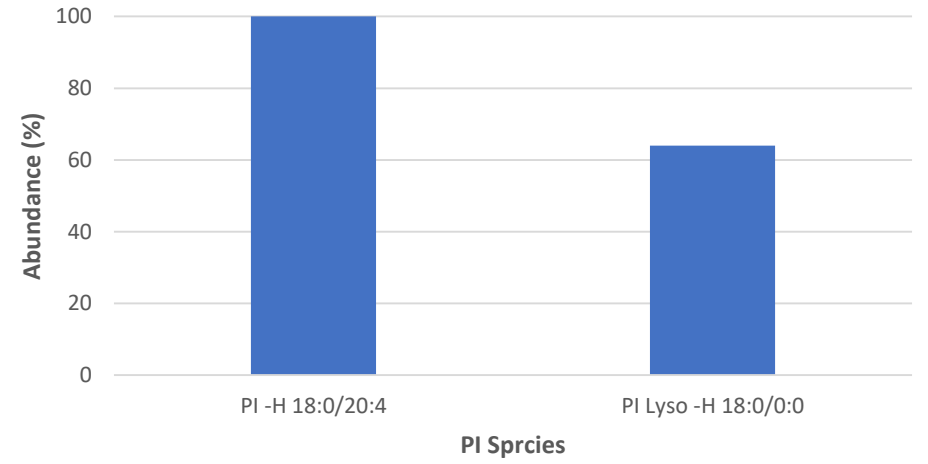
F10-SM-R1-Neg



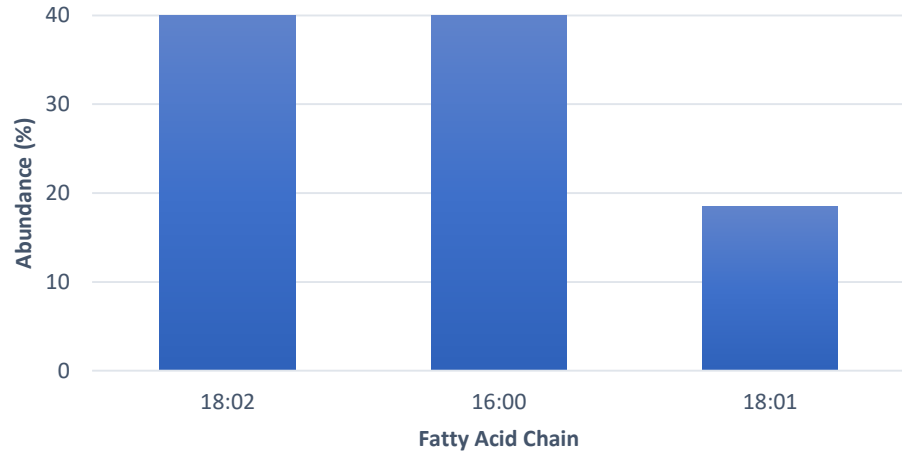
F10-PE-R1-Neg



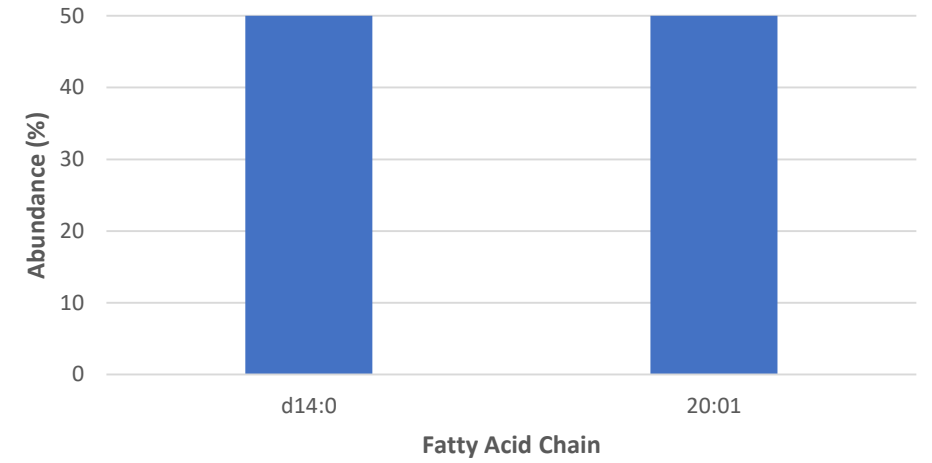
F10-PI-R1-Neg



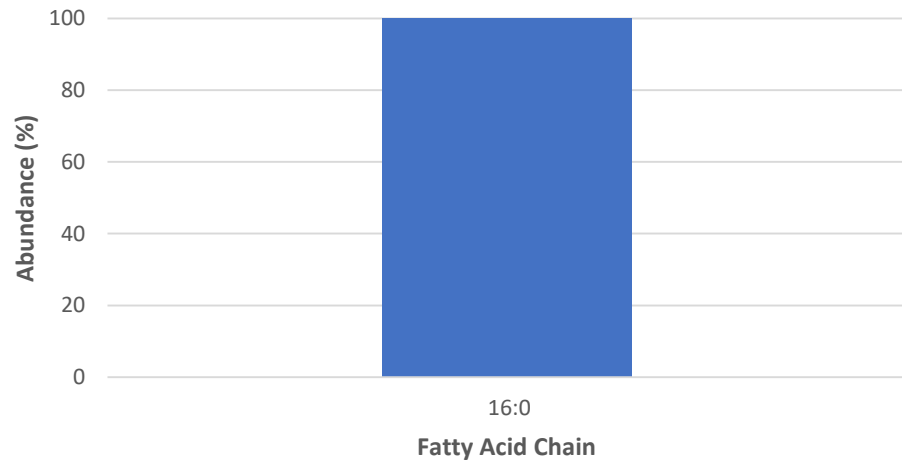
F10-PC-FA-R1-Neg



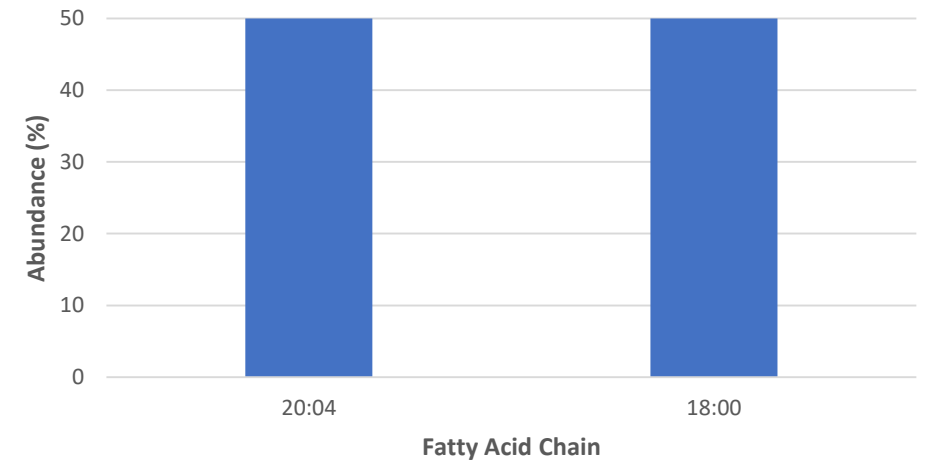
F10-SM-FA-R1-Neg

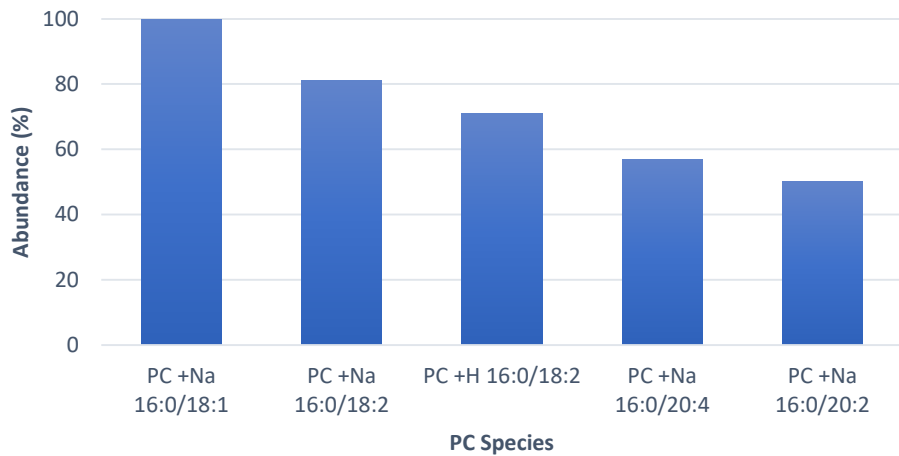
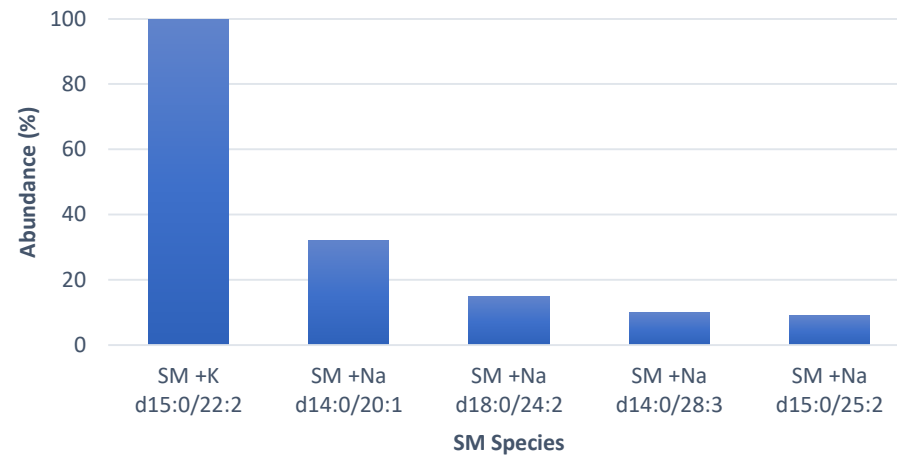
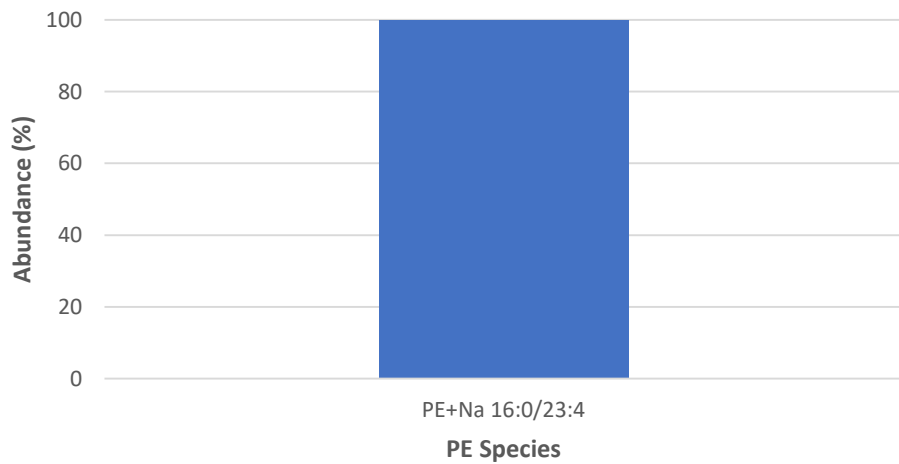
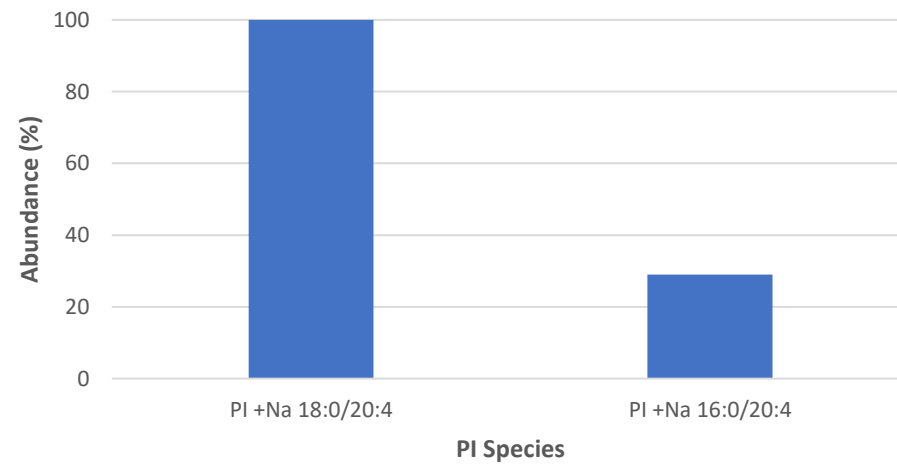


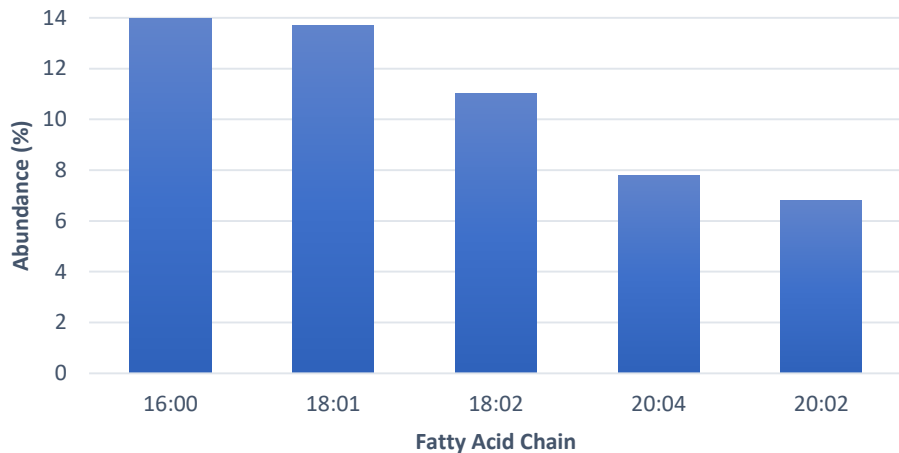
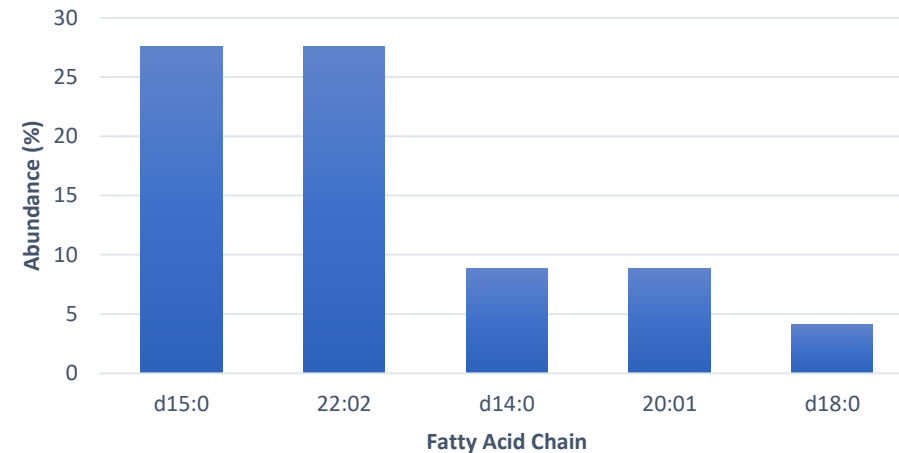
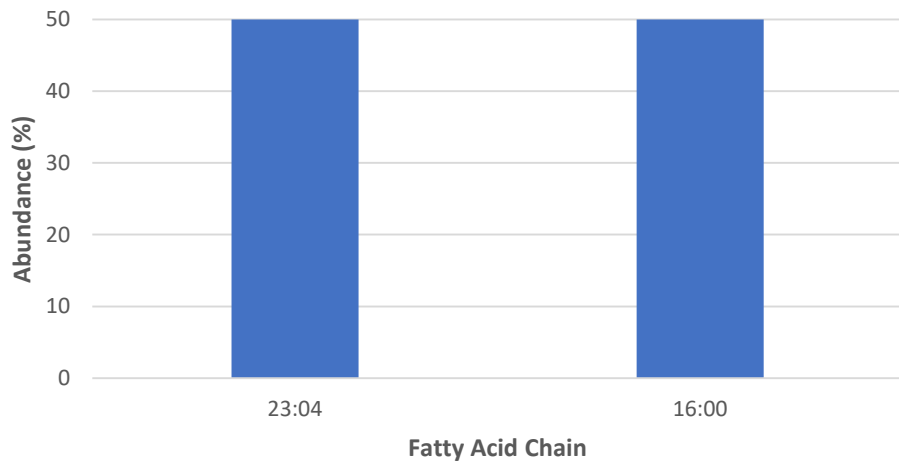
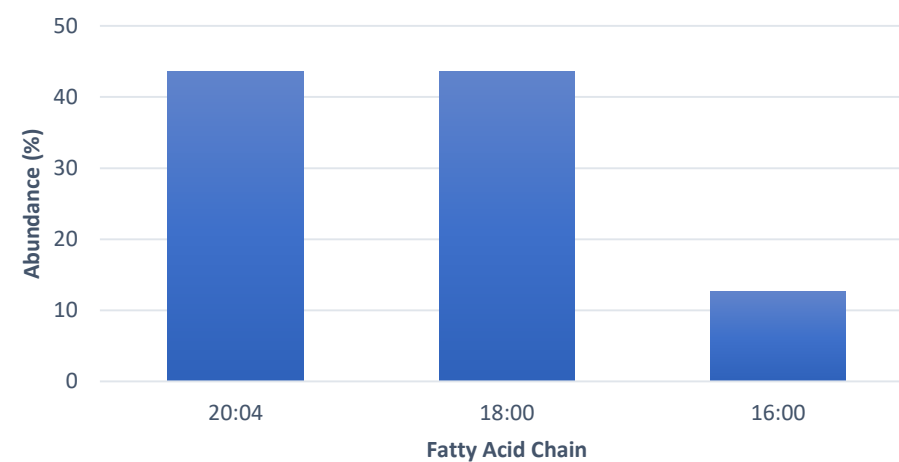
F10-PE-FA-R1-Neg



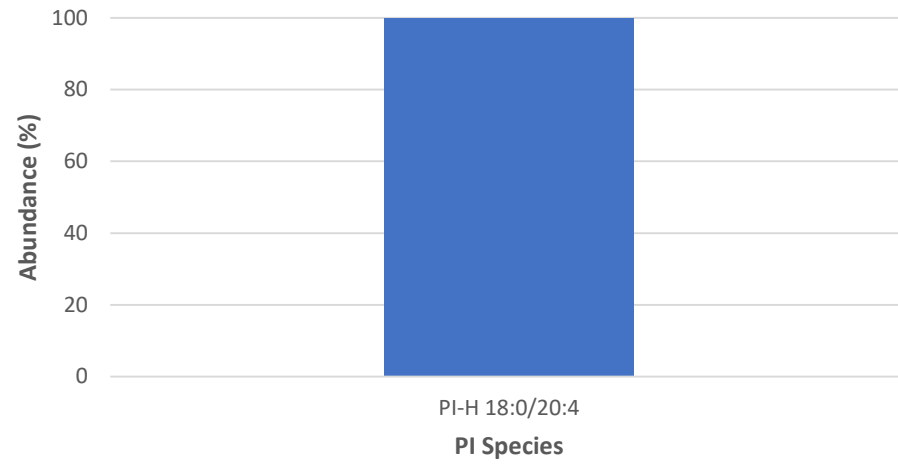
F10-PI-FA-R1-Neg



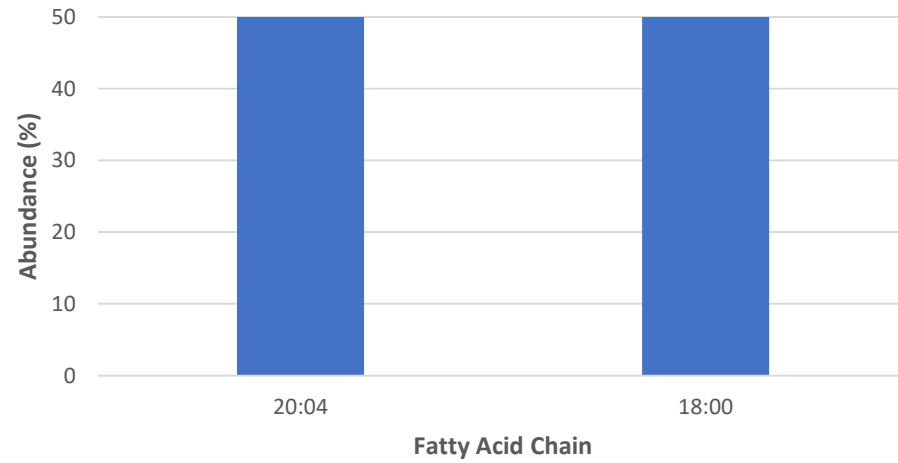
F10-PC-R2**F10-SM-R2****F10-PE-R2****F10-PI-R2**

F10-PC-FA-R2**F10-SM-FA-R2****F10-PE-FA-R2****F10-PI-FA-R2**

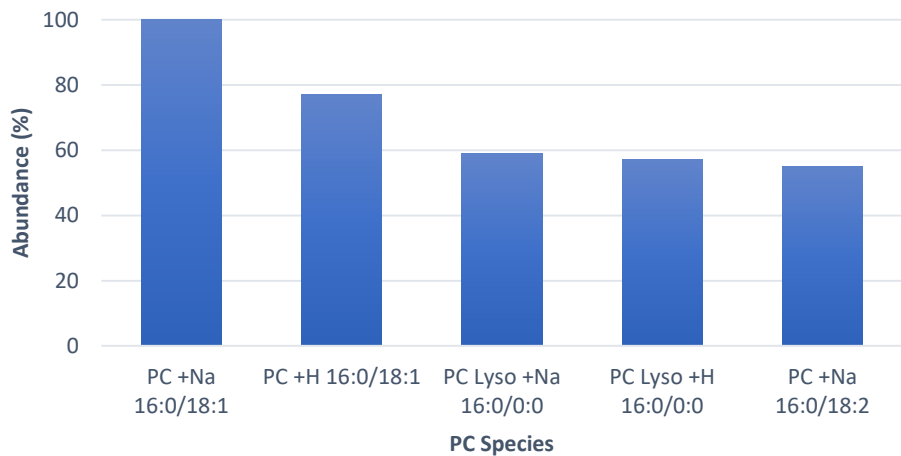
F10-PI-R2-Neg



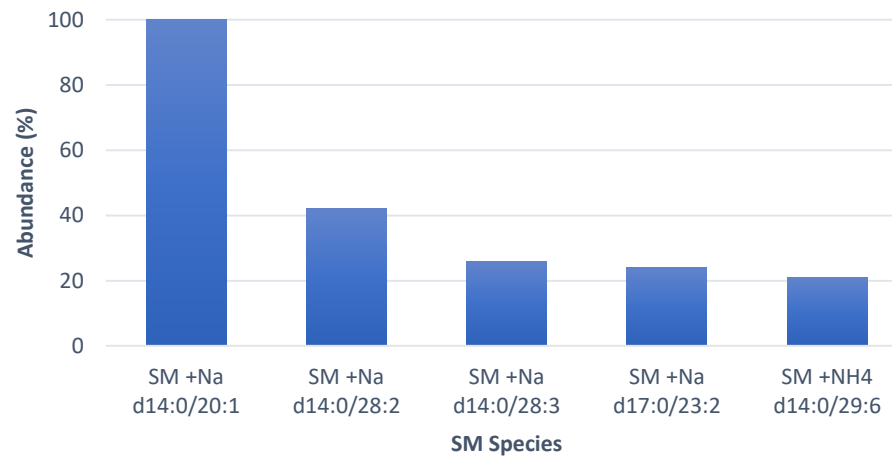
F10-PI-FA-R2-Neg



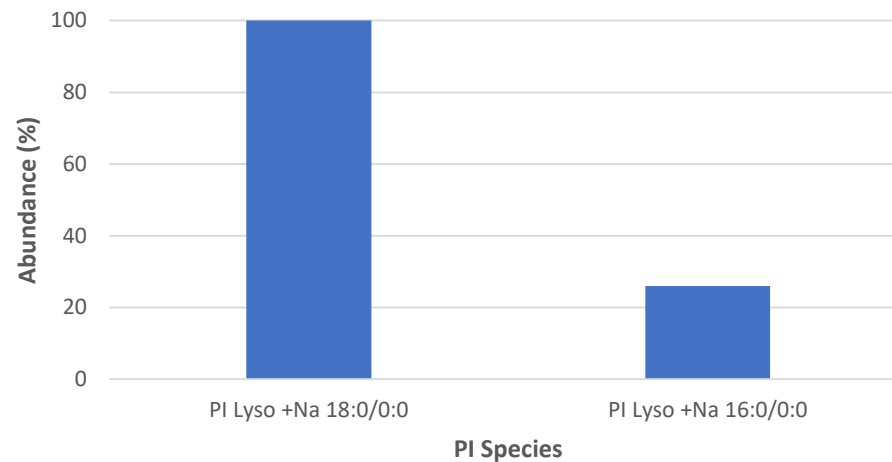
F10-PC-R3



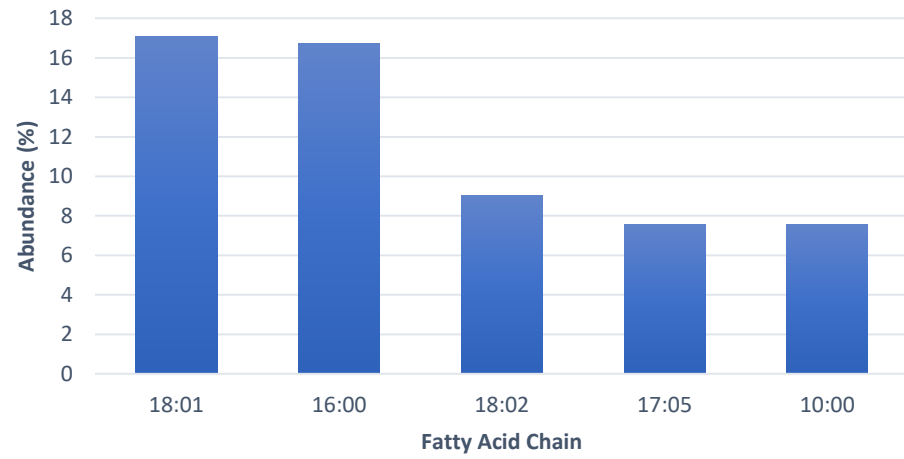
F10-SM-R3



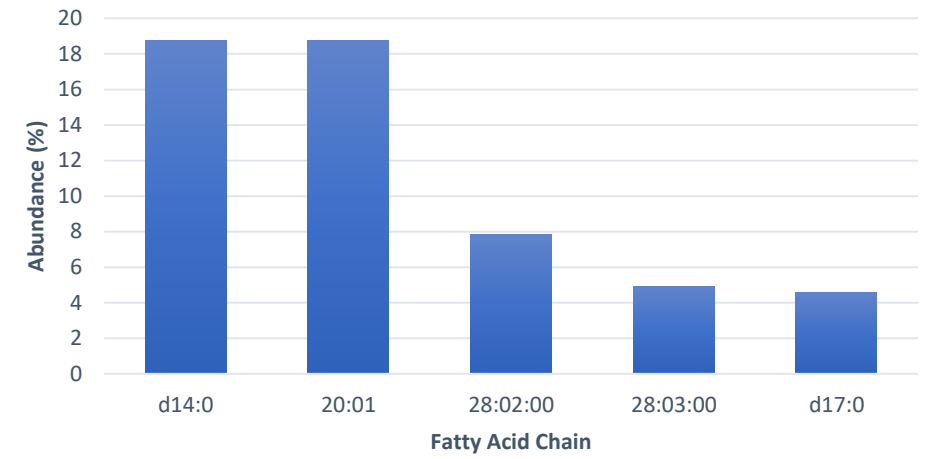
F10-PI-R3



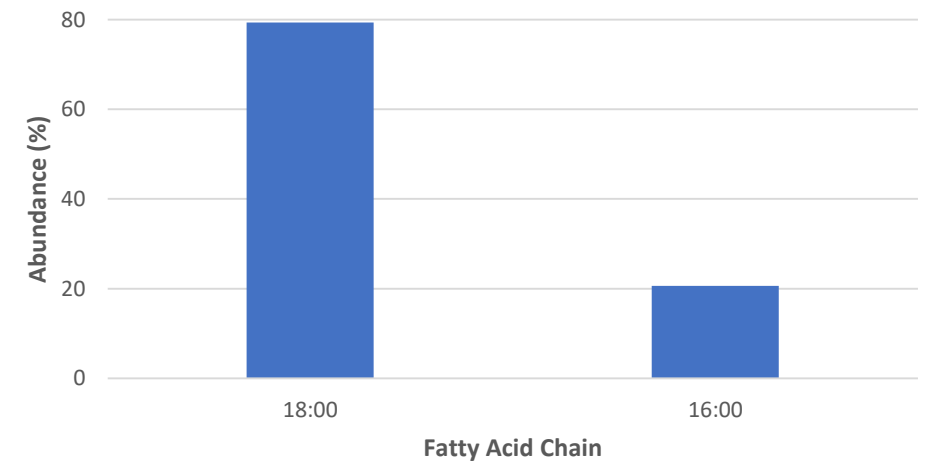
F10-PC-FA-R3



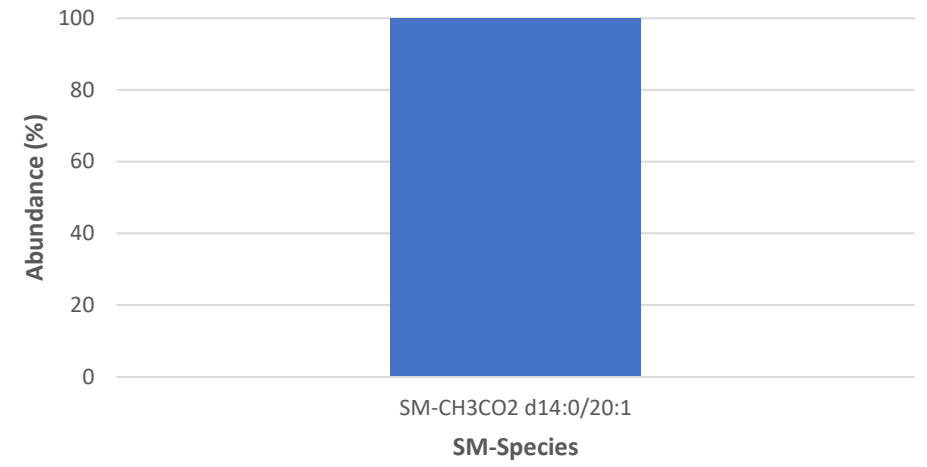
F10-SM-FA-R3



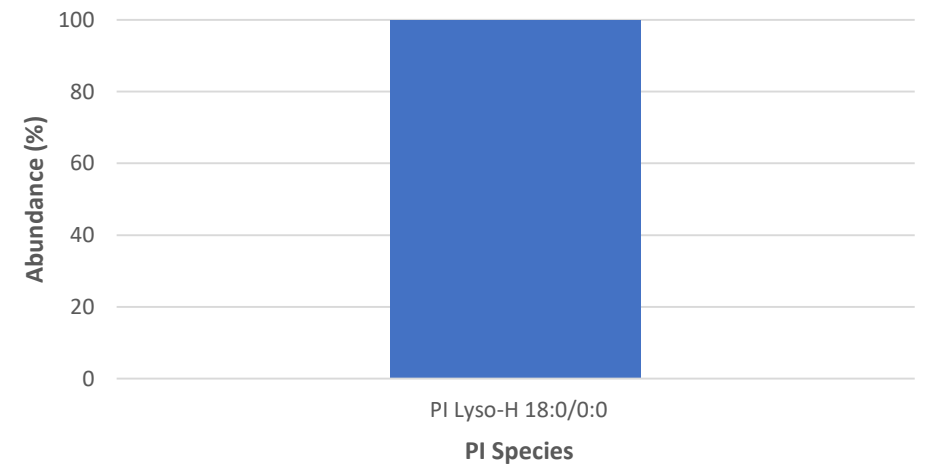
F10-PI-FA-R3



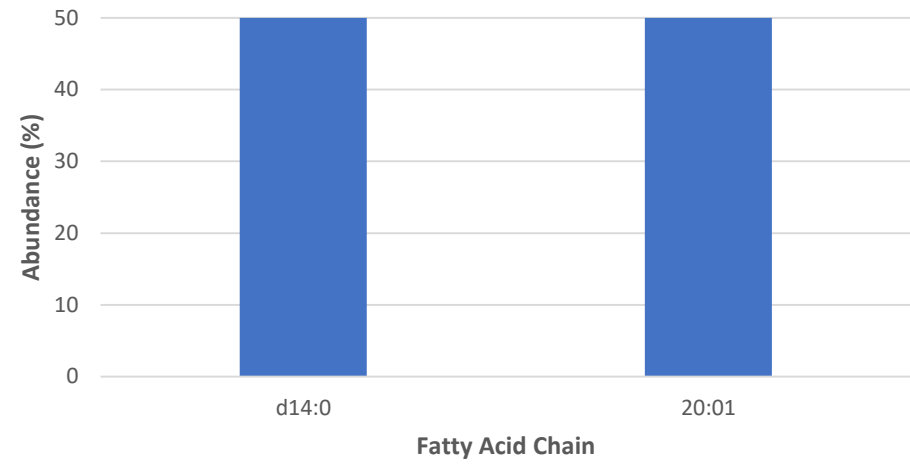
F10-SM-R3-Neg



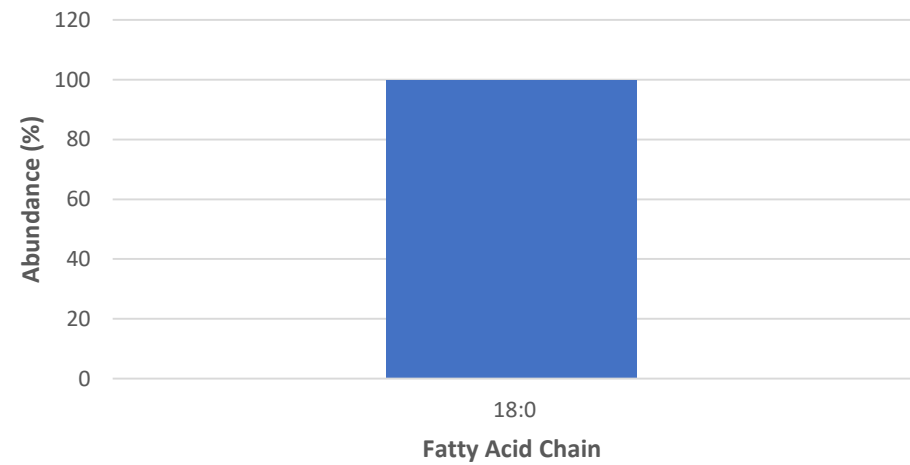
F10-PI-R3-Neg



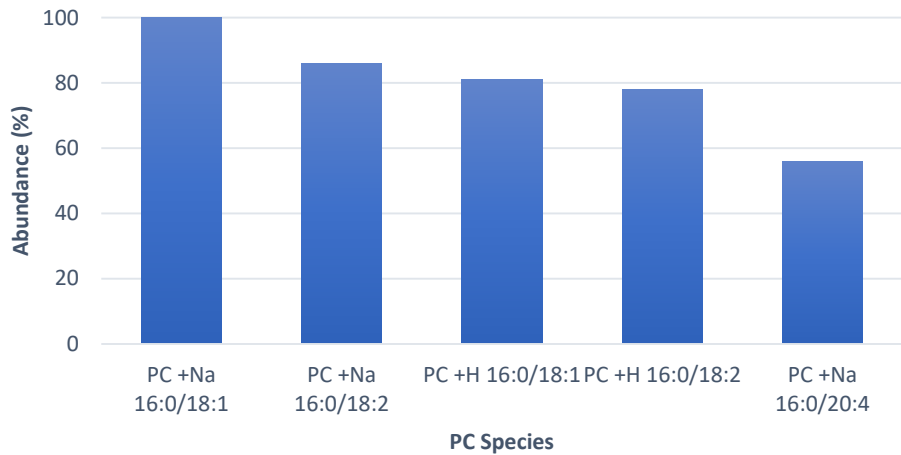
F10-SM-FA-R3-Neg



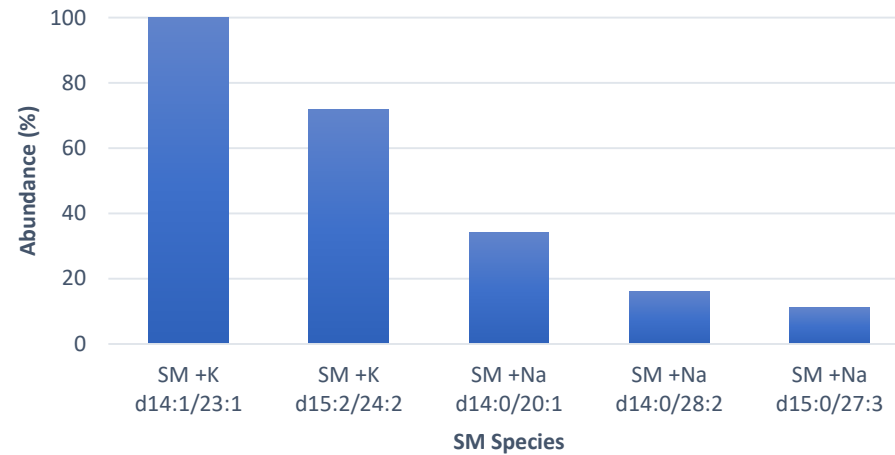
F10-PI-FA-R3-Neg



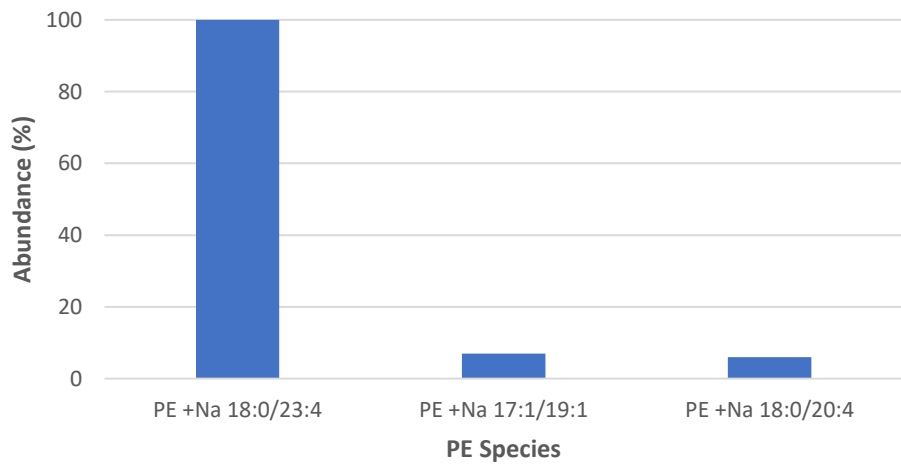
F10-PC-R4



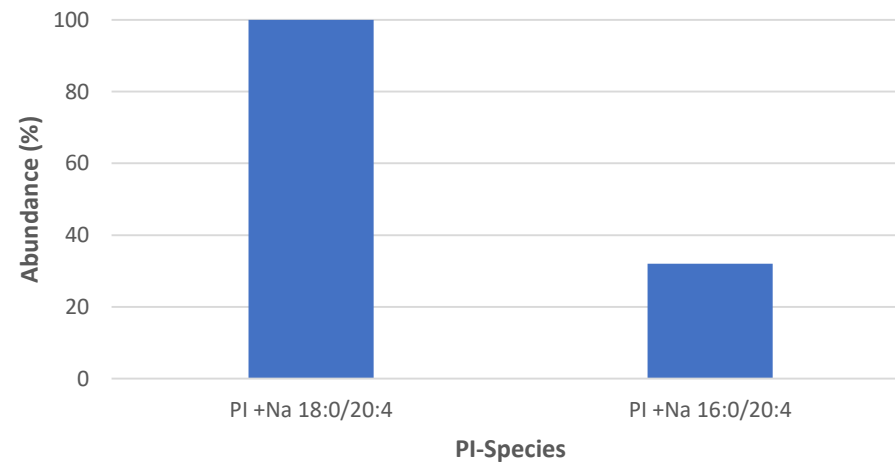
F10-SM-R4



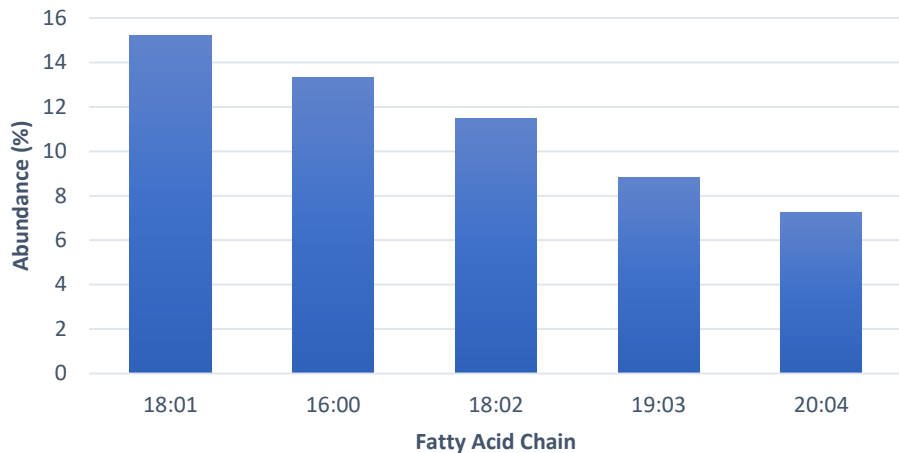
F10-PE-R4



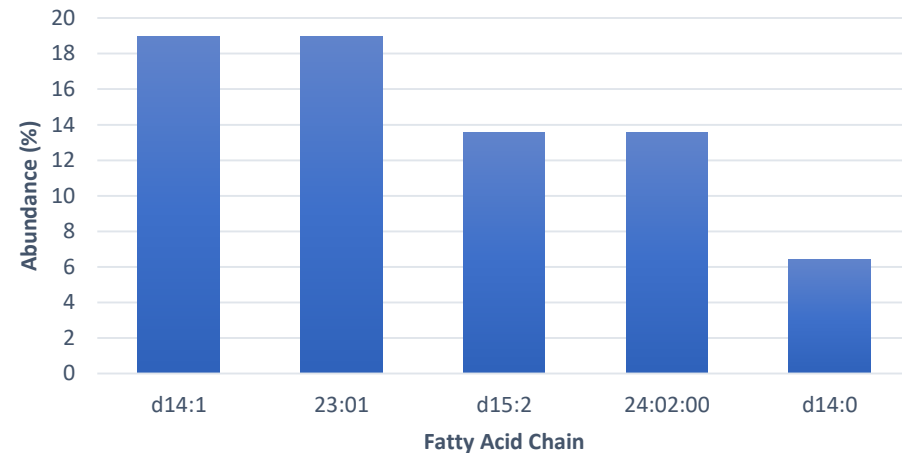
F10-PI-R4



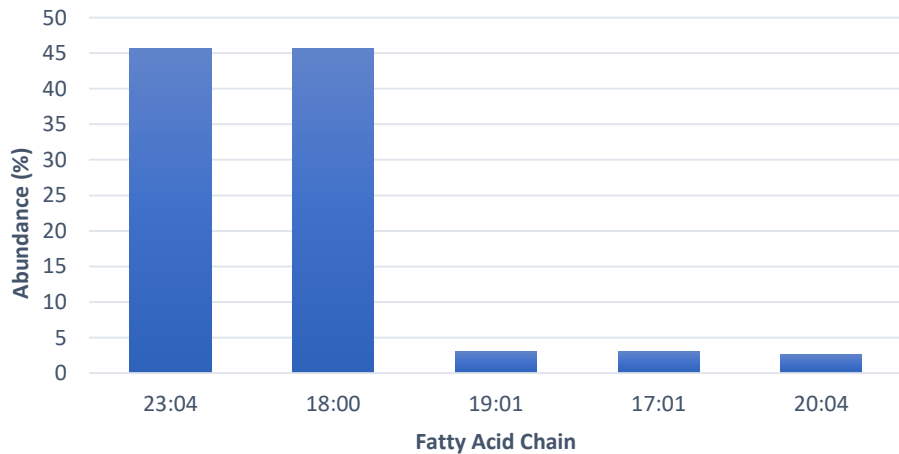
F10-PC-FA-R4



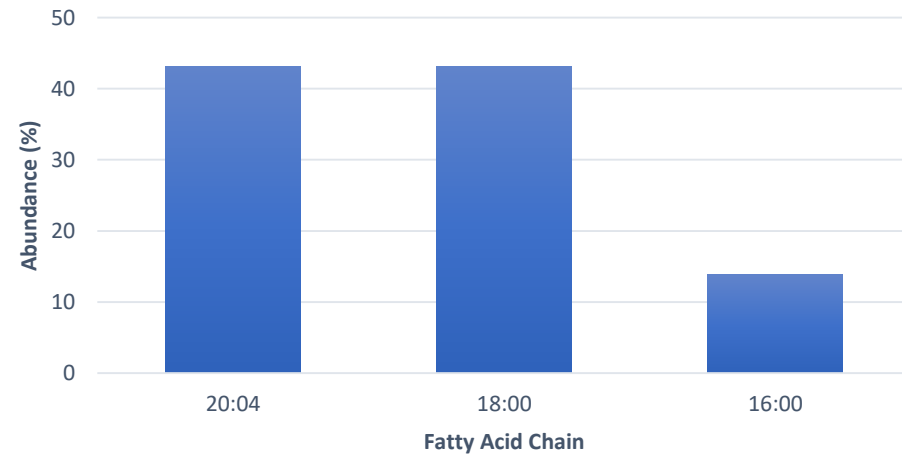
F10-SM-FA-R4



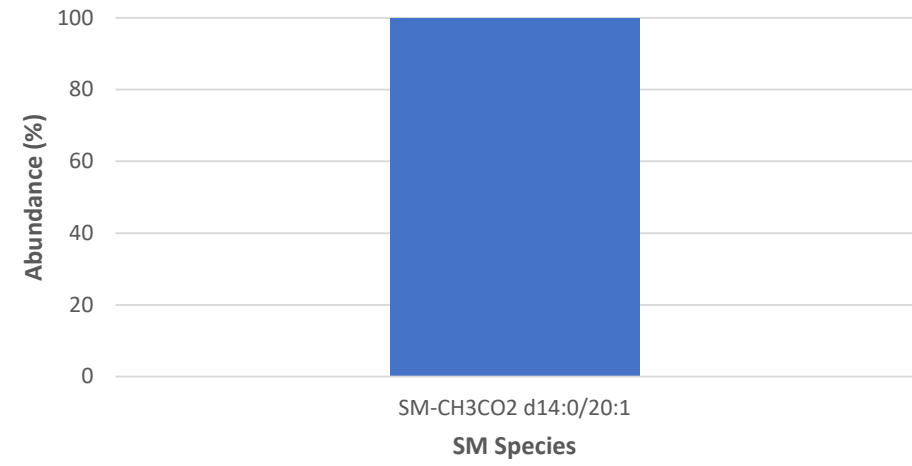
F10-PE-FA-R4



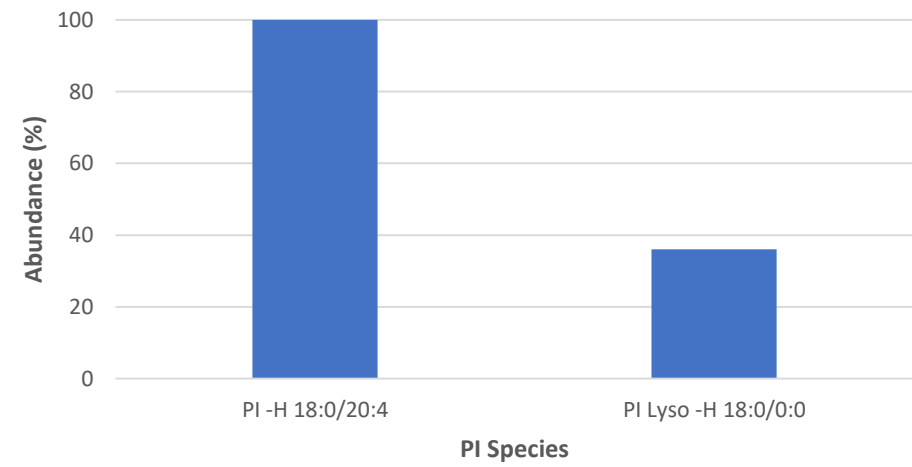
F10-PI-FA-R4



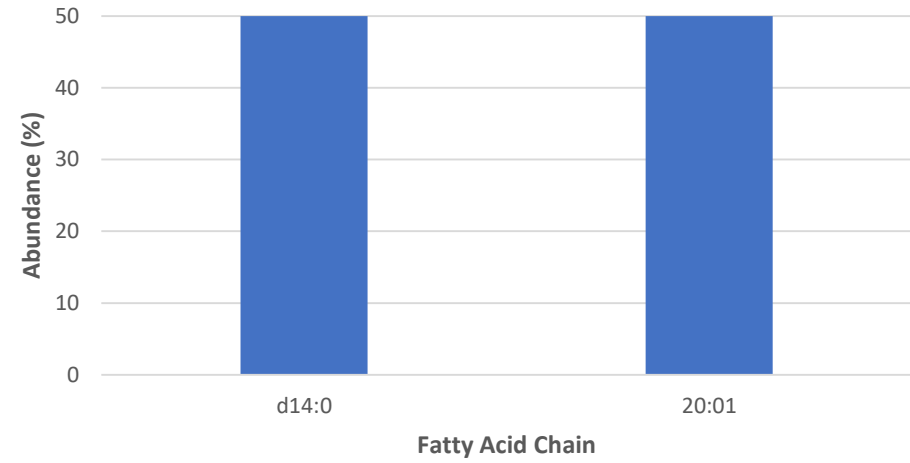
F10-SM-R4-Neg



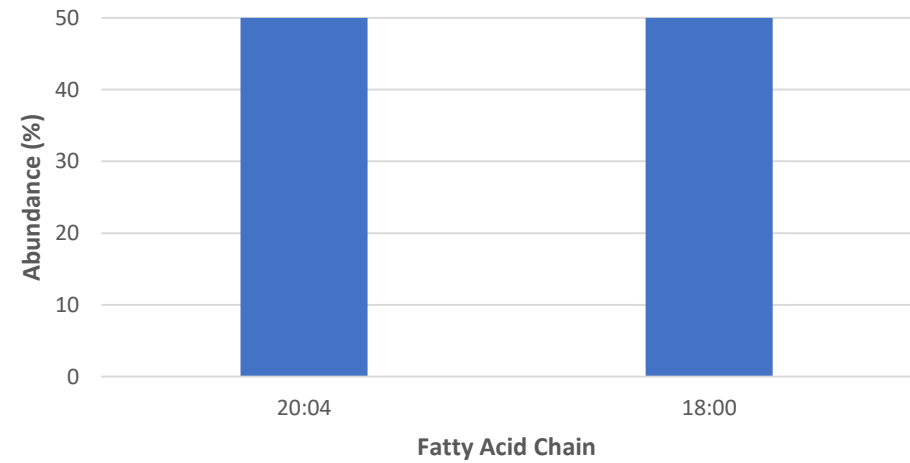
F10-PI-R4-Neg

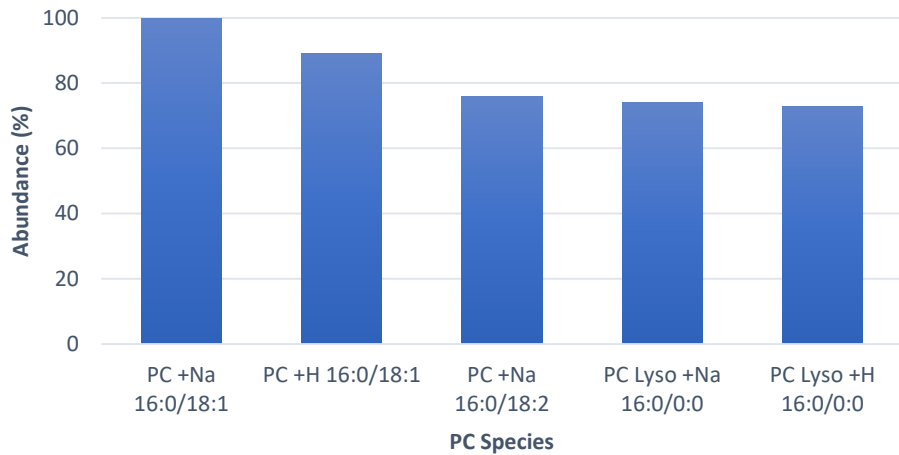
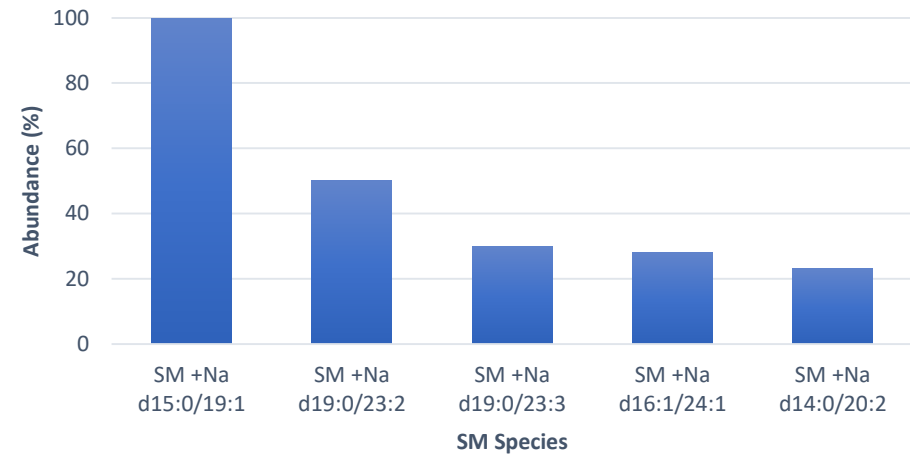
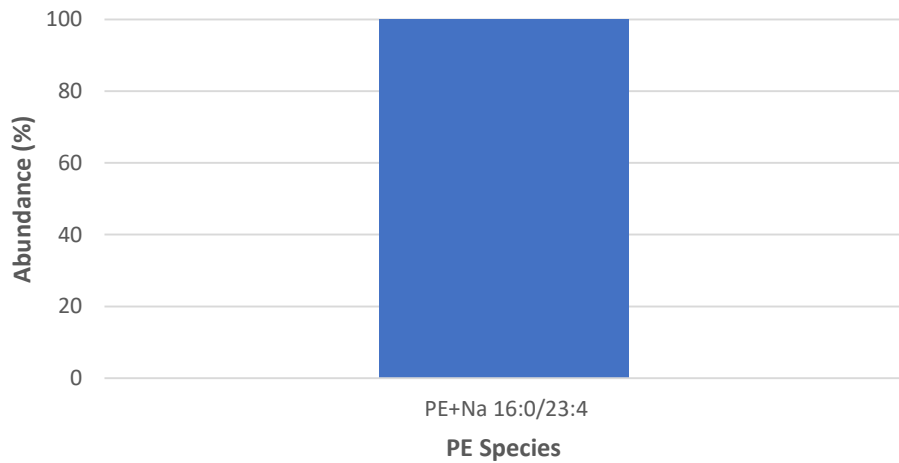
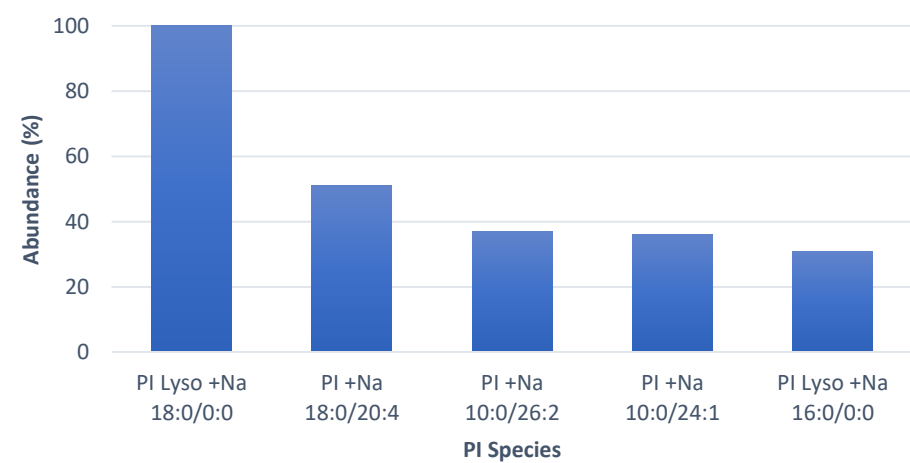


F10-SM-FA-R4-Neg

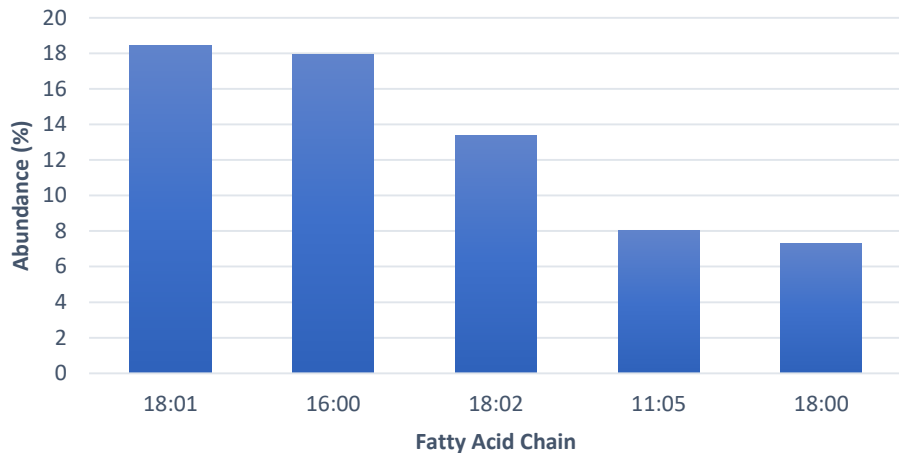


F10-PI-FA-R4-Neg

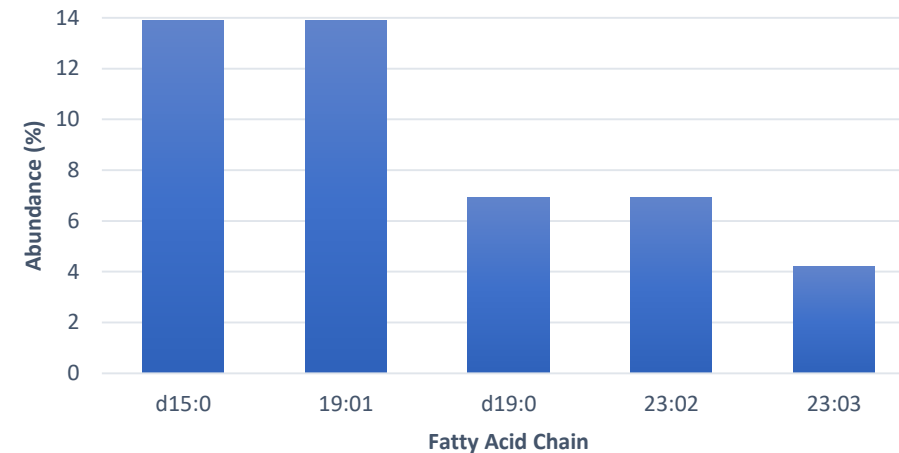


F10-PC-R5**F10-SM-R5****F10-PE-R5****F10-PI-R5**

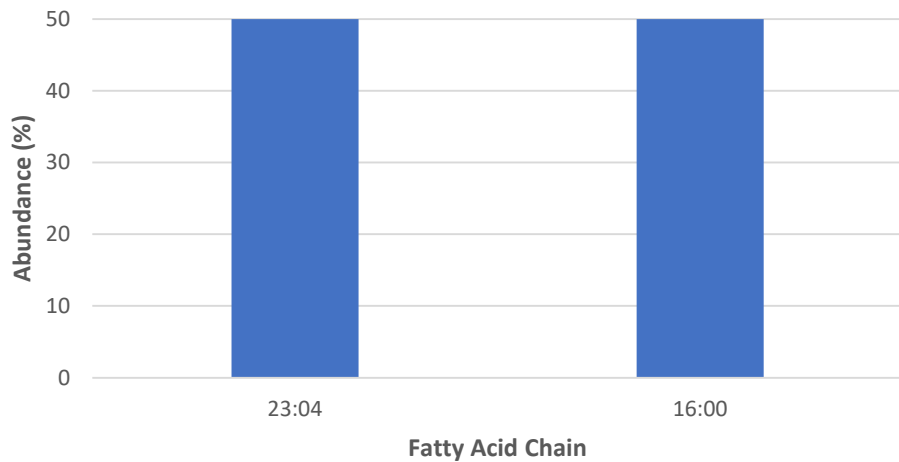
F10-PC-FA-R5



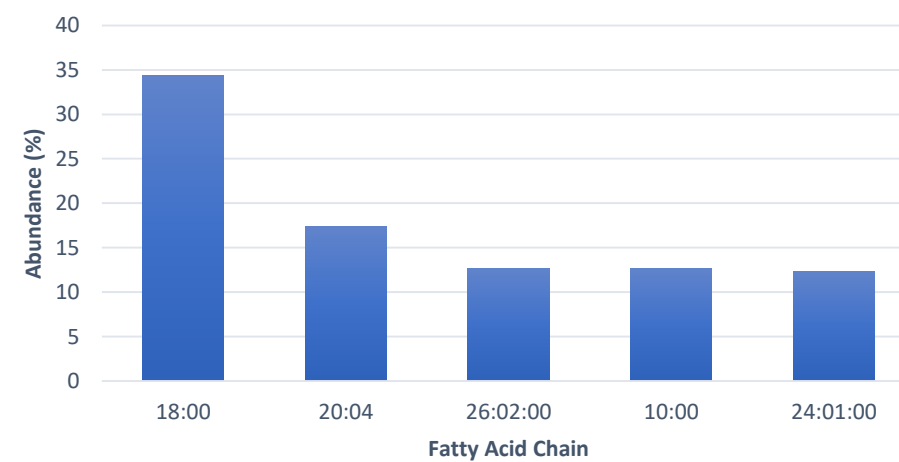
F10-SM-FA-R5



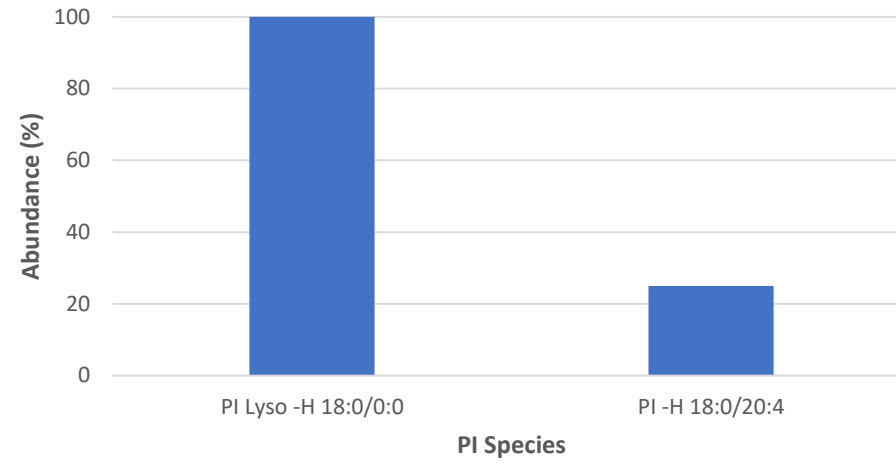
F10-PE-FA-R5



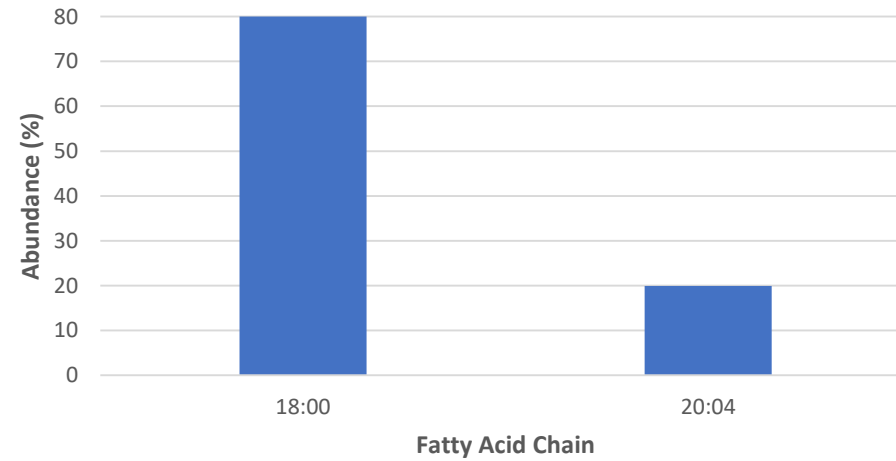
F10-PI-FA-R5



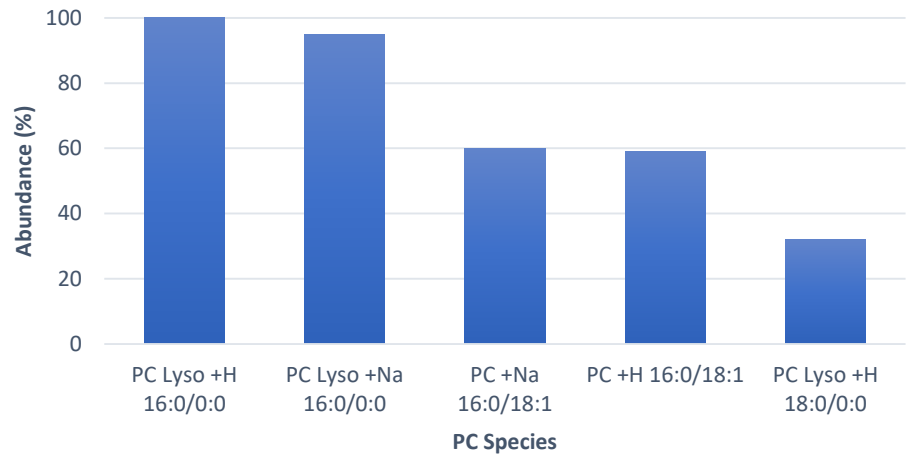
F10-PI-R5-Neg



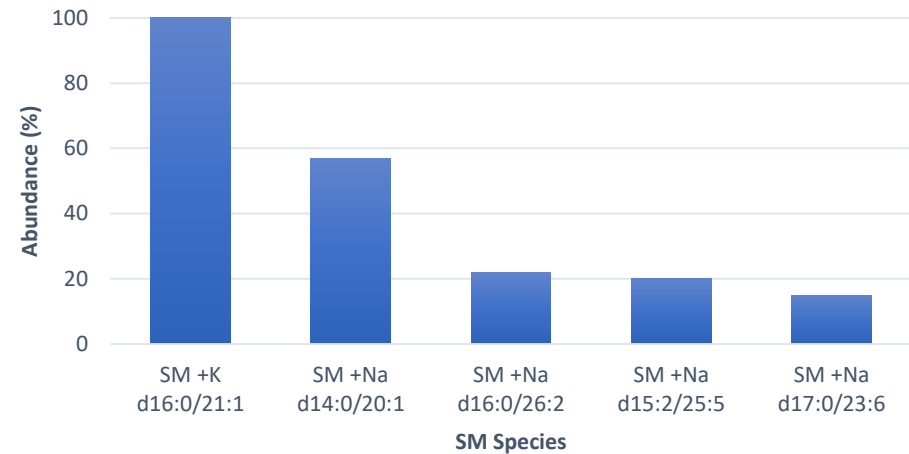
F10-PI-FA-R5-Neg



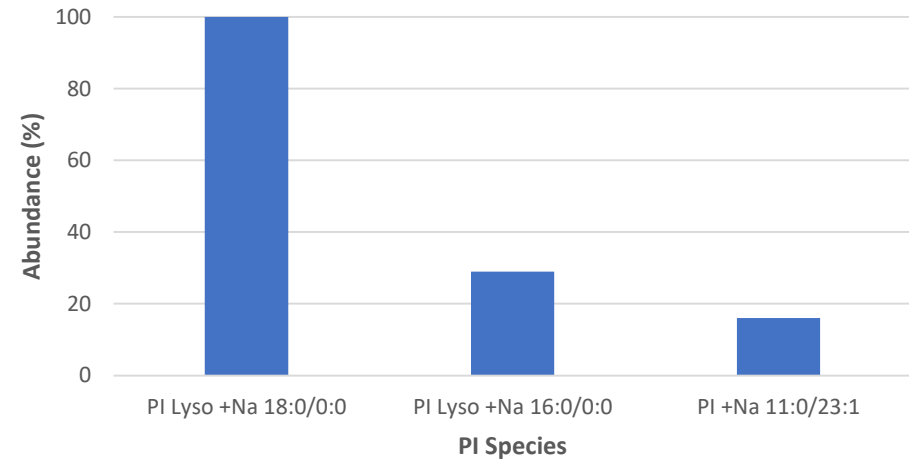
F11-PC-R1

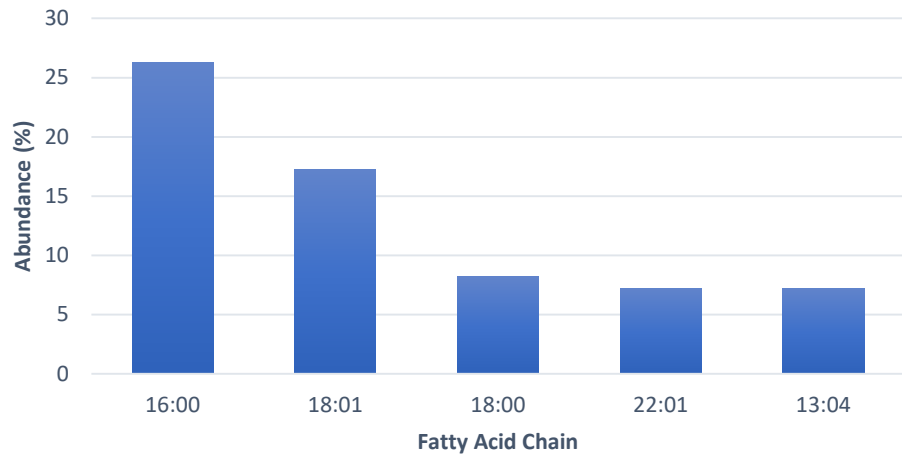
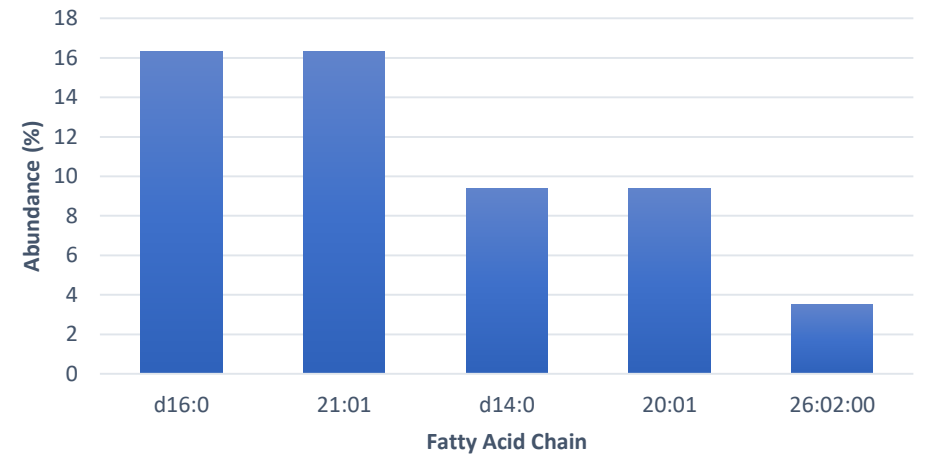
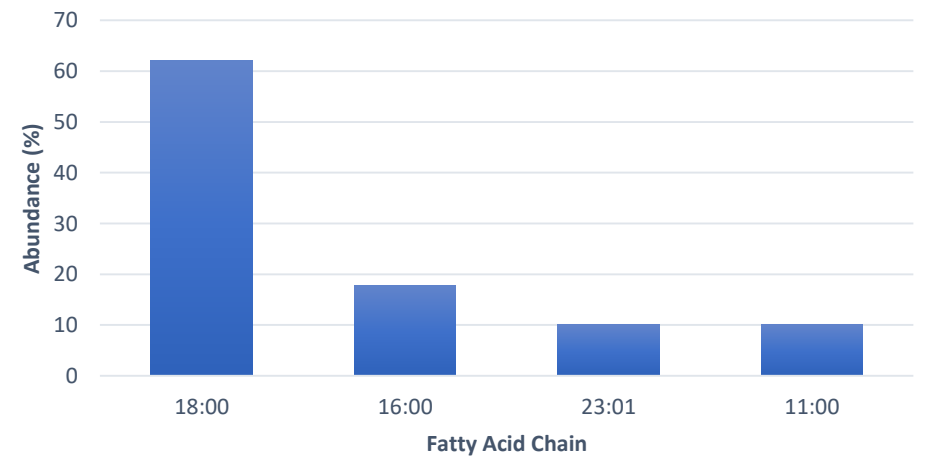


F11-SM-R1

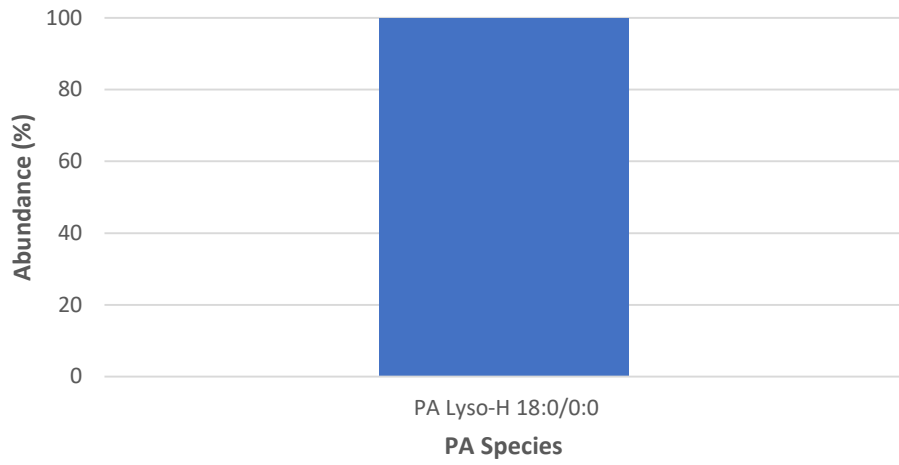


F11-PI-R1

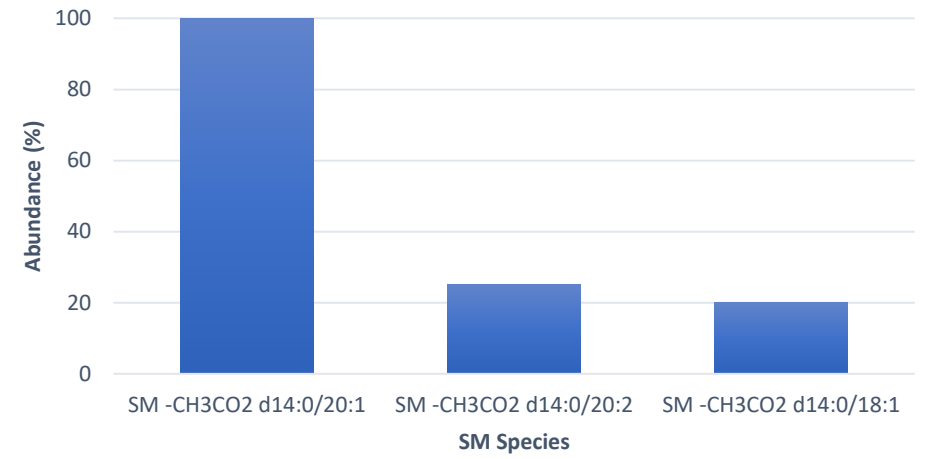


F11-PC-FA-R1**F11-SM-FA-R1****F11-PI-FA-R1**

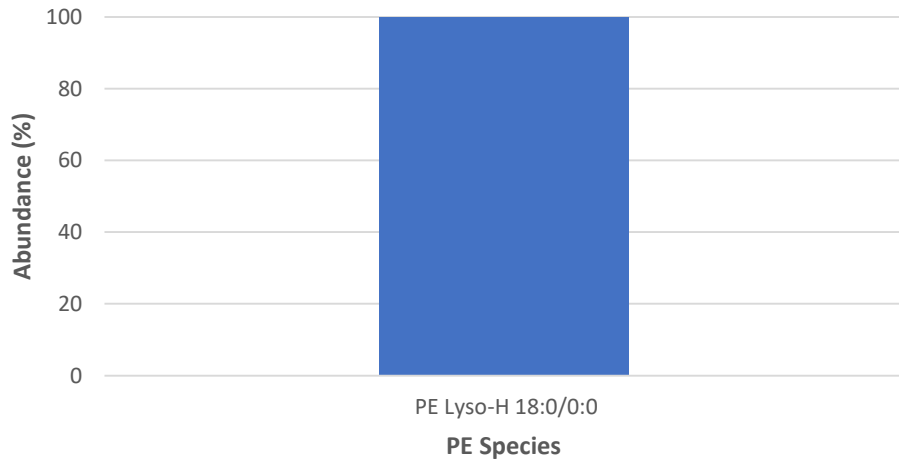
F11-PA-R1- Neg



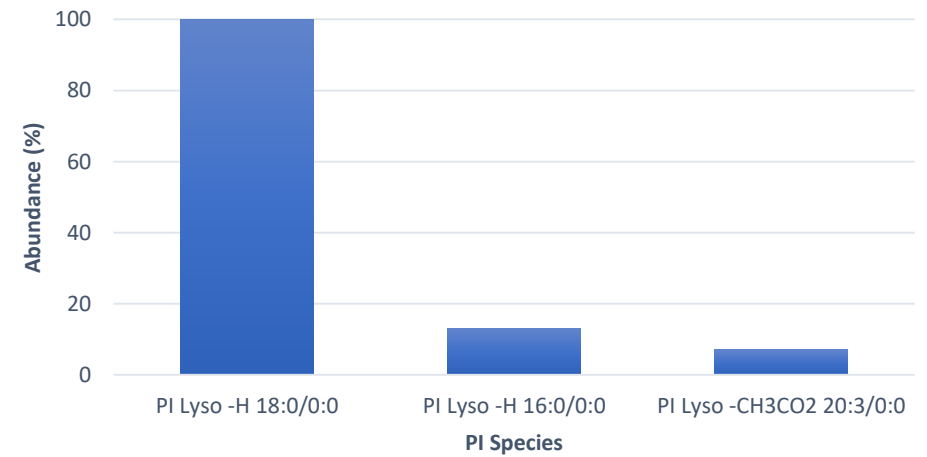
F11-SM-R1-Neg



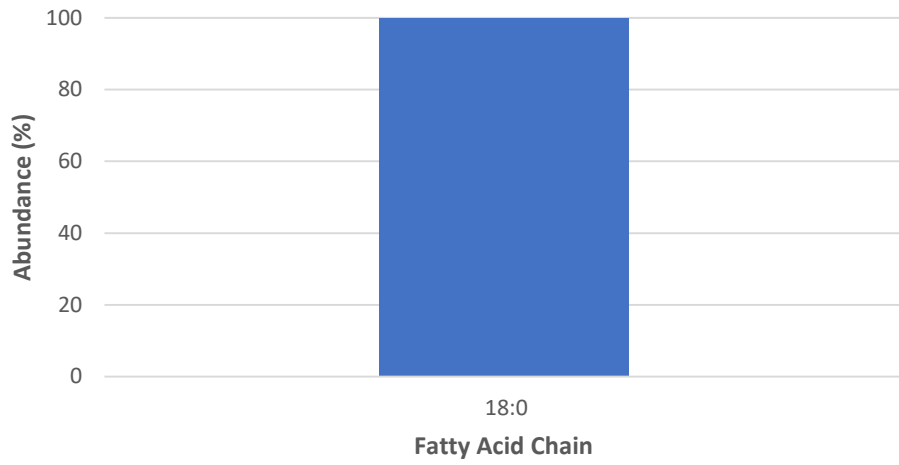
F11-PE-R1-Neg



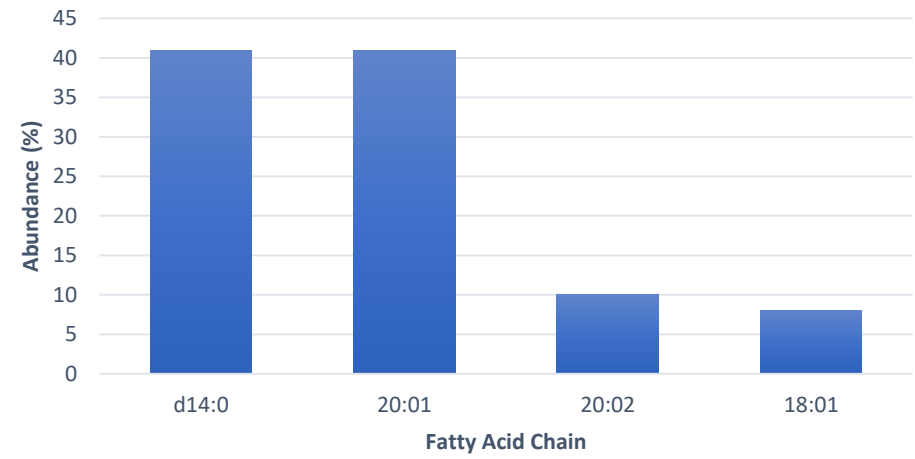
F11-PI-R1-Neg



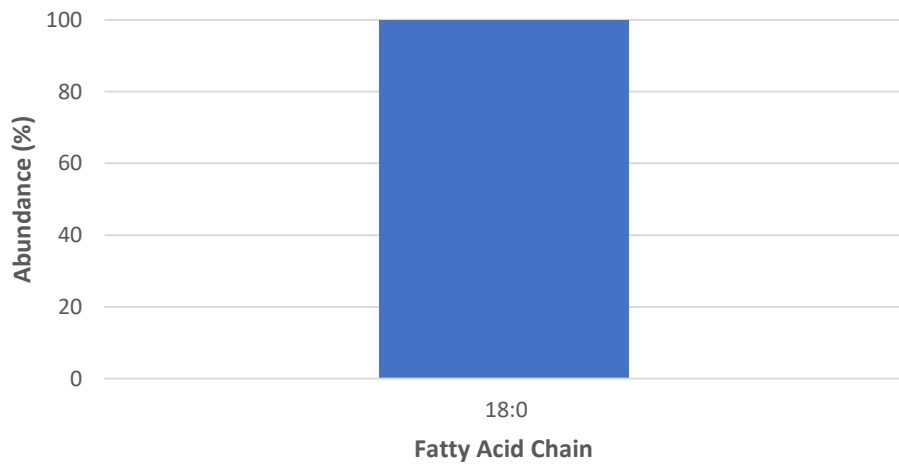
F11-PA-FA-R1-Neg



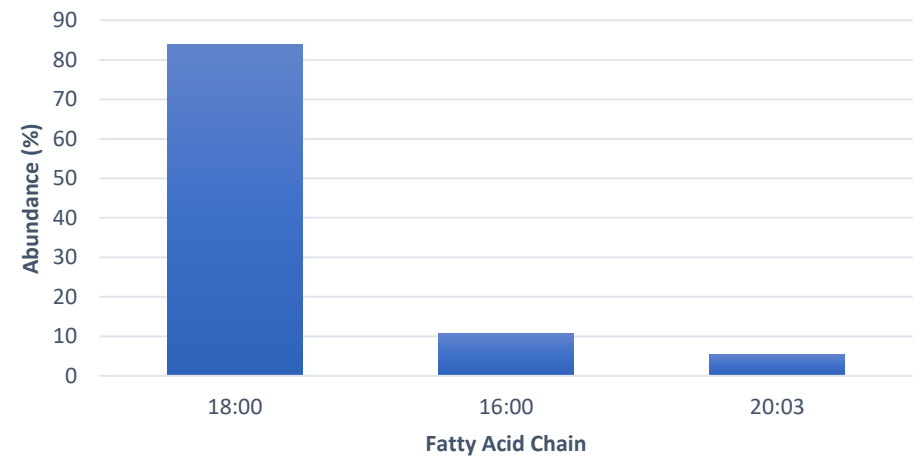
F11-SM-FA-R1-Neg



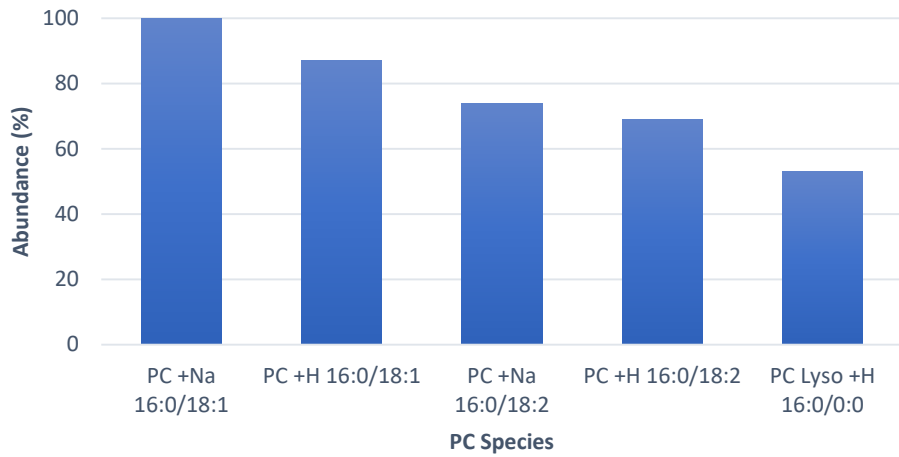
F11-PE-FA-R1-Neg



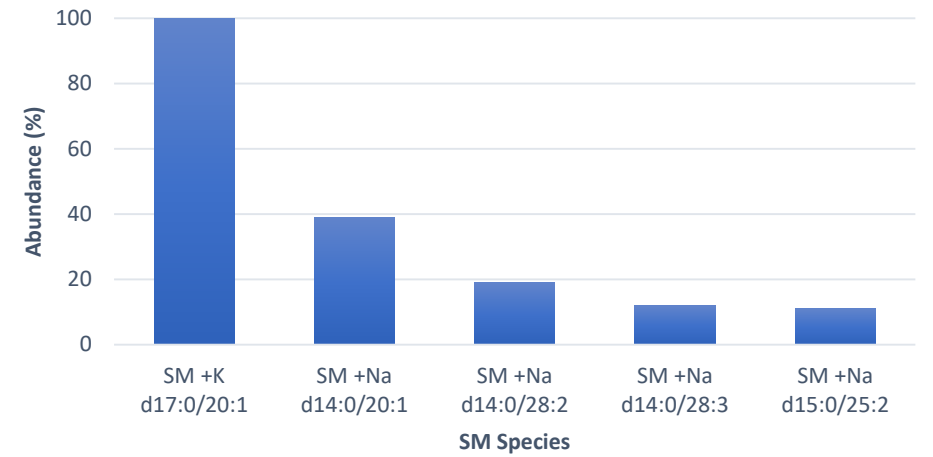
F11-PI-FA-R1-Neg



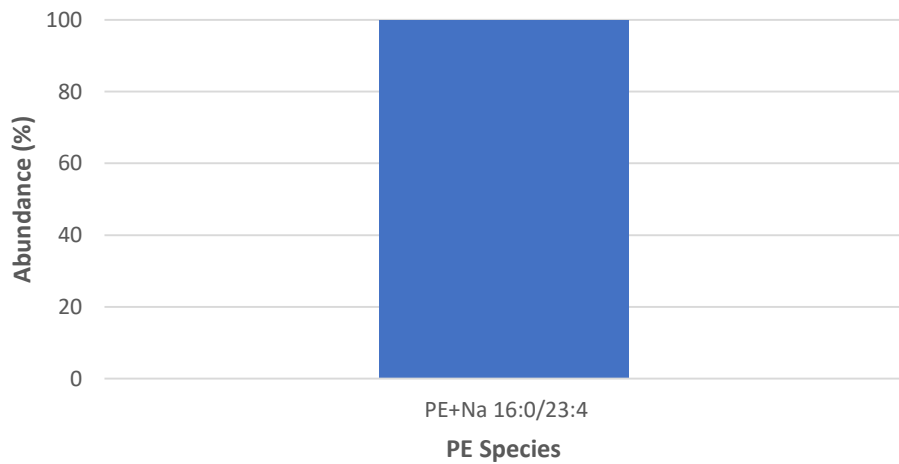
F11-PC-R2



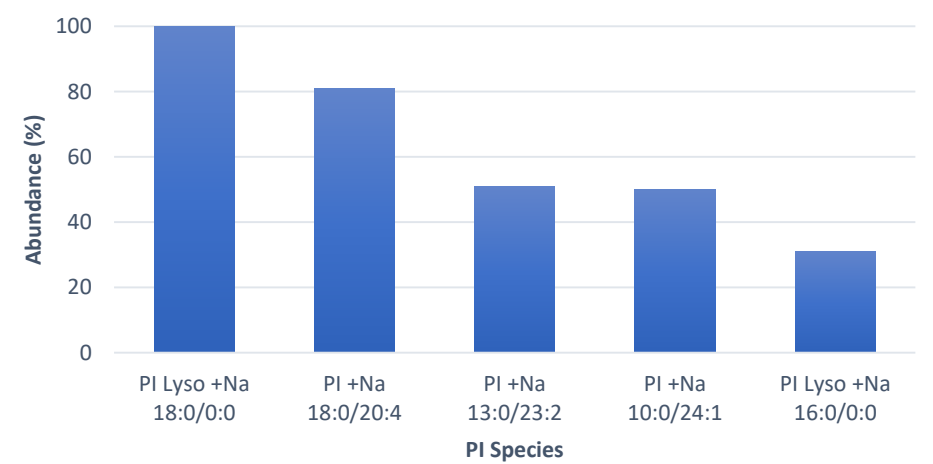
F11-SM-R2



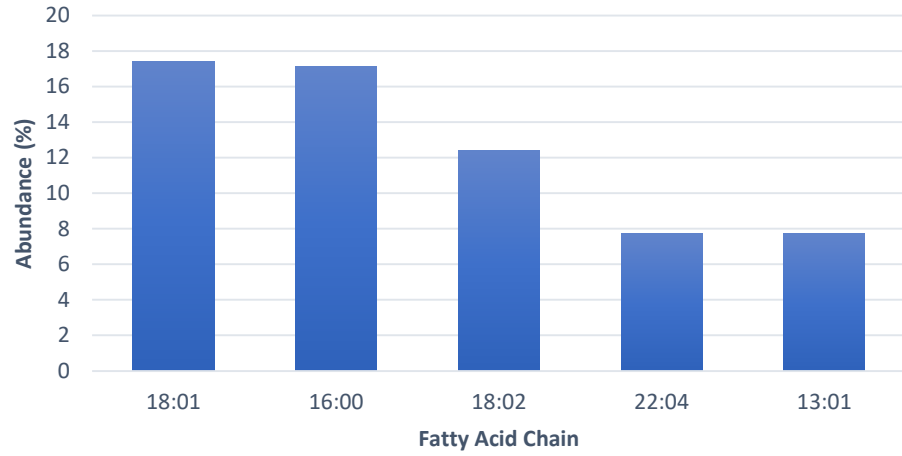
F11-PE-R2



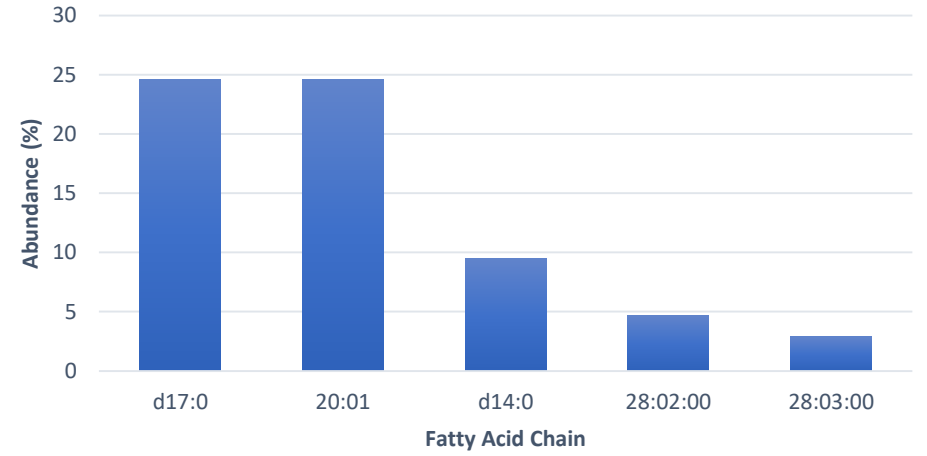
F11-PI-R2



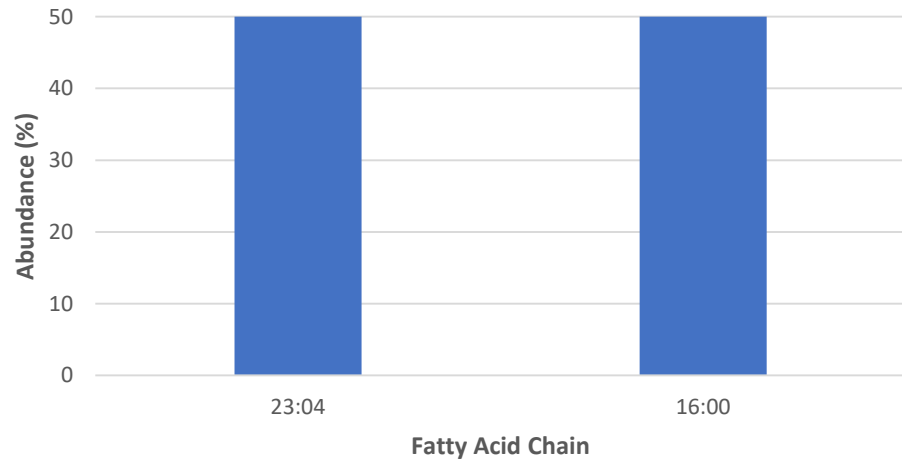
F11-PC-FA-R2



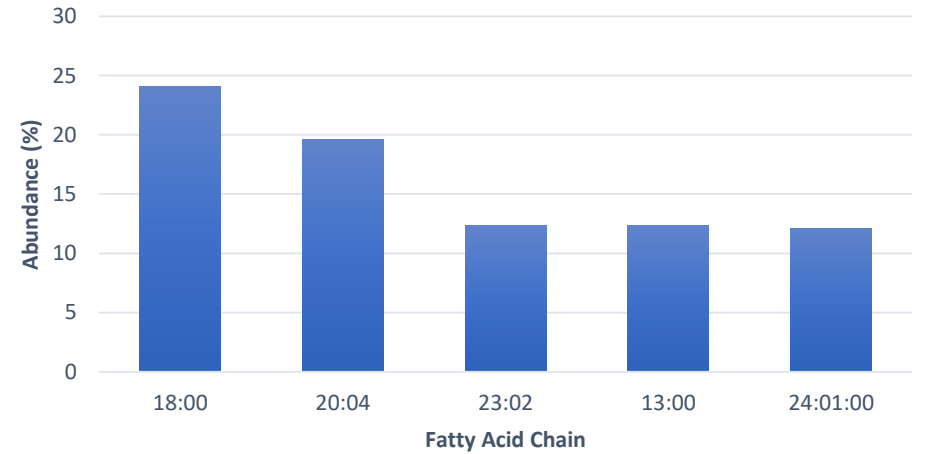
F11-SM-FA-R2



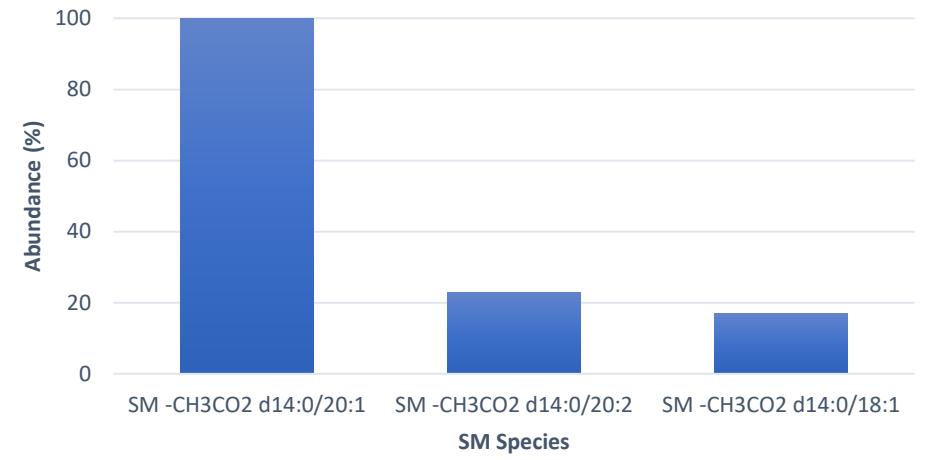
F11-PE-FA-R2



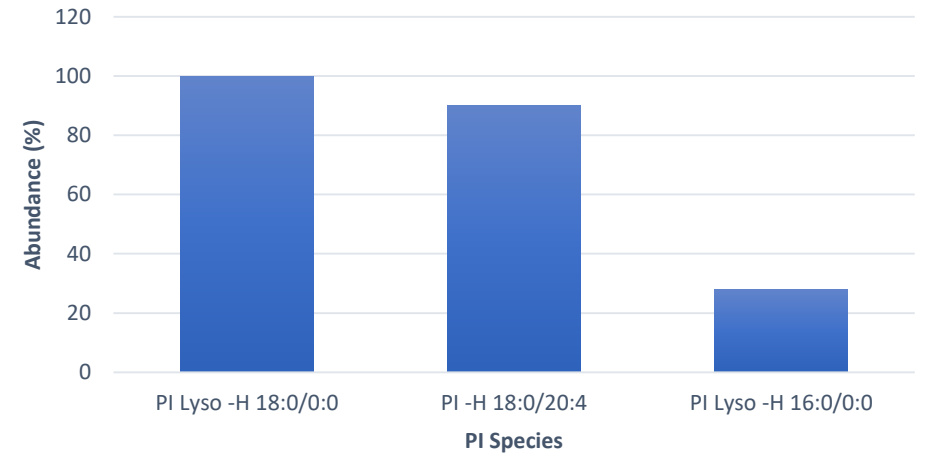
F11-PI-FA-R2



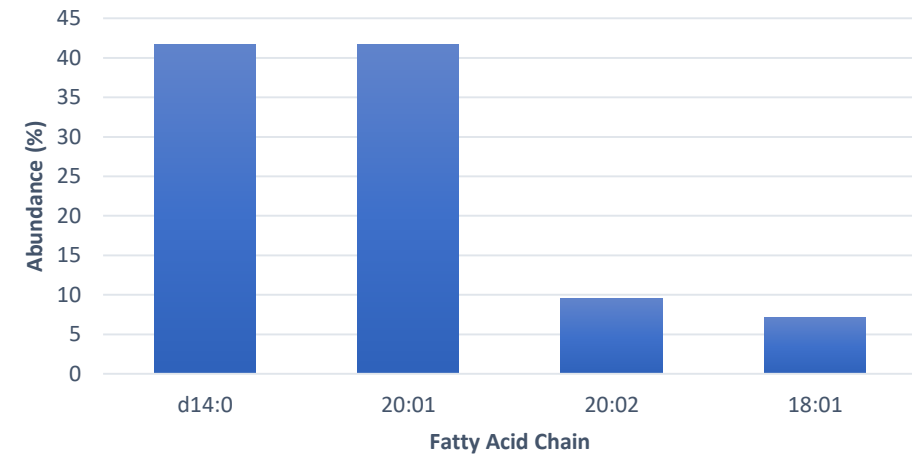
F11-SM-R2-Neg



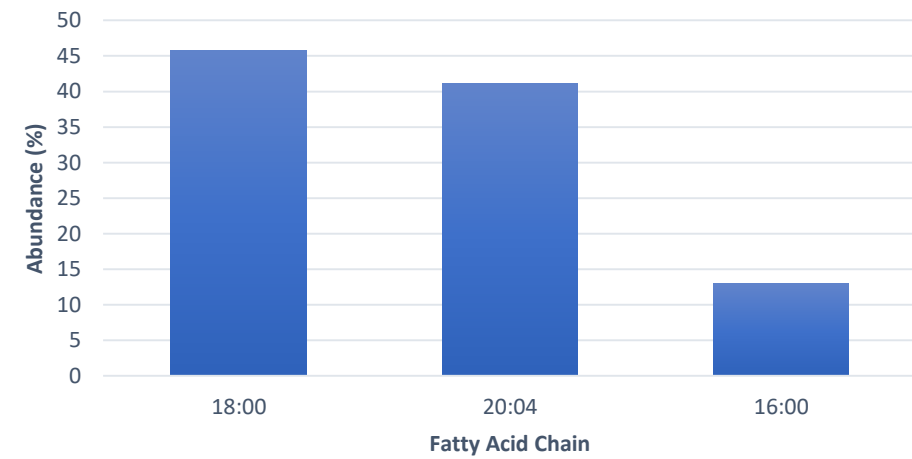
F11-PI-R2-Neg

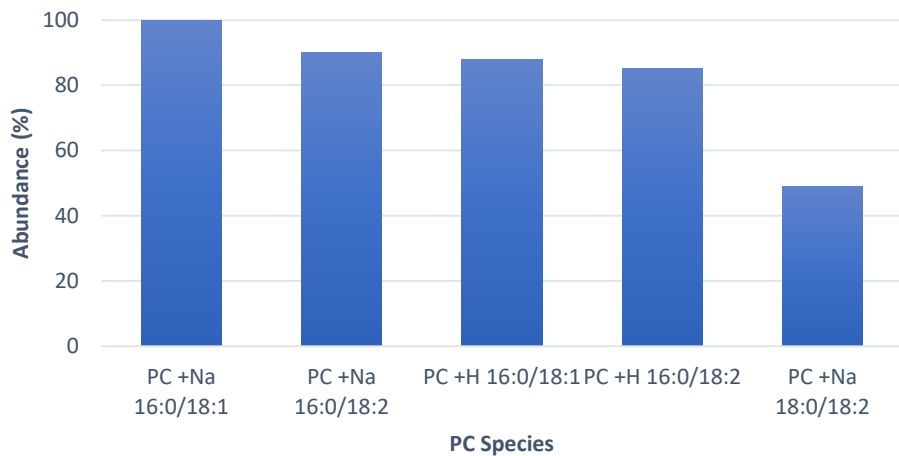
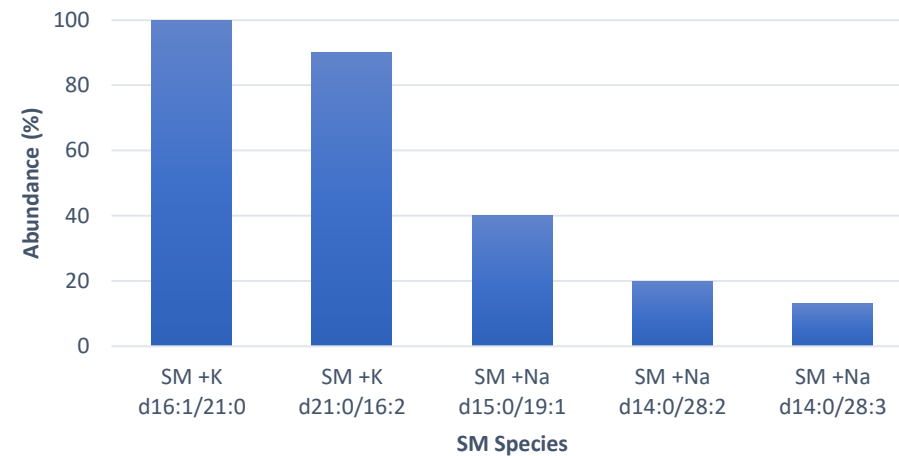
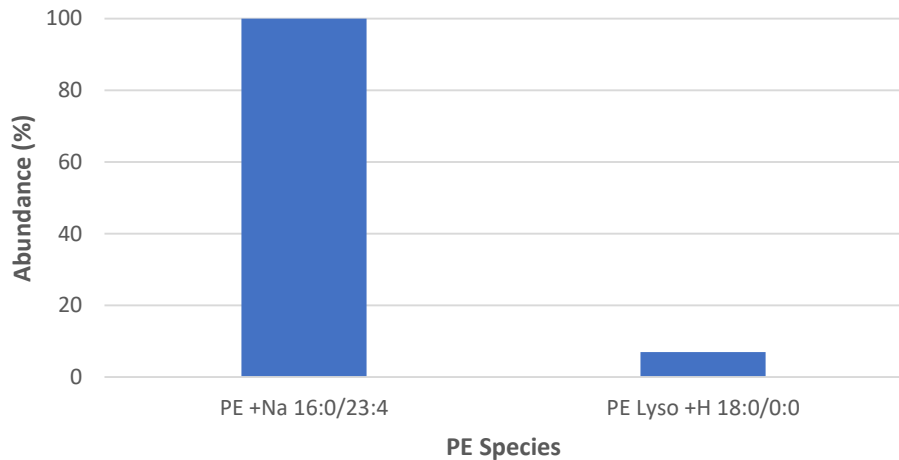
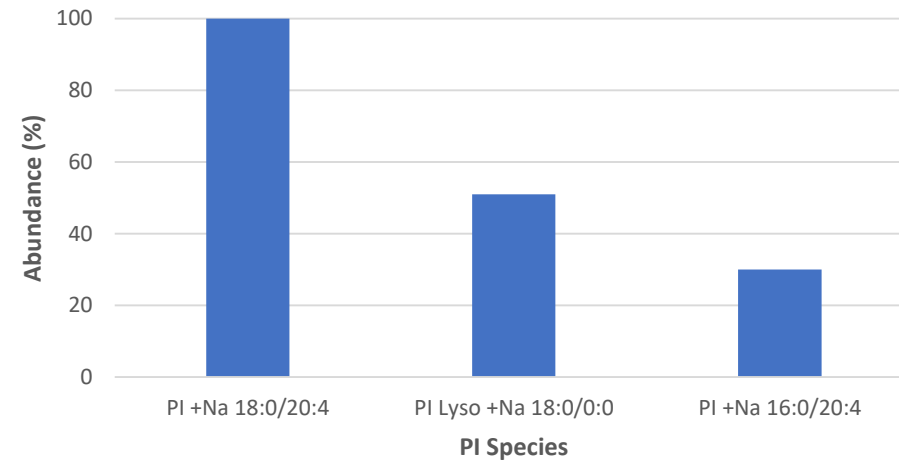


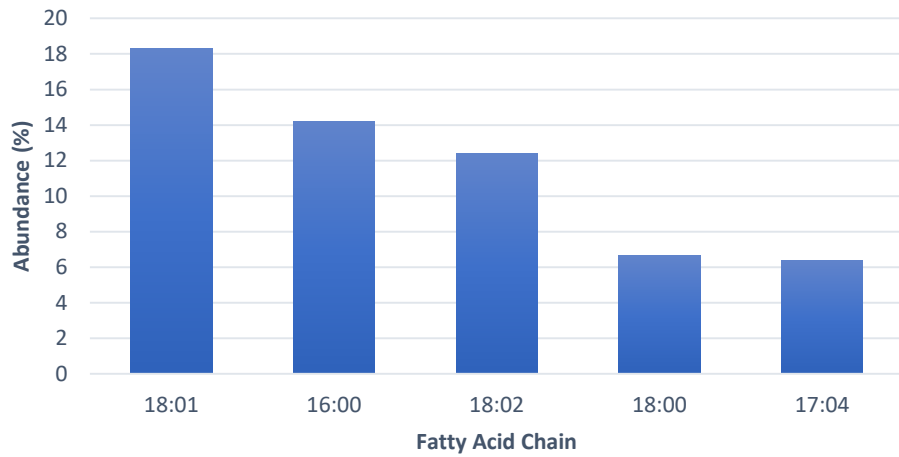
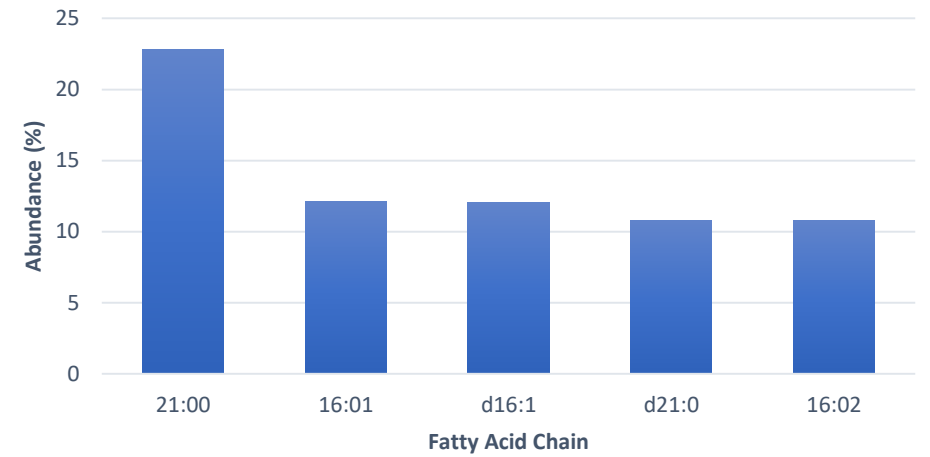
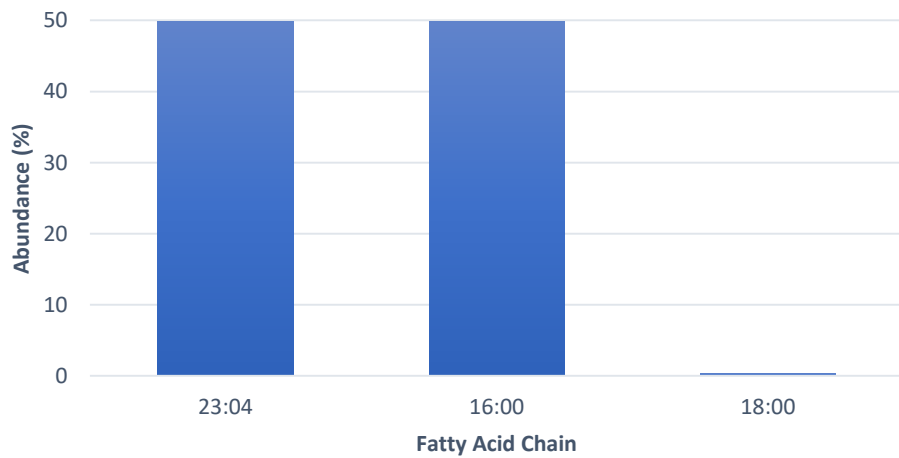
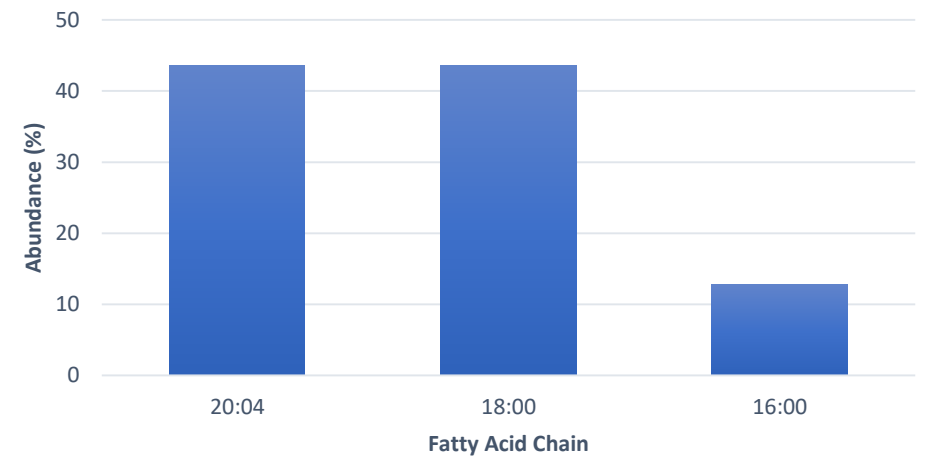
F11-SM-FA-R2-Neg



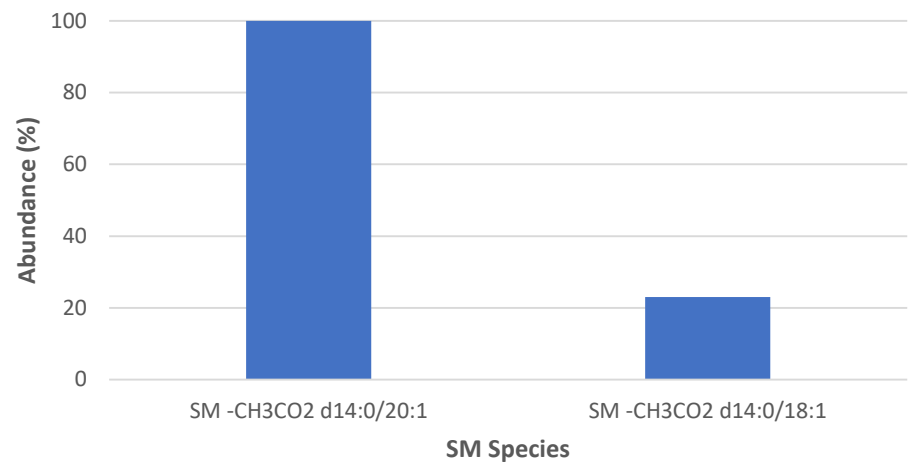
F11-PI-FA-R2-Neg



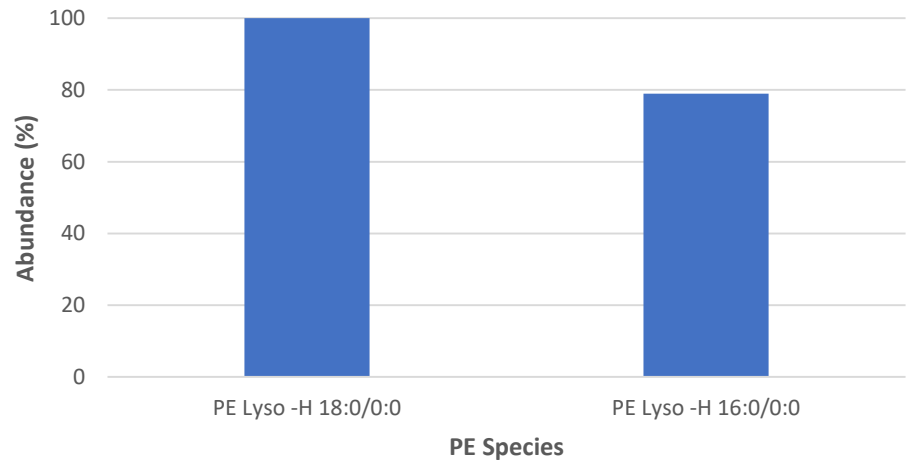
F11-PC-R3**F11-SM-R3****F11-PE-R3****F11-PI-R3**

F11-PC-FA-R3**F11-SM-FA-R3****F11-PE-FA-R3****F11-PI-FA-R3**

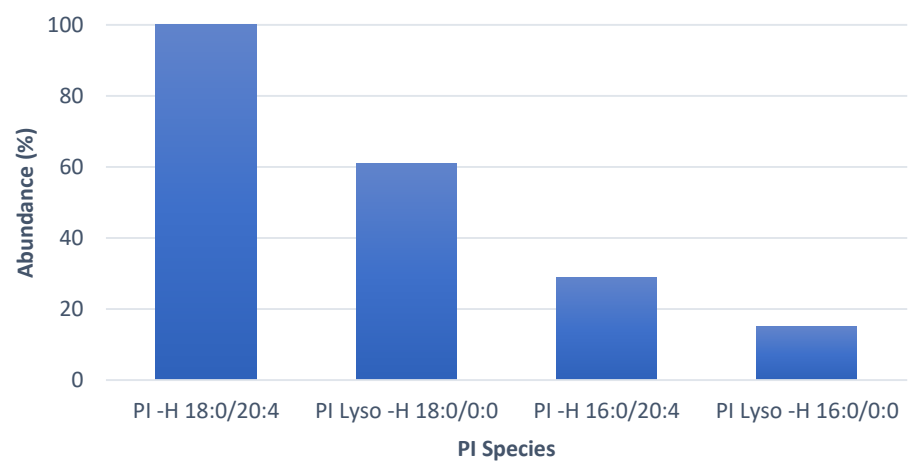
F11-SM-R3-Neg



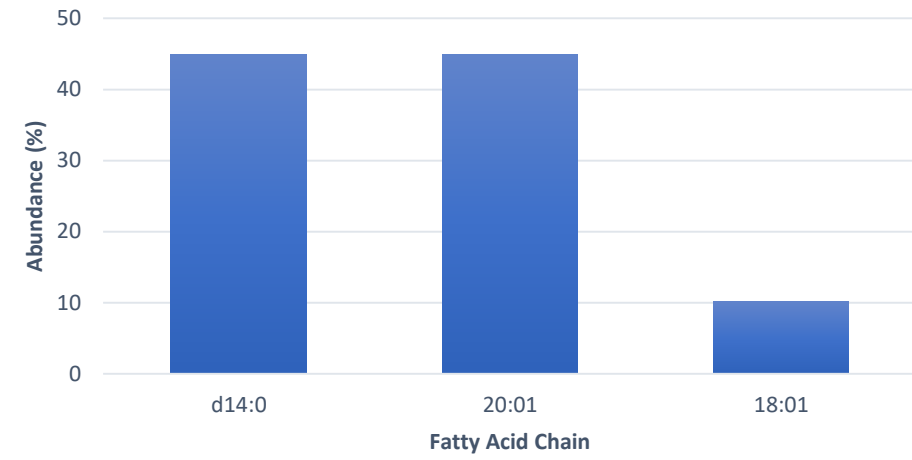
F11-PE-R3-Neg



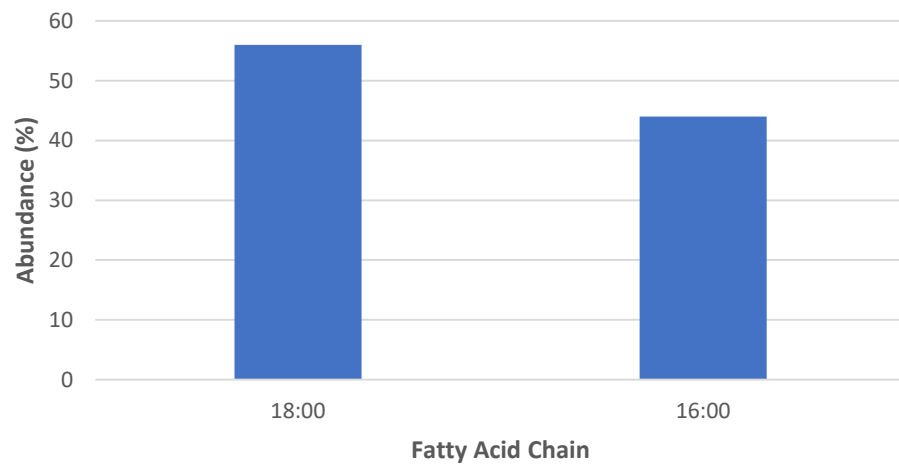
F11-PI-R3-Neg



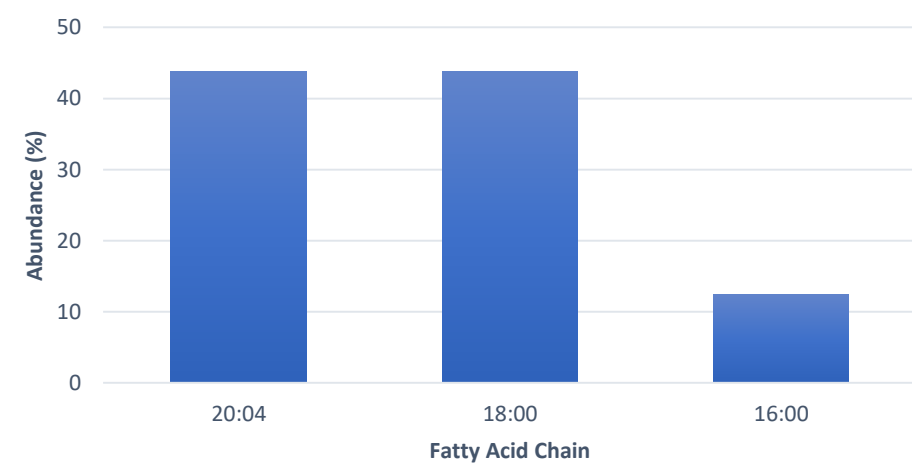
F11-SM-FA-R3-Neg

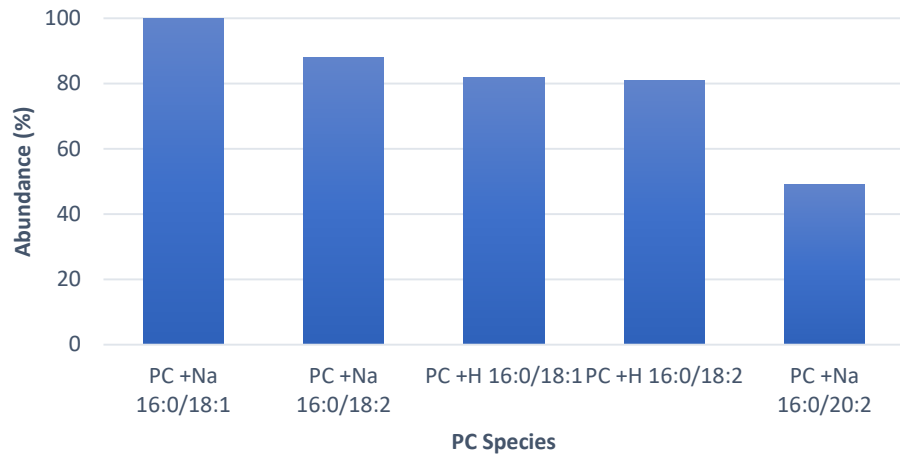
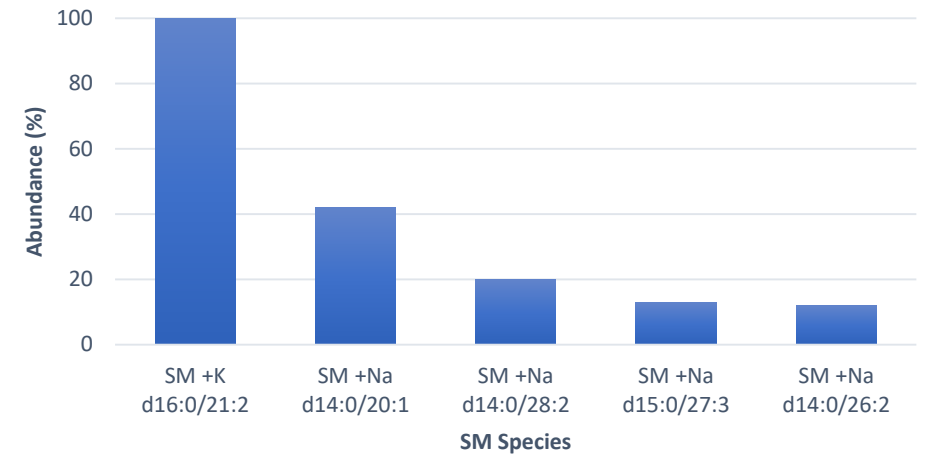
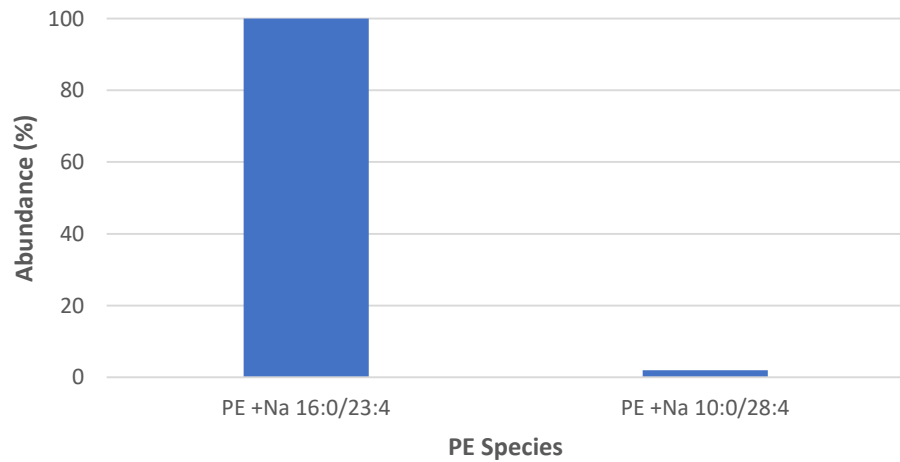
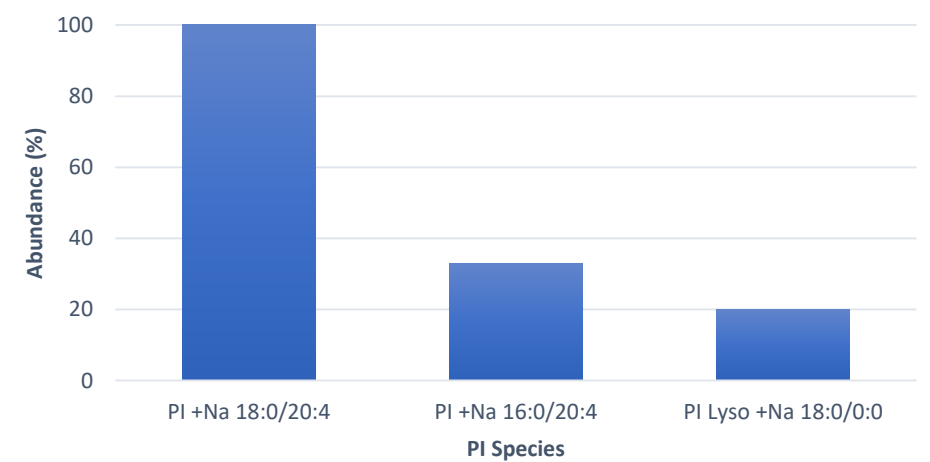


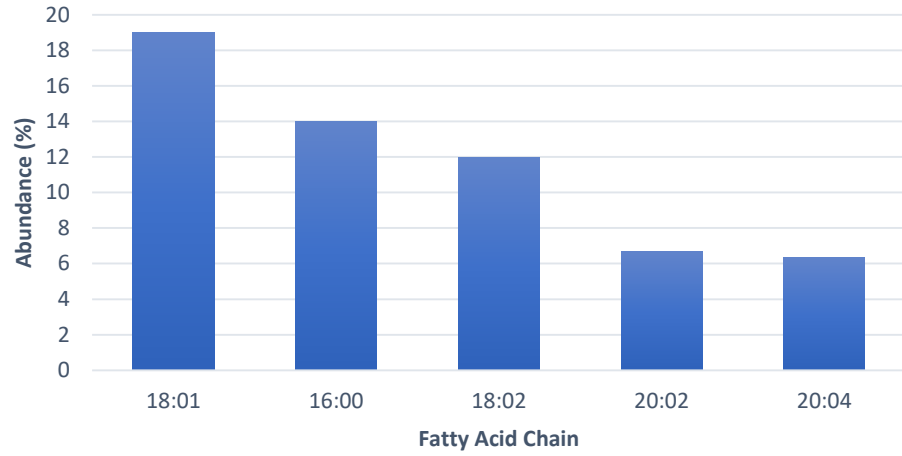
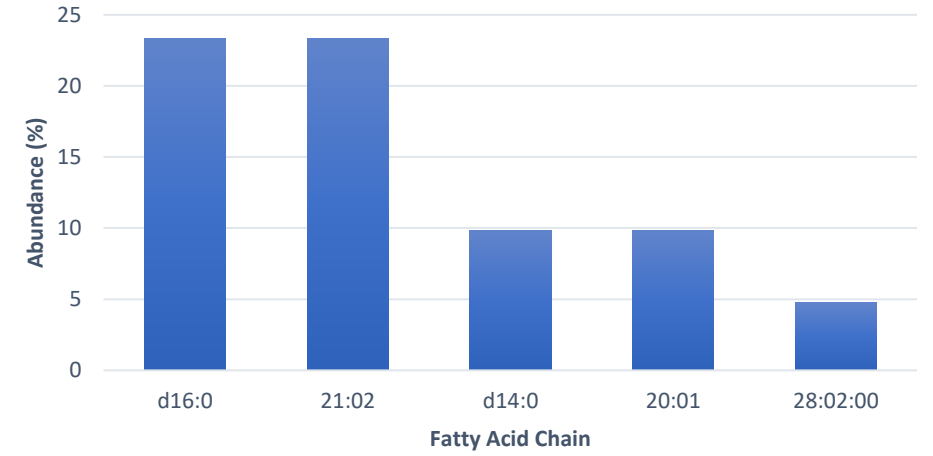
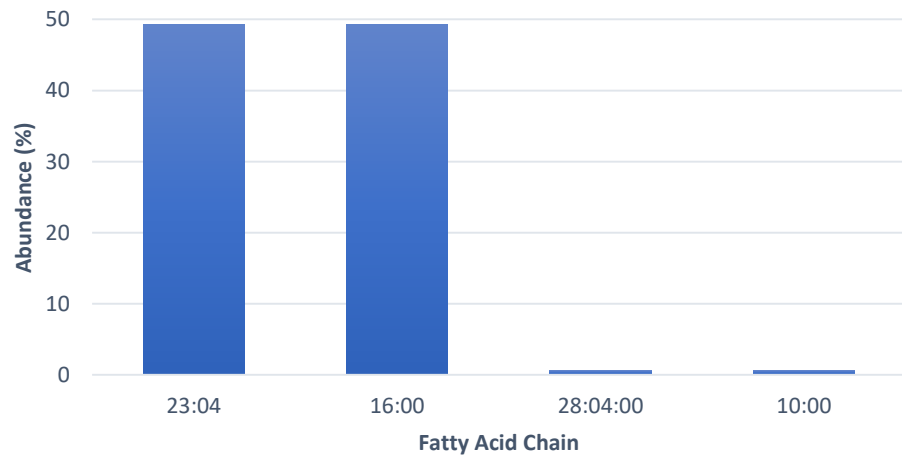
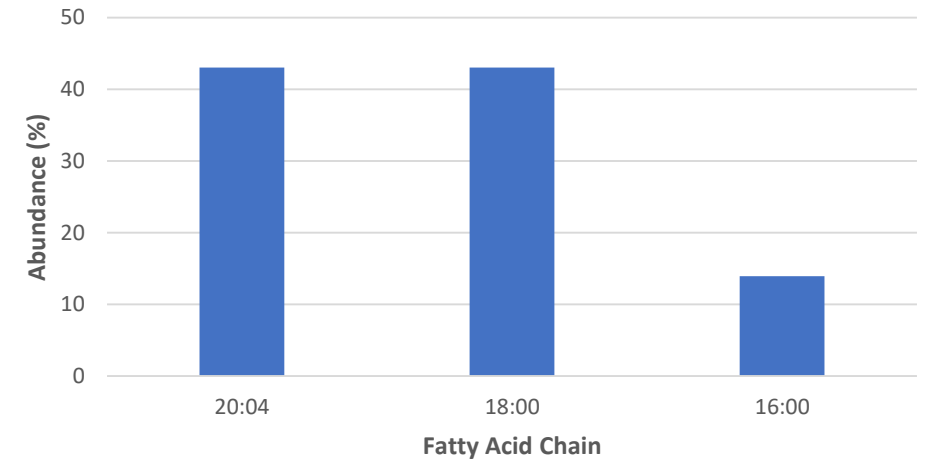
F11-PE-FA-R3-Neg



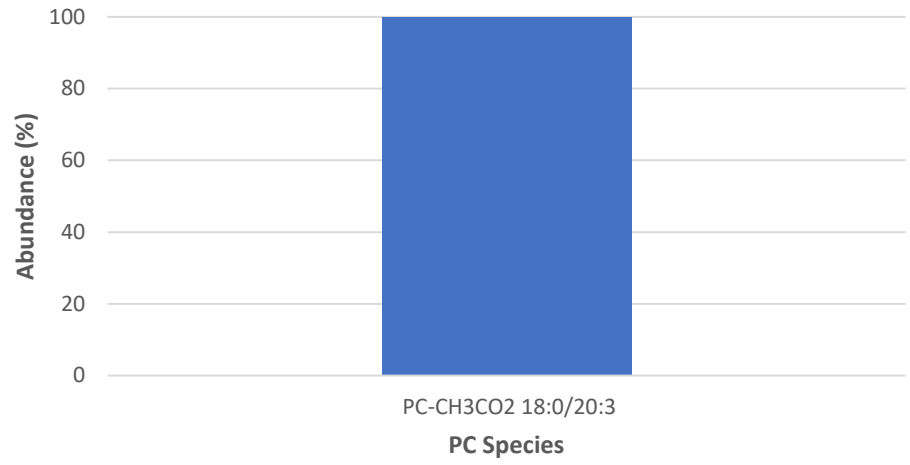
F11-PI-FA-R3-Neg



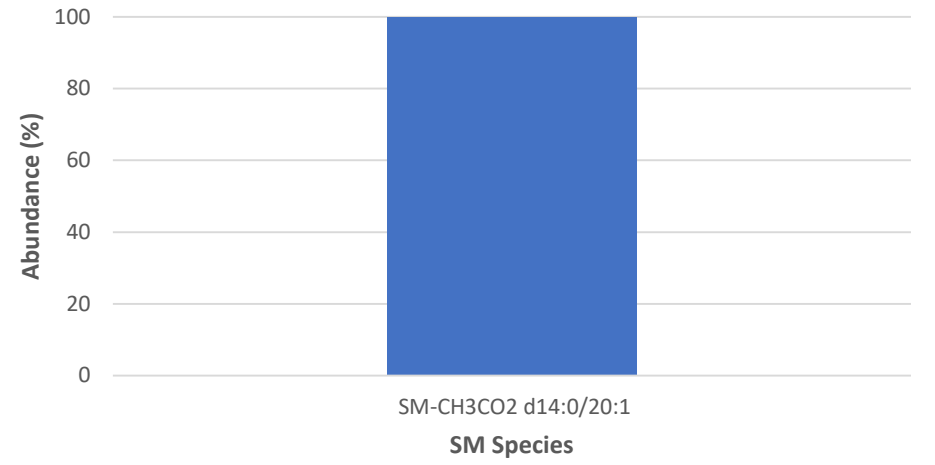
F11-PC-R4**F11-SM-R4****F11-PE-R4****F11-PI-R4**

F11-PC-FA-R4**F11-SM-FA-R4****F11-PE-FA-R4****F11-PI-FA-R4**

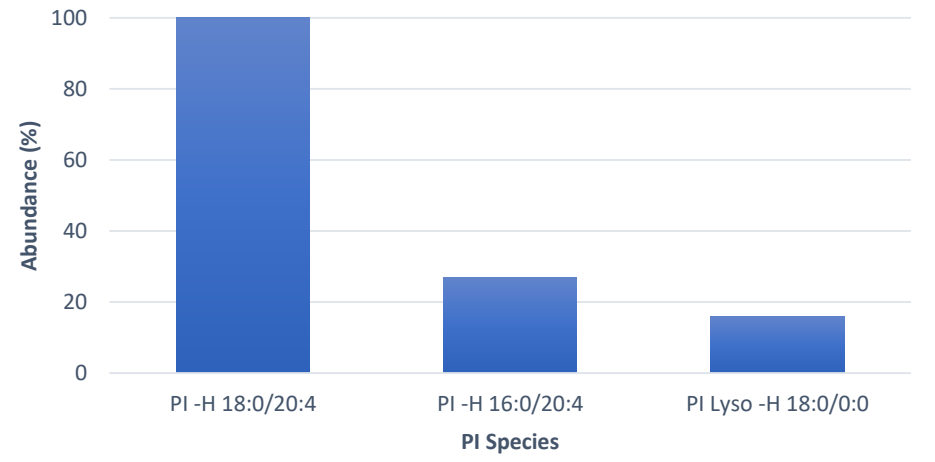
F11-PC-R4-Neg



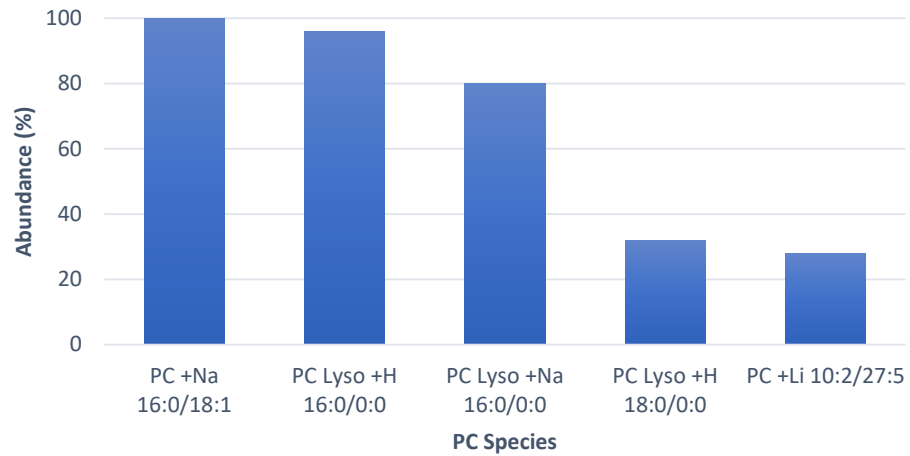
F11-SM-R4-Neg



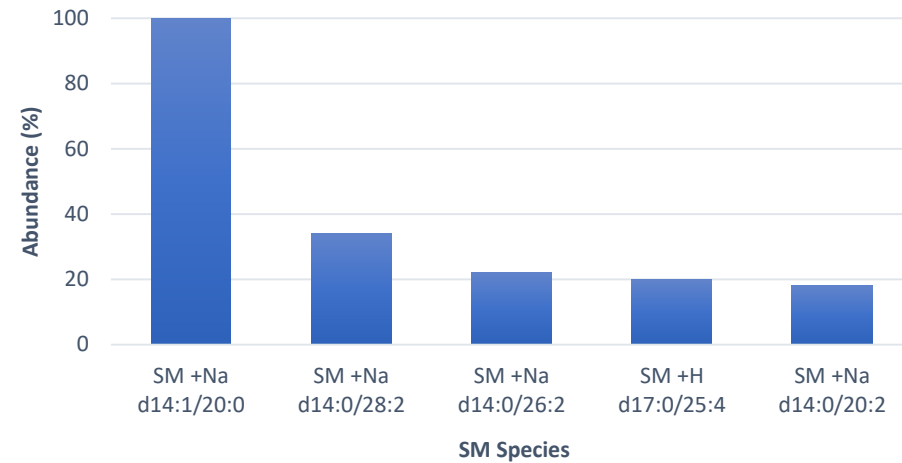
F11-PI-R4-Neg



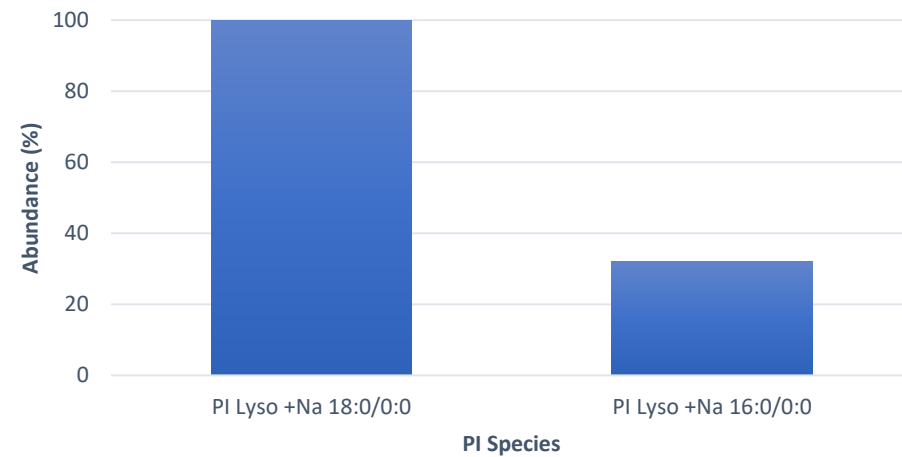
F11-PC-R5



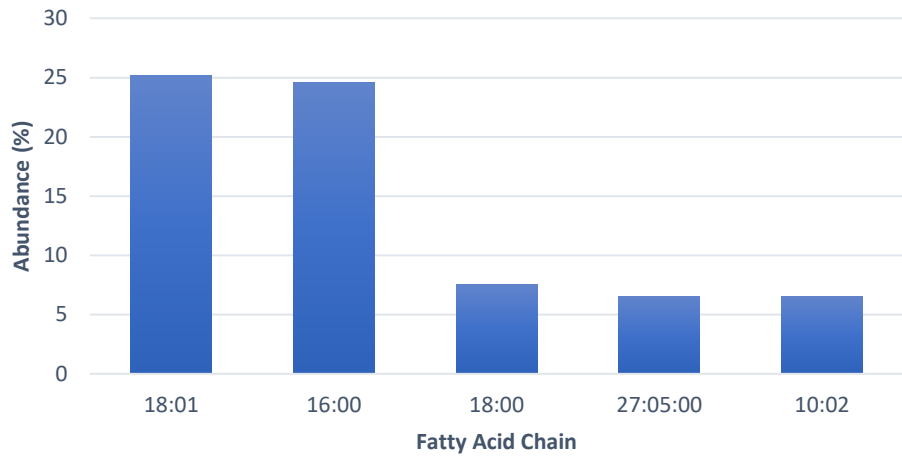
F11-SM-R5



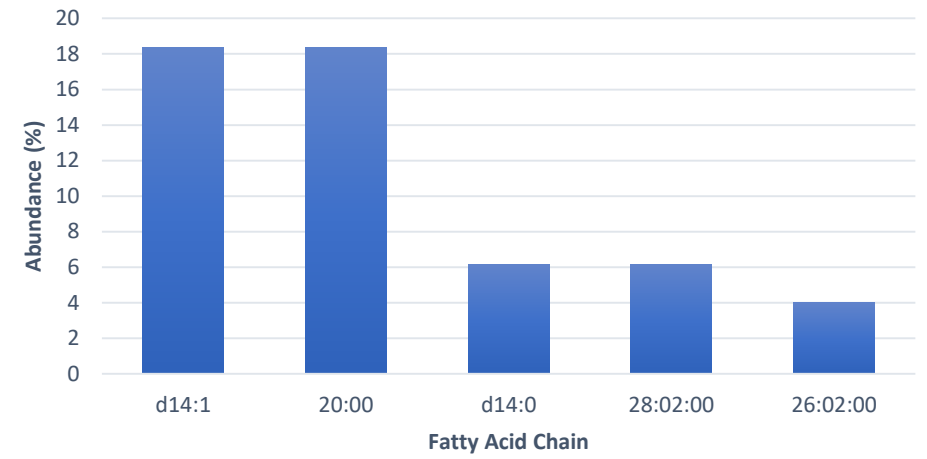
F11-PI-R5



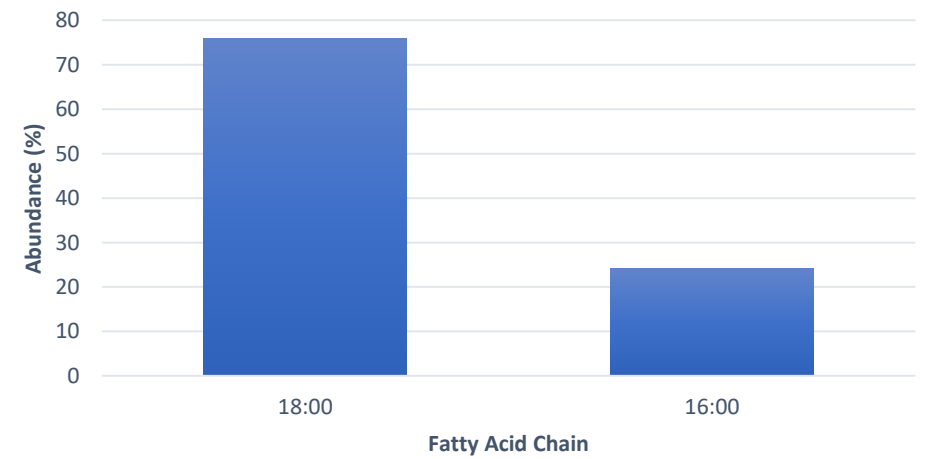
F11-PC-FA-R5



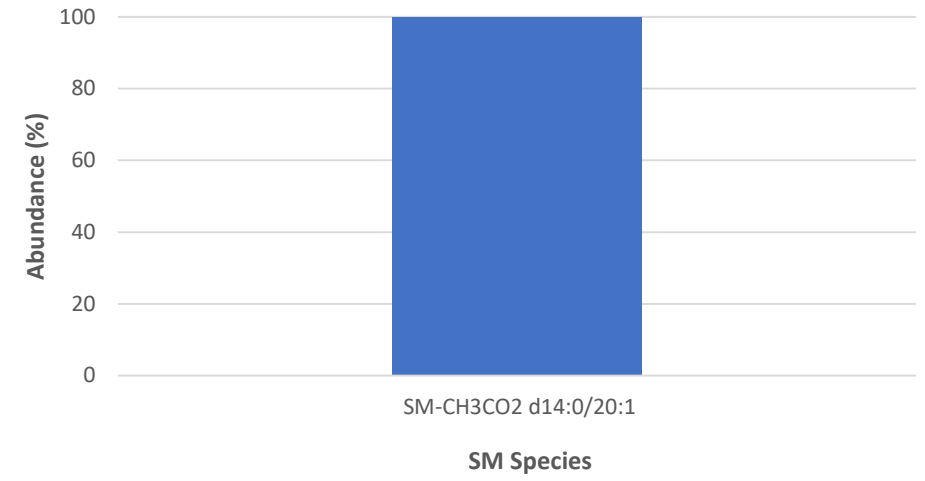
F11-SM-FA-R5



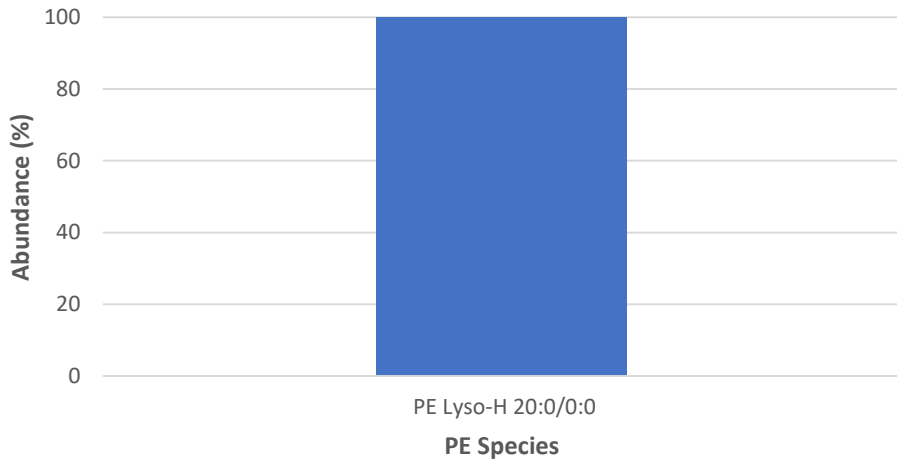
F11-PI-FA-R5



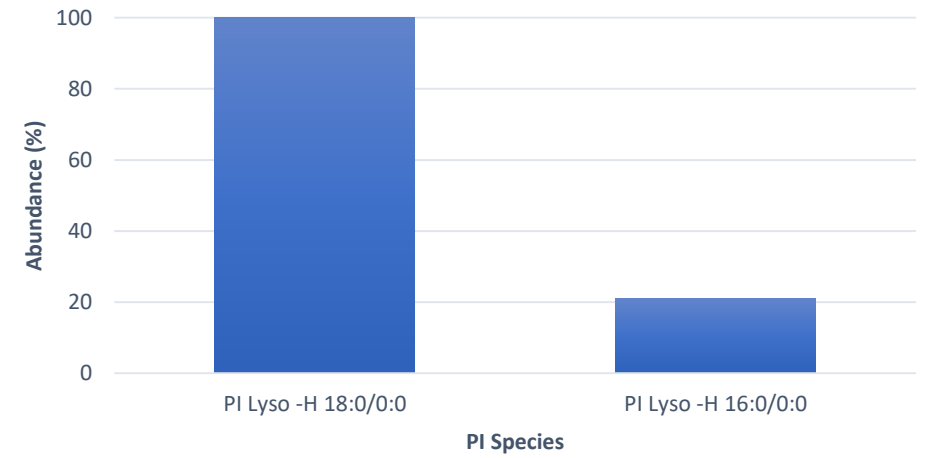
F11-SM-R5-Neg



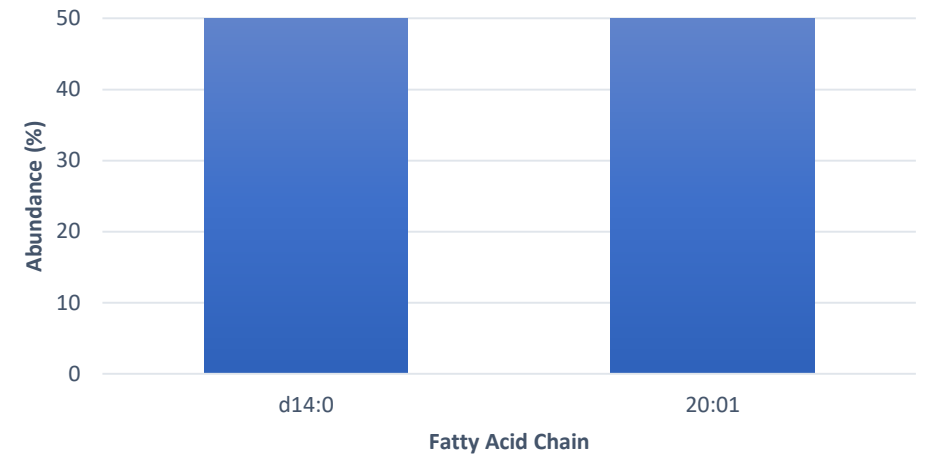
F11-PE-R5-Neg



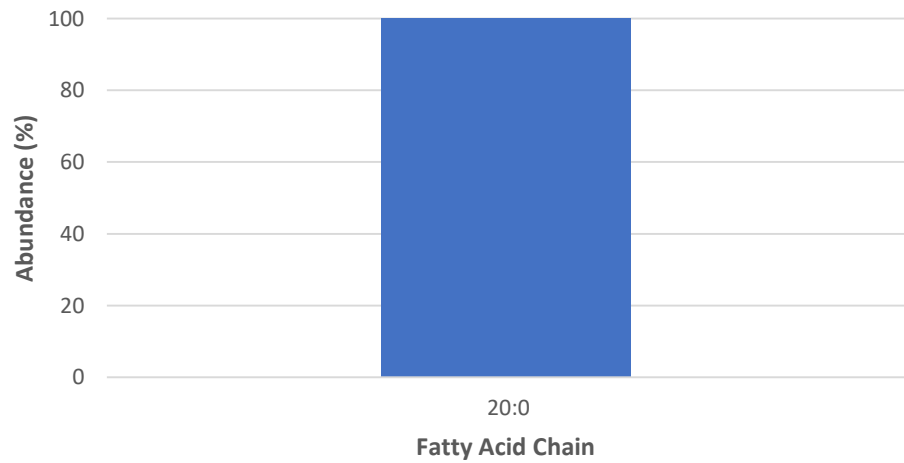
F11-PI-R5-Neg



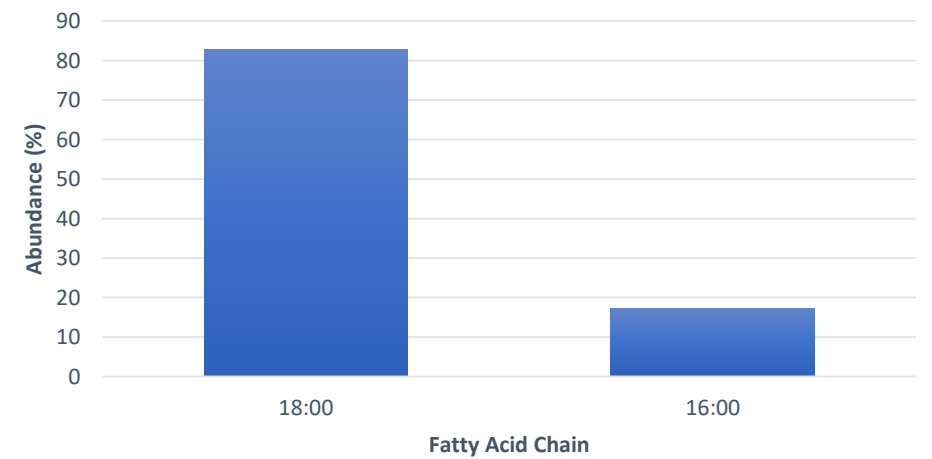
F11-SM-FA-R5-Neg



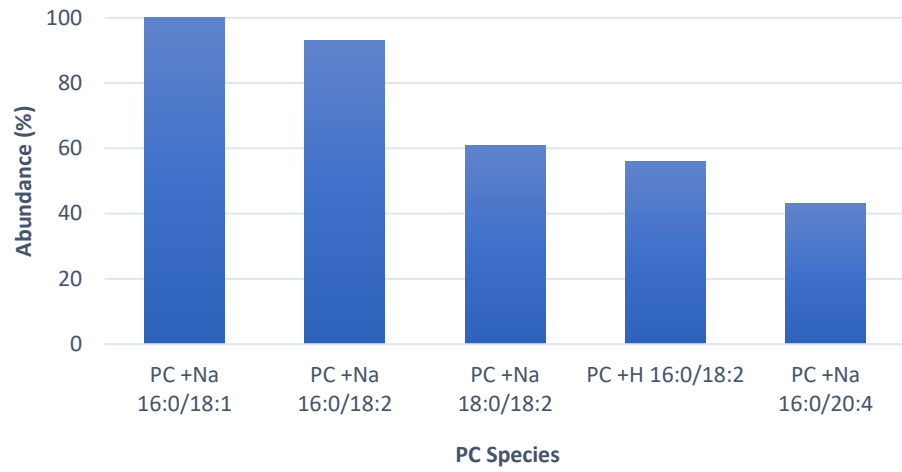
F11-PE-FA-R5-Neg



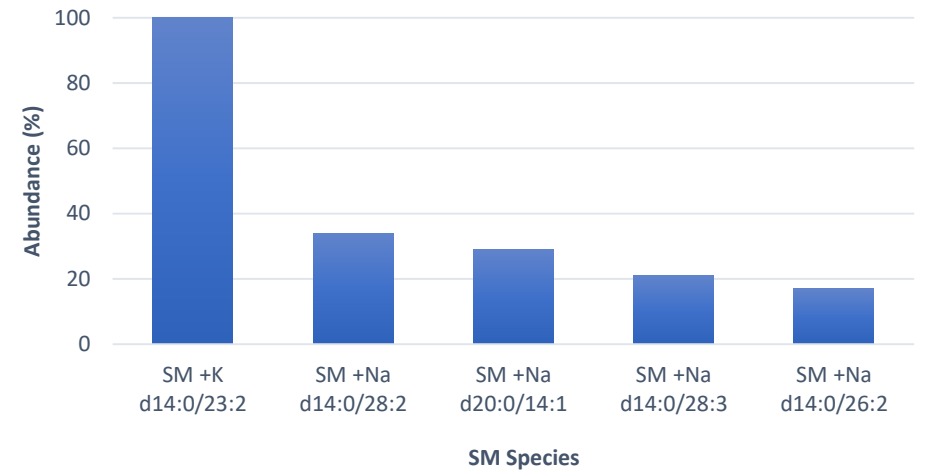
F11-PI-FA-R5-Neg



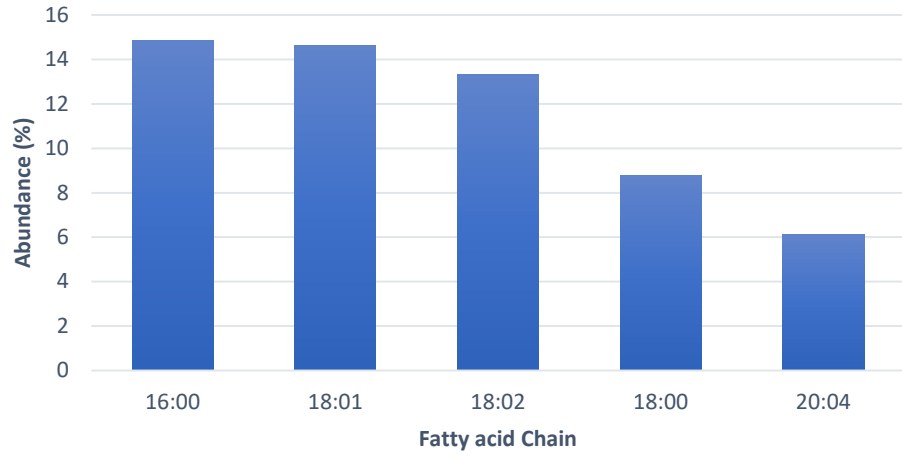
F12-PC-R1



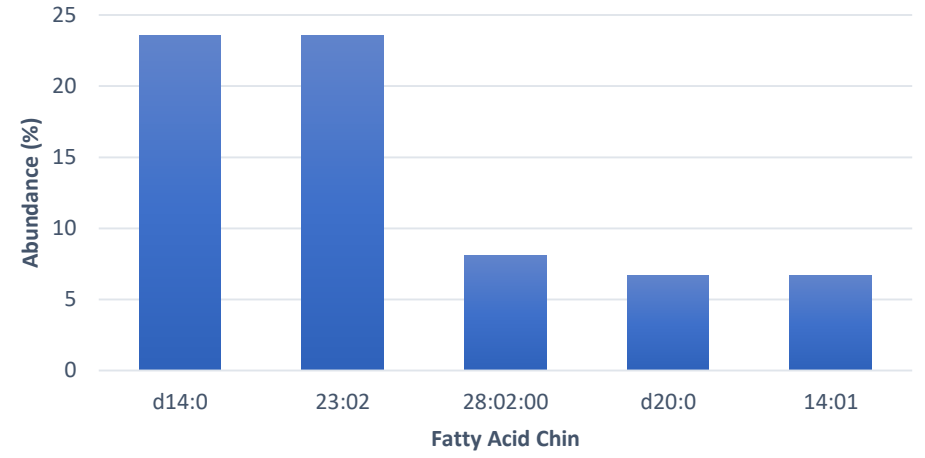
F12-SM-R1



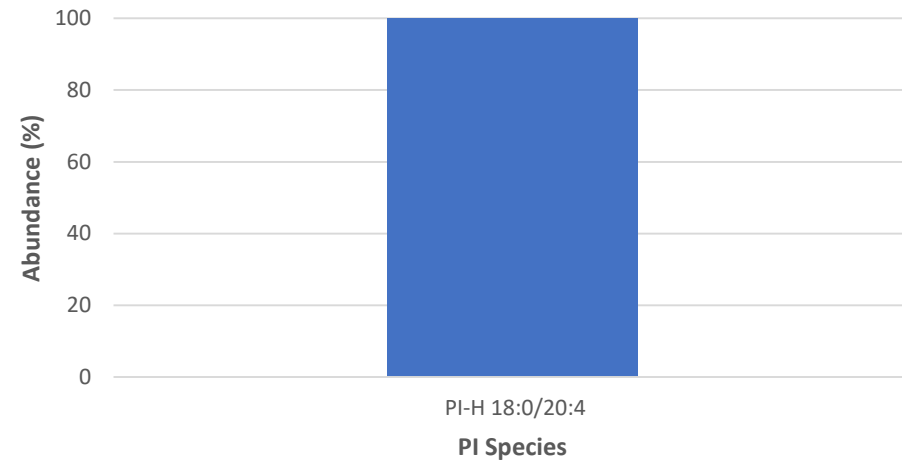
F12-PC-FA-R1



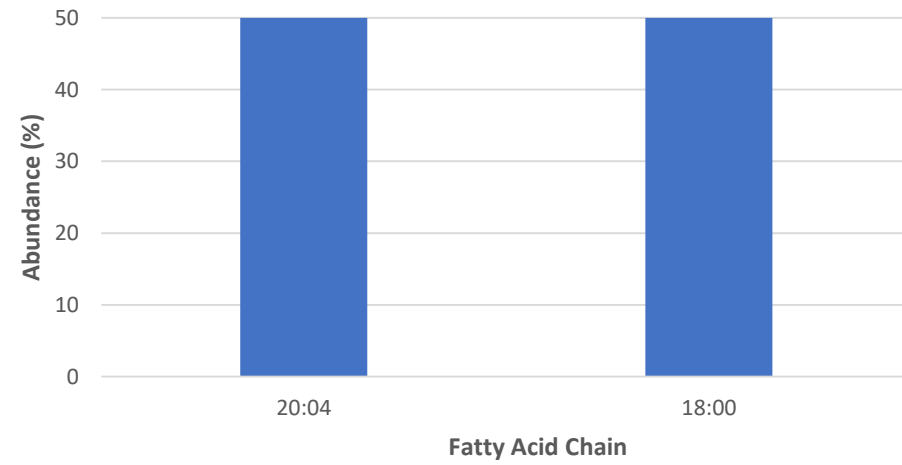
F12-SM-FA-R1



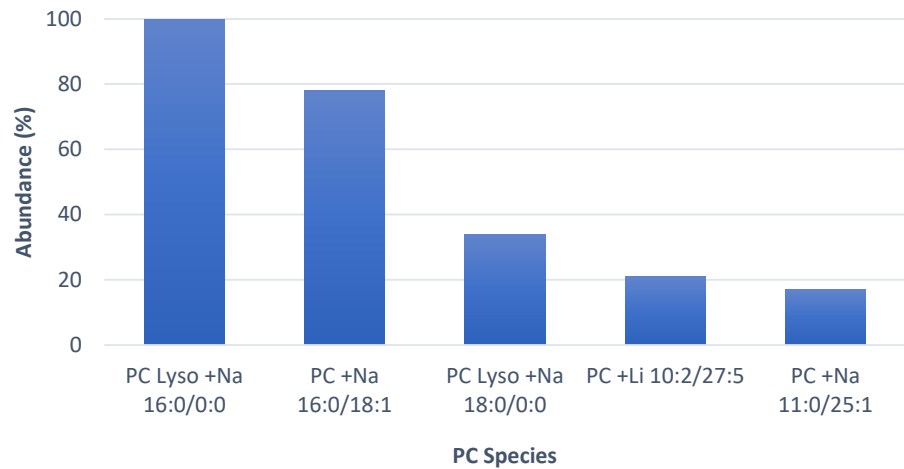
F12-PI-R1-Neg



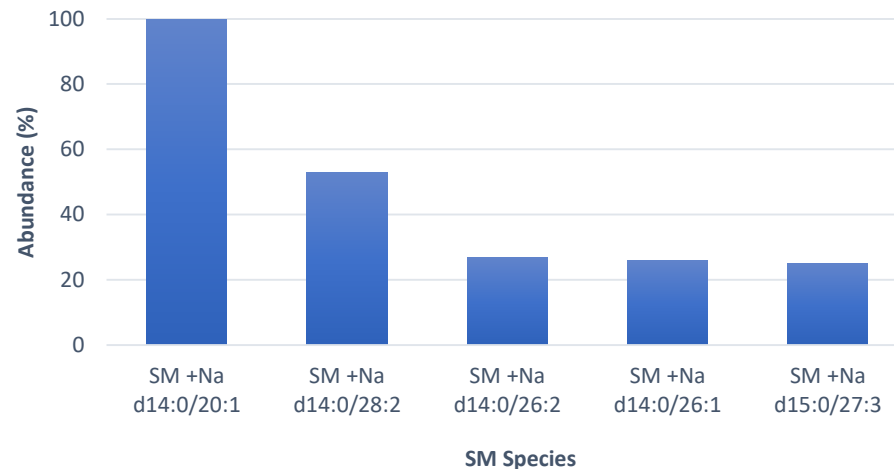
F12-PI-FA-R1-Neg



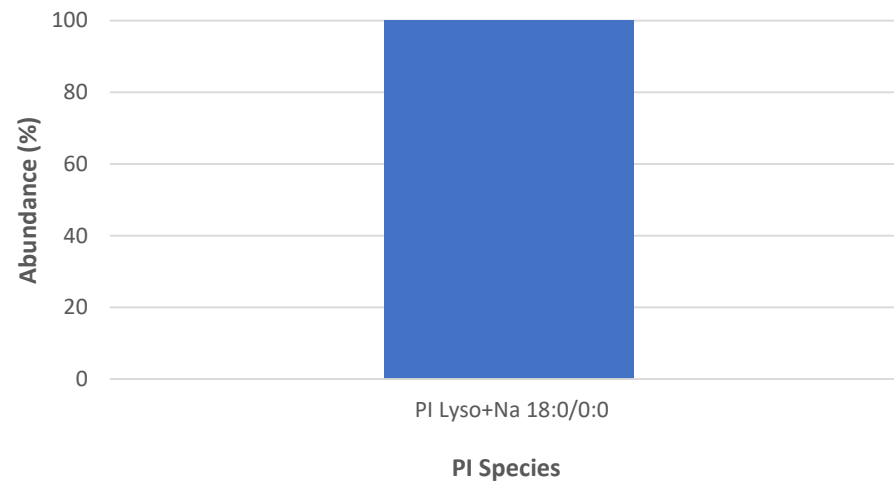
F12-PC-R2



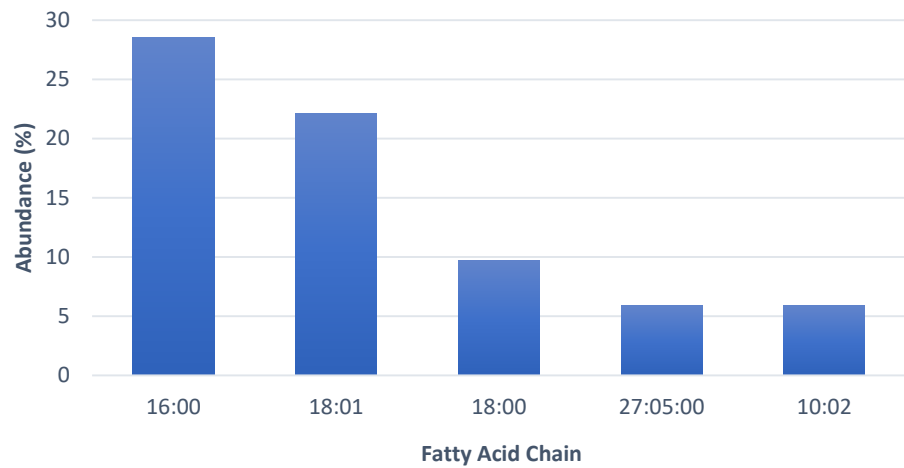
F12-SM-R2



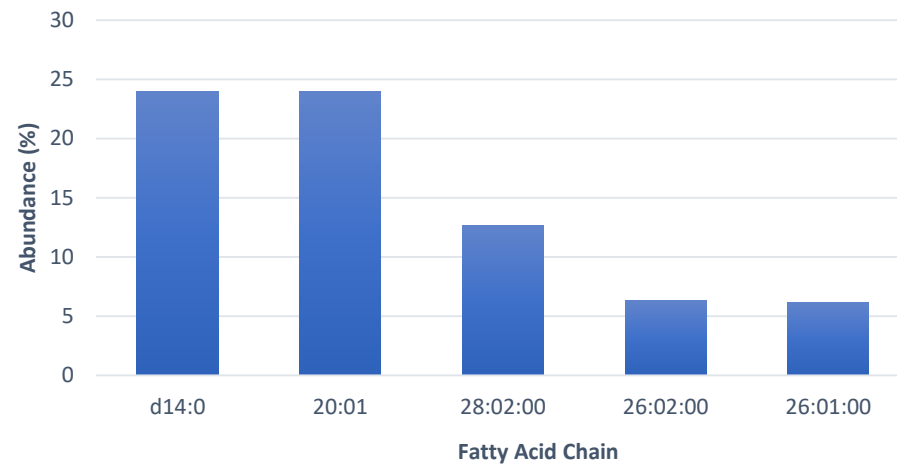
F12-PI-R2



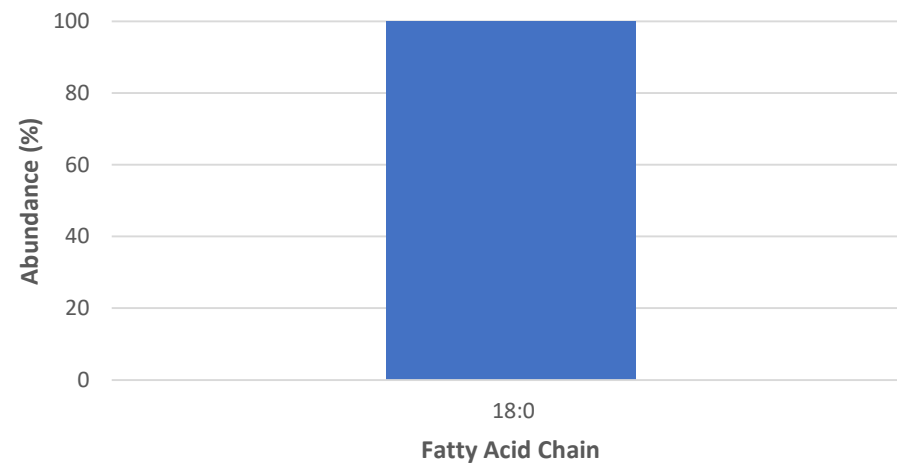
F12-PC-FA-R2



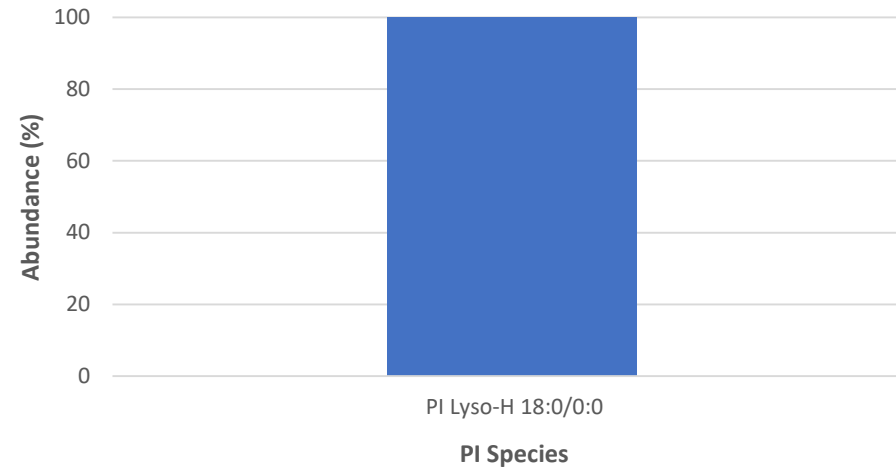
F12-SM-FA-R2



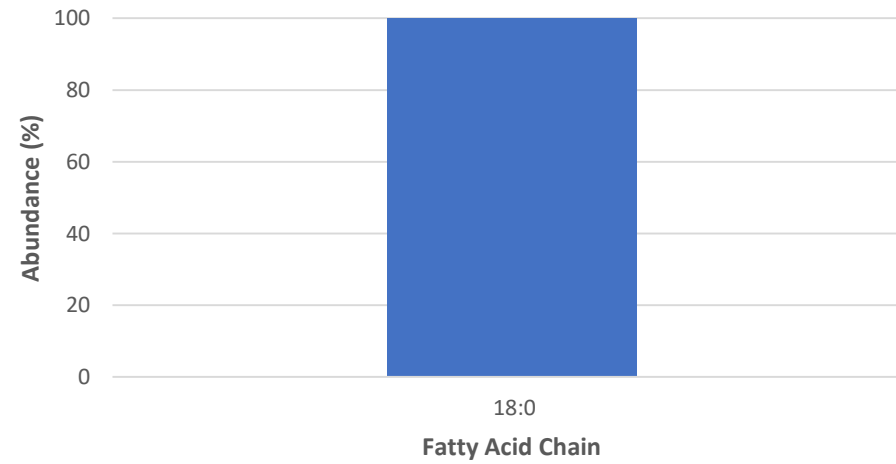
F12-PI-FA-R2



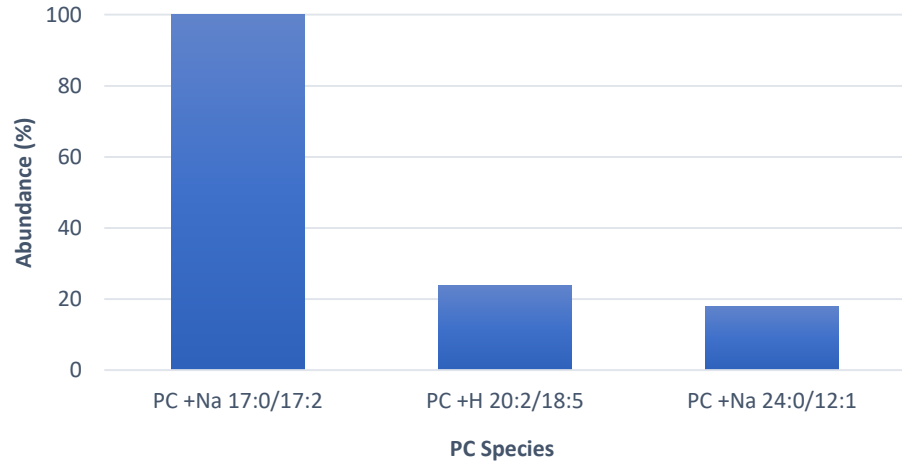
F12-PI-R2 Neg



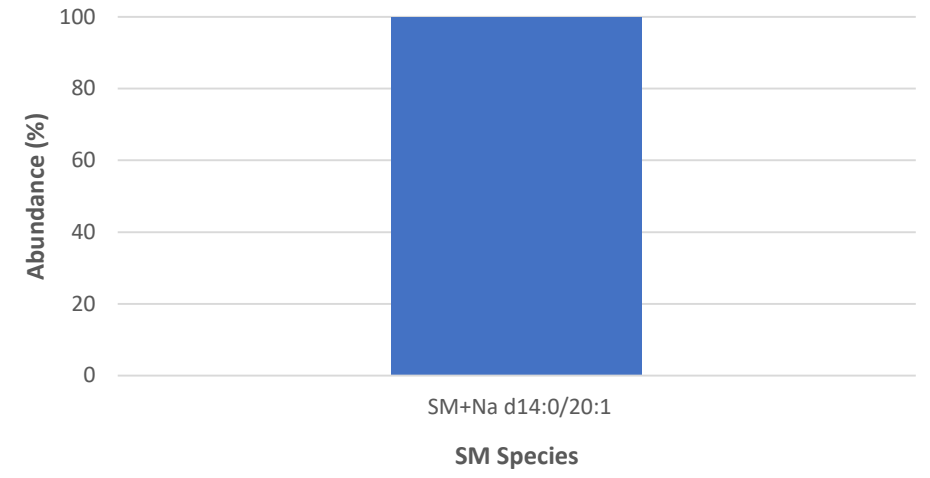
F12-PI-FA-R2 Neg



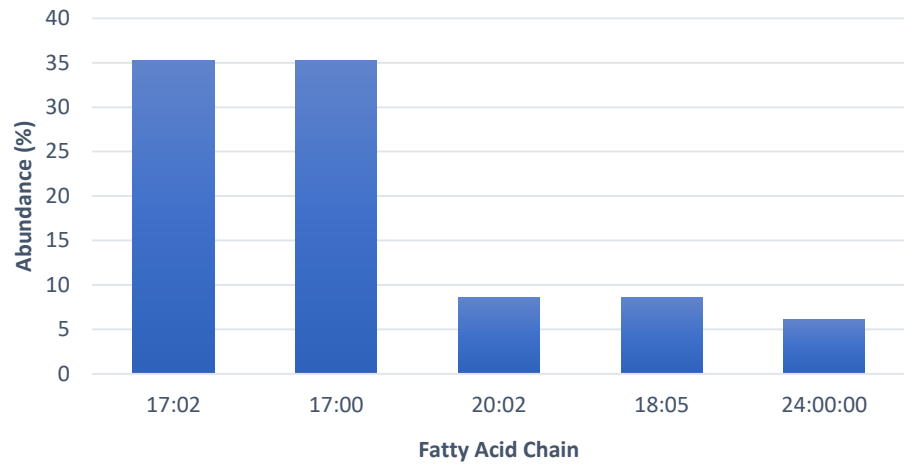
F12-PC-R3



F12-SM-R3



F12-PC-FA-R3



F12-SM-FA-R3

